



Advancements in **Porous Silicon** and **Silicon-On-Insulator** Membranes for Biosensing and Irradiation Recovery

Laurent A. FRANCIS

Electrical Engineering Dpt., ICTEAM Institute, UCLouvain (Louvain-la-Neuve, Belgium)

Louvain la Neuve, located in Belgium





Louvain la Neuve – then (1972)



Louvain la Neuve – now







UCL - ICTEAM Institute

- Electrical Engineering (ELEN)
- Computing Science Engineering (INGI)
- Mathematical Engineering (INMA)
- WELCOME and WINFAB technology platforms
- About 40 professors
- More than 200 researchers
- 20 computer scientists and technicians

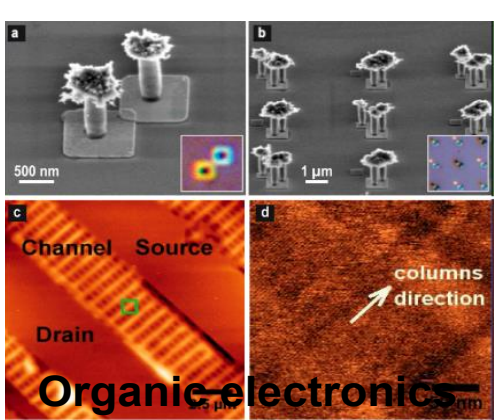




WINFAB platform for micro-nano-fabrication

- 1000 m² of clean rooms on 2 levels
- Cleanliness: Critical work areas in class 1 / ISO 3 (stand-by)
 « less than 100 particules ≥300 nm/m³ of air »
- Activities: more than 40 specialized pieces of equipment,
 50 to 80 users, more than 20 R&D projects in parallel
- Supports research activities from micro down to nano scale in
 - Biosensors
 - MEMS-NEMS
 - SOI-CMOS co-integration
 - Organic electronics
 - Nanoelectronics
 - Photovoltaics











Wallonia Electronics & Communications Measurements

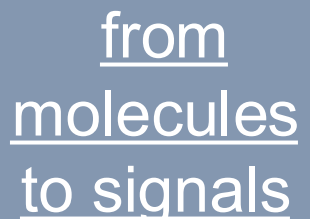


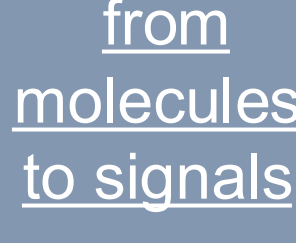


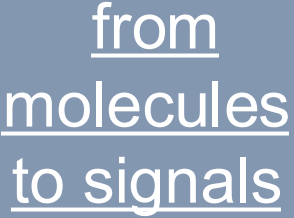


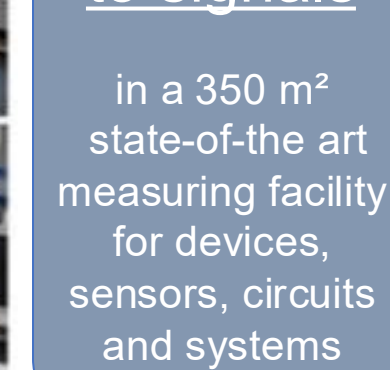


Welcome to multiparametric characterizations

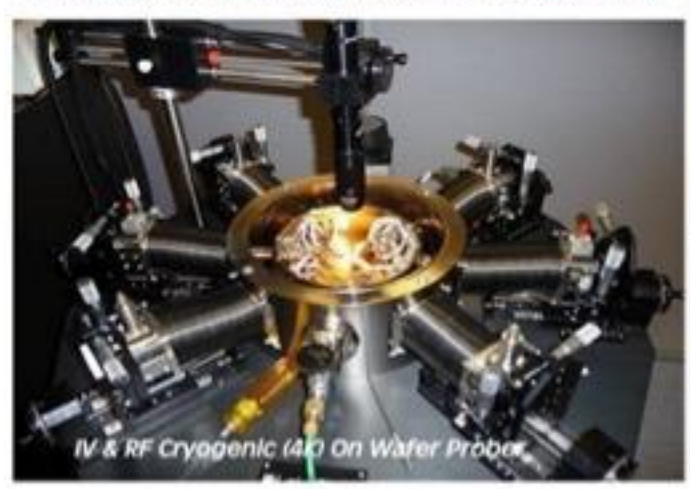


















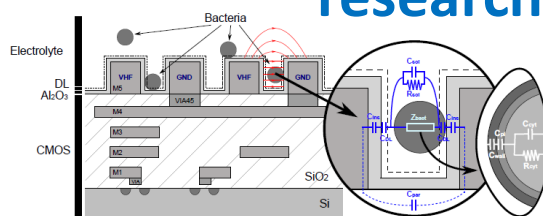
2.13 MEuros equipment over 10 years – over 120 yearly users from 4 corners of the globe open to research, PhD/Master studies, industry http://www.uclouvain.be/welcome info-welcome@uclouvain.be





From microsensors to microsystems for health, environment and monitoring applications

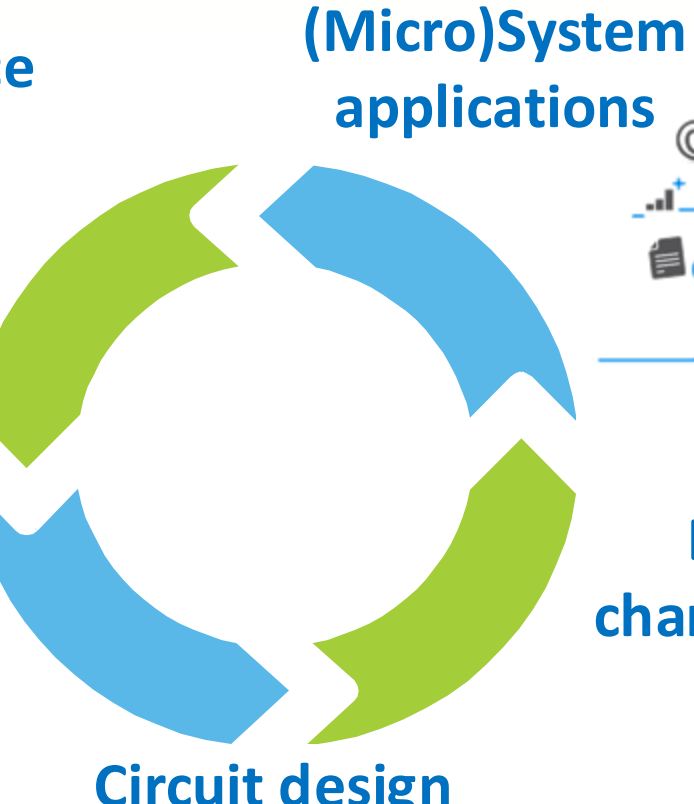
> **Process / device** research



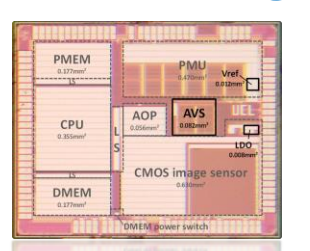
Microfabrication



Many collaborations within UCL and abroad!



Circuit design

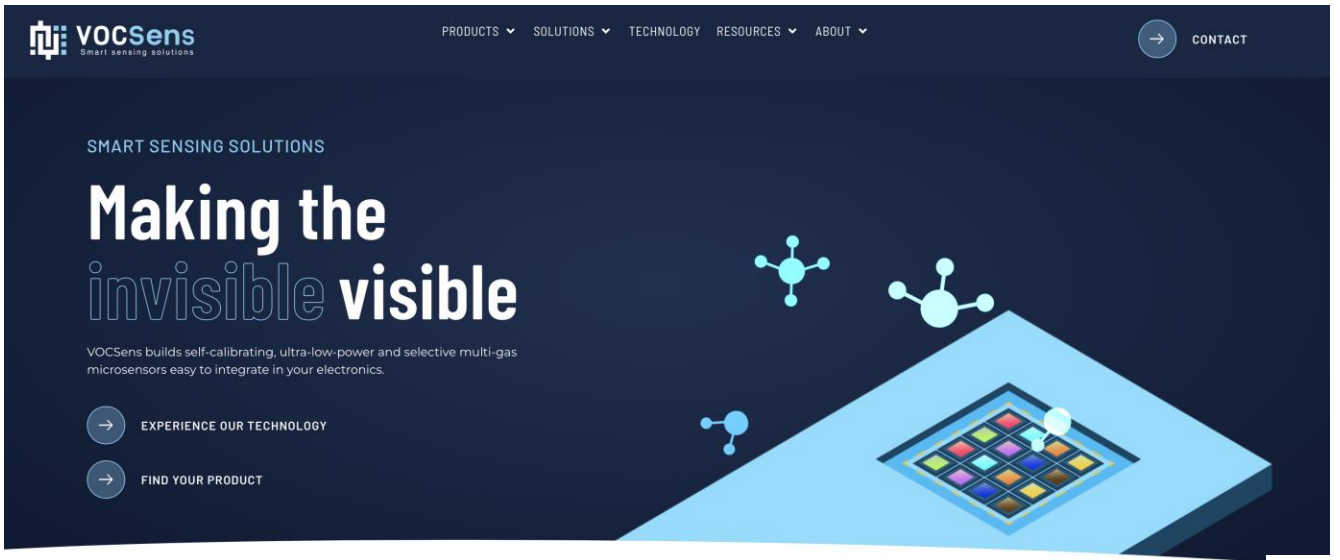


Electrical characterization



Institute of Information and Communication Technologies, Electronics and Applied Mathematics





UCLouvain spin off

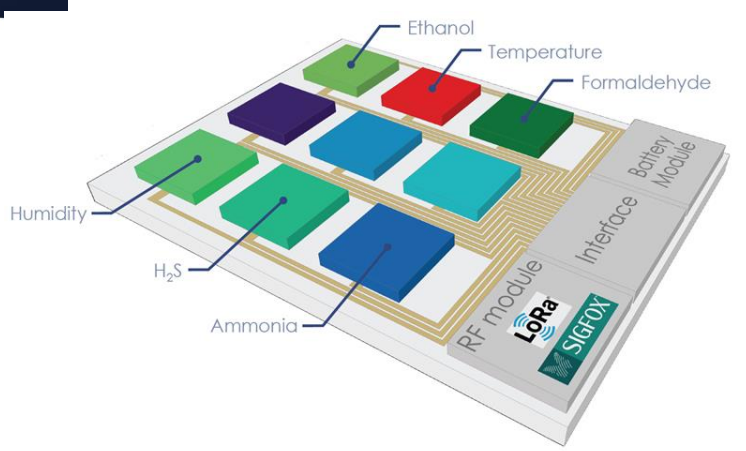
EnviCam®-3x is our cutting-edge product line of multi-gas microsensors, designed to enable precise measurement and control of multiple gases and VOCs across various industries.

With EnviCam®-3x, businesses can better meet regulatory compliance requirements while fostering a healthier and safer environment.











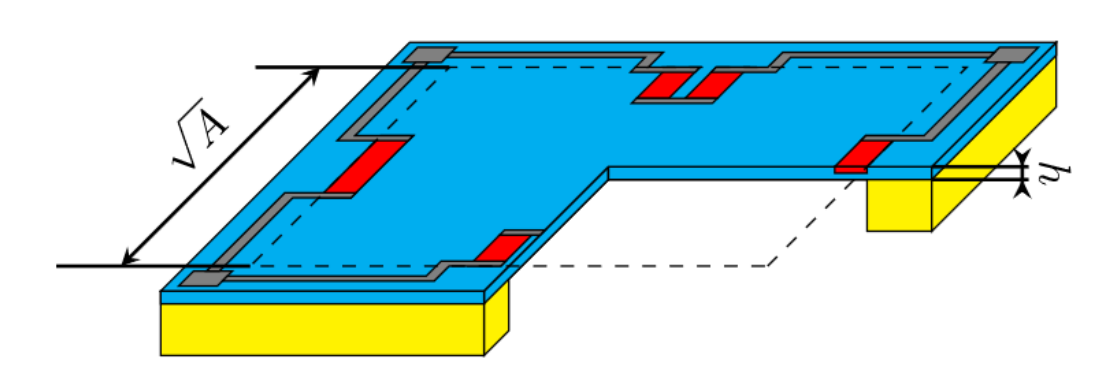


R&D in integrated micro-sensors

Gas, Flow, Pressure, Humidity, Temperature, Heat Light, Radiation, Magnetic field, Electrical arcs Biomolecules (DNA, Proteins, Bacteria...)
Microfluidics, Fluid properties

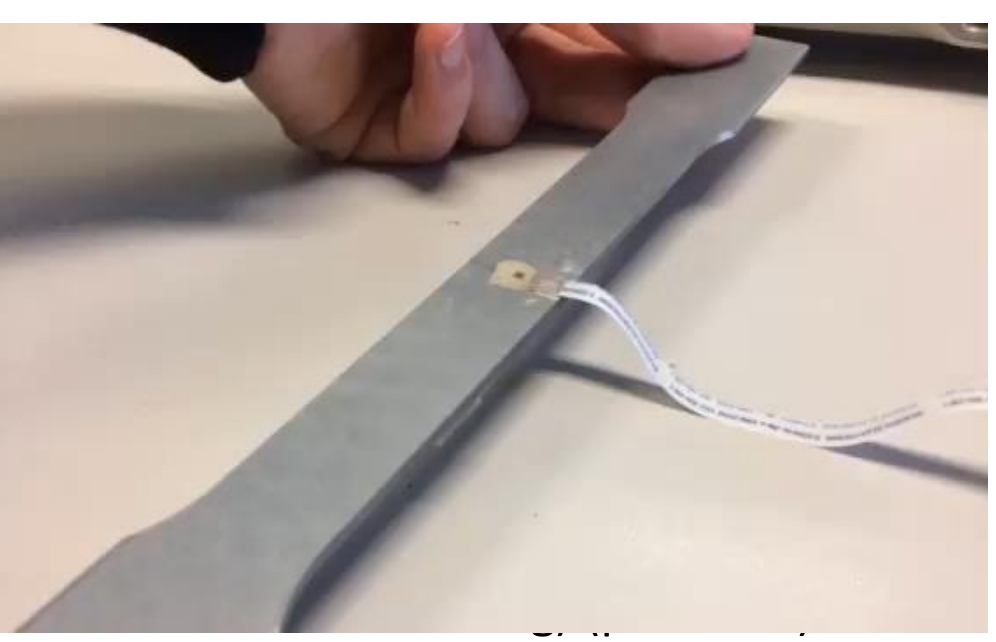
& energy harvesting

PV (Si, CIGS, CZTS) RF (CMOS rectifiers)



Record performance for

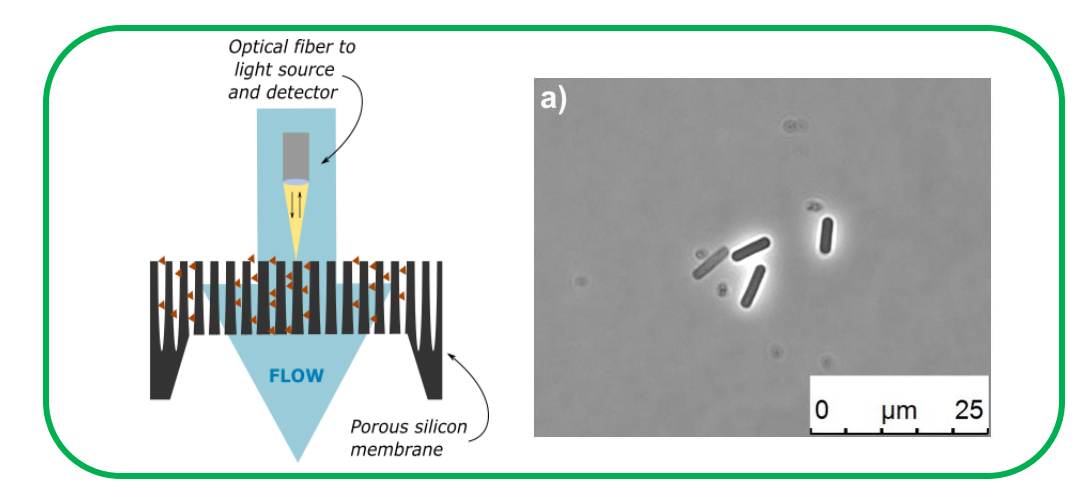
- μW / HT / GF > 1000 Strain gauges on Si (str
- mbar pressure sensor (eye implant)
- 10µm-thick Si proton beam detector (hadrontherapy)
- few-bacteria detection (point-of-care)
- UV sensing (SPAD)...



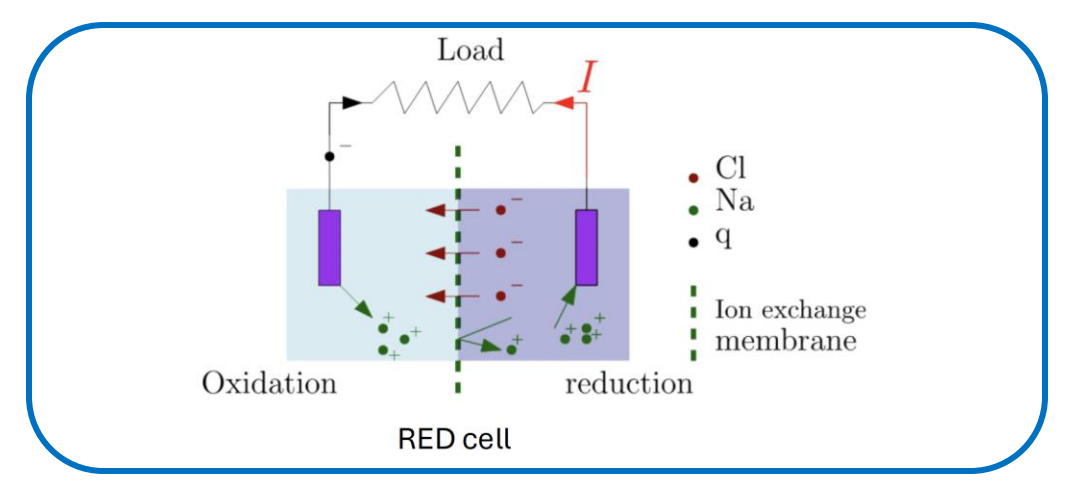


_icteam

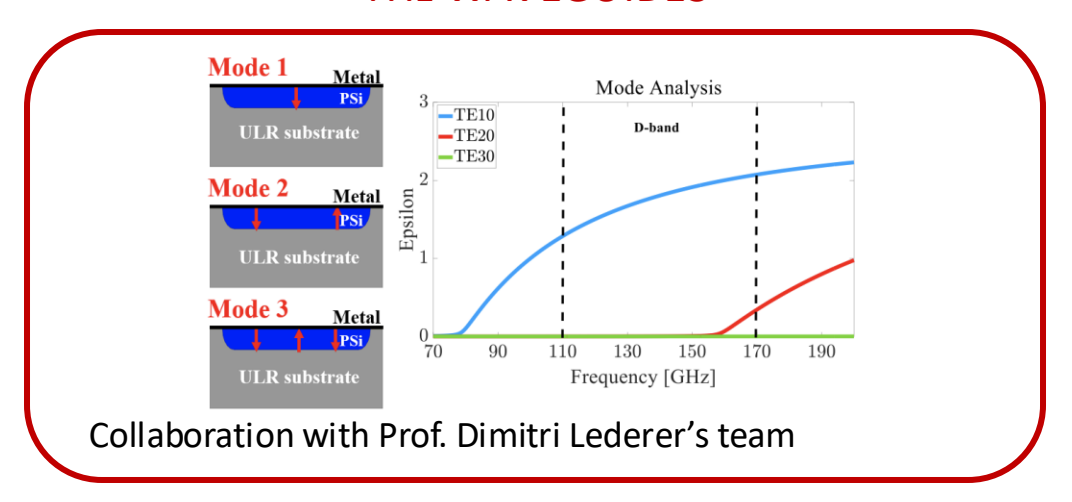
BACTERIAL DETECTION IN COMPLEX SAMPLES



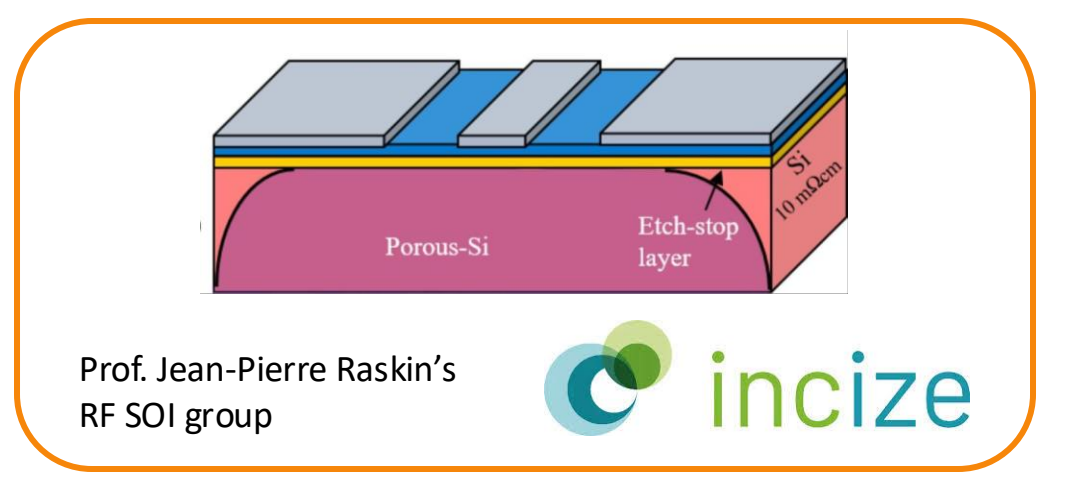
BLUE ENERGY & IONTRONICS



THz WAVEGUIDES

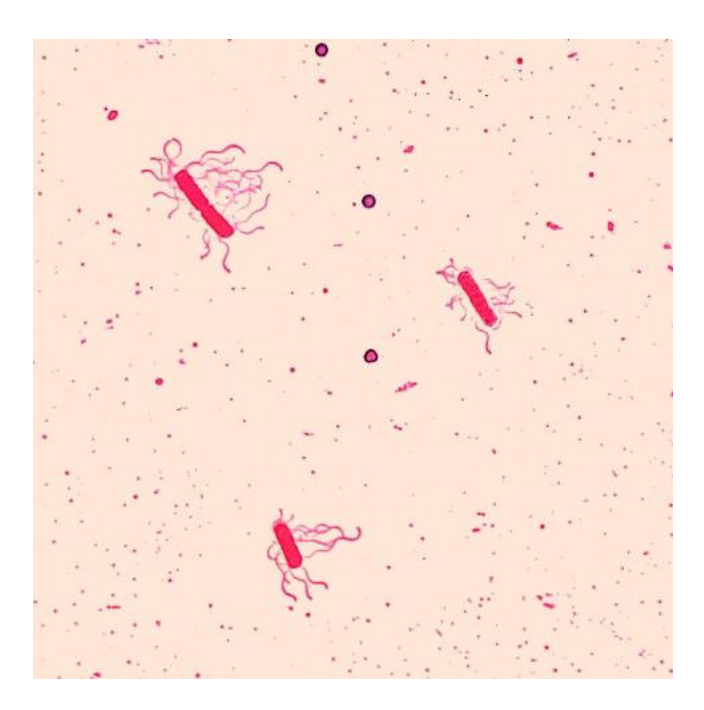


RF SUBSTRATES



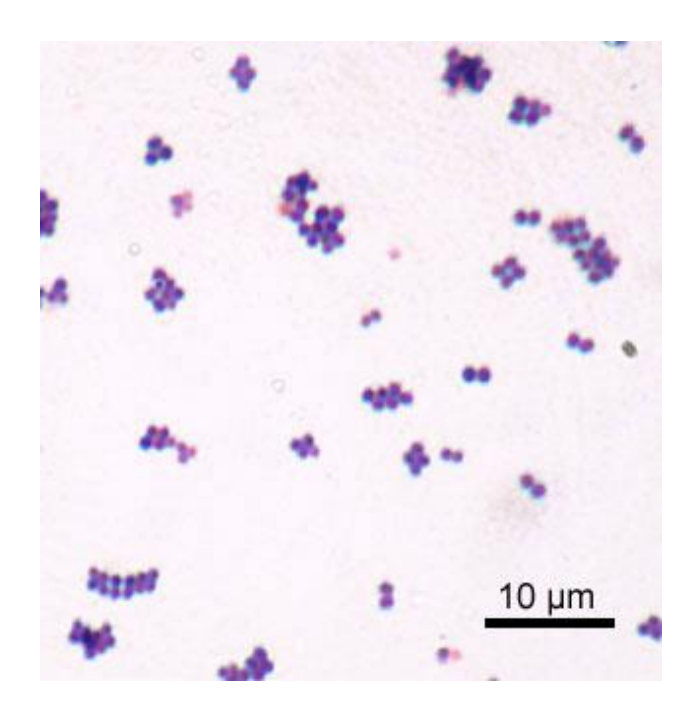
Porous Silicon Membrane for biosensing

BACTERIA?



B. cereus

Gastrointestinal, respiratory tract, nosocomial, eye, CNS, urinary tract and cutaneous infections, endocarditis, osteomyelitis. The potential of this bacterium to cause life threatening infections has increased.

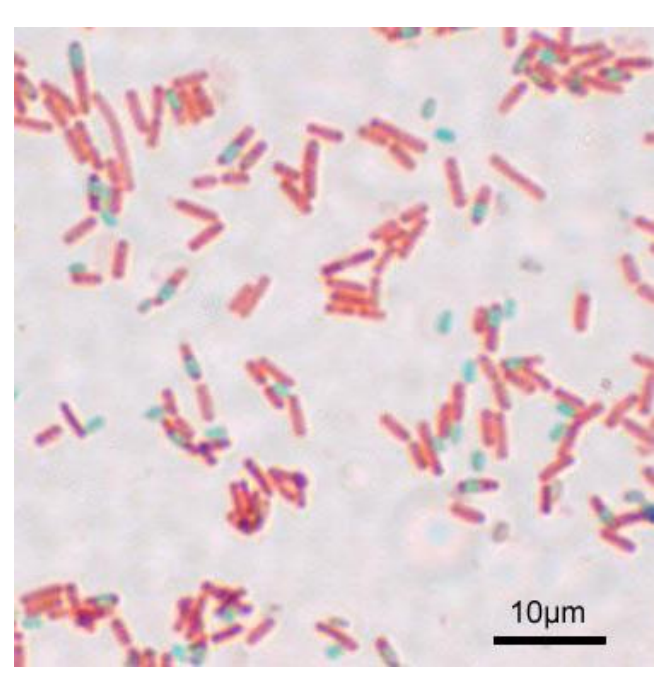


S. aureus (S. epidermidis)

Minor skin infections: boils, abscesses, impetigo;

More serious infections: meningitis, osteomyelitis, pneumonia, septic phlebitis, endocarditis;

MRSA, displays antibiotic resistance



B. subtilis

« Not a frank human pathogen, but has on several occasions been isolated from human infections.

Infections attributed to *B. subtilis* include **bacteremia**, **endocarditis**, **pneumonia**, and **septicemia**. »

[https://www.epa.gov/sites/default/files/2015-09/documents/fra009.pdf]

RTL info

Ne consommez pas ce fromage : présence possible de E. Coli STEC



Le fromage « VALENCAY » à base de lait cru de la marque Cloche d'or est rappelé par les autorités sanitaires pour risque de contamination à...

Il y a 1 jour



Infections à la bactérie Stec dans des homes : le parquet de Bruxelles ouvre une enquête judiciaire



Fin août, des contaminations par la bactérie Escherichia coli productrice de shigatoxines (STEC) avaient touché des...

Il y a 5 jours



Bactérie Stec dans des homes : le parquet de Bruxelles ouvre une enquête sur les contaminations



Les contaminations à la bactérie ont causé neuf décès et provoqué des symptômes chez plus de 70 personnes.

Il y a 5 jours



Infections à la bactérie Stec dans des homes: voici la source la plus probable de l'épidémie



La viande bovine hachée crue est la source de contamination par la bactérie Escherichia coli productrice de Shiga-toxines (Stec) la plus...

Il y a 5 jours

wt VRT

De la viande bovine crue hachée serait la cause la plus probable de l'épidémie de Stec mortelle dans des maisons de repos



L'Agence fédérale pour la sécurité de la chaîne alimentaire (Afsca), l'Agence pour une vie de qualité (AVIQ), le Departement des Soins...

Il y a 5 jours



Les victimes de la bactérie Stec se multiplient en Belgique, des cas en province de Luxembourg

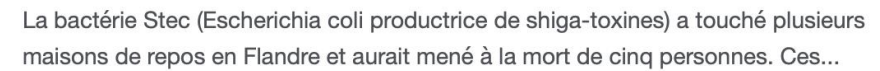


La bactérie Stec est une variante dangereuse d'Escherichia coli capable de produire une toxine puissante. Selon la professeure Sandra Van...

Il y a 4 semaines



Bactérie Stec: un premier enfant contaminé dans une crèche



Il y a 1 mois



Artsenkrant

Contaminations STEC en MRS: de la viande bovine hachée crue en cause



Des contaminations par la bactérie E. coli productrice de Shiga-toxines (STEC) ont été détectées dans 11 maisons de repos lors du mois...

Il y a 5 jours

Le Vif

Qu'est-ce que la bactérie Stec, qui menace les maisons de repos? Le point en 3 questions



«C'est une bactérie d'origine animale, mais qui peut se retrouver dans toutes sortes de produits, précise Cécile Meex. Les animaux porteurs...

Il y a 1 mois

RTL info

Bactérie E-Coli Stec: le parquet de Bruxelles ouvre une enquête judiciaire



Société bruxelles Sciences et Santé vidéos Sujet par sujet Ecoli Stec maison de repos décès afsca alimentation nourriture viande hachée...

Il y a 4 jours

Rappel massif de fromages : ce que l'on sait des 21 personnes contaminées par la Listeria

Mercredi 13 août, Santé publique France a donné plus de détails sur les 21 cas de listériose détectés en France et qui pourrait avoir un...

Il v a 1 mois



Rappel massif de fromages pour des soupçons de contamination par la bactérie Listeria : épisode du podcast Enquêtes

Plus de 40 lots de fromages ont été retirés de la vente en France en raison d'un risque de listériose. Santé Publique France a recensé 21...

Il y a 1 mois

Le Dauphiné Libéré

Consommation. Plus de 40 fromages rappelés, un « lien possible » avec 21 cas de listériose dont deux décès

Le site Rappel Conso alerte les consommateurs sur plus de 40 lots de fromages vendus notamment par la plupart des grandes surfaces.

Il y a 1 mois

•3 France 3 Régions

21 cas possibles de listériose, dont deux décès... Plusieurs fromages de la laiterie creusoise Chavegrand rappelés pour suspicion de listéria

Plus de 40 lots de fromages ont été rappelés pour suspicion de contamination par la listeria monocytogenes, le mardi 12 août.

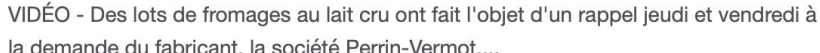
Il v a 1 mois

₩ BFMTV

21 févr. 2025

Morbier, tomme...Des fromages au lait cru rappelés à la suite de suspicions de contamination à la bactérie E. coli

la demande du fabricant, la société Perrin-Vermot....





France 3 Régions

Contaminations à la Listeria : une quinzaine de fromages rappelés par les supermarchés en France

Plusieurs fromages vendus dans la grande distribution ne doivent pas être consommés. Ils font l'objet de rappels nationaux depuis le début...

Il y a 1 mois



Le Dauphiné Libéré

Consommation. Raclette, morbier, tomme: des fromages au lait cru potentiellement contaminés par une bactérie

Des fromages des marques Jean Perrin et Nos régions ont du talent sont potentiellement contaminés par la bactérie Escherichia coli et...

19 févr. 2025



Radio SCOOP

Du fromage à raclette rappelé dans toute la France

Plusieurs fromages au lait cru (raclette, morbier, tomme) sont rappelés en raison d'un risque de contamination à E. coli, une bactérie...

19 févr. 2025



•3 France 3 Régions

La bactérie Listeria retrouvée dans des fromages de Cîteaux, la vente suspendue : "c'est un très gros préjudice"

C'est au cours d'auto-tests pratiqués sur leur production de fromages que les moines de Cîteaux ont stoppé la fabrication.

12 mai 2025



Le Figaro

E. coli : deux fillettes contaminées par la bactérie, l'une d'elles frôle la mort

Élise, 7 ans, est hospitalisée à Lyon depuis décembre dernier pour une contamination par la bactérie E. coli, présente dans du fromage.















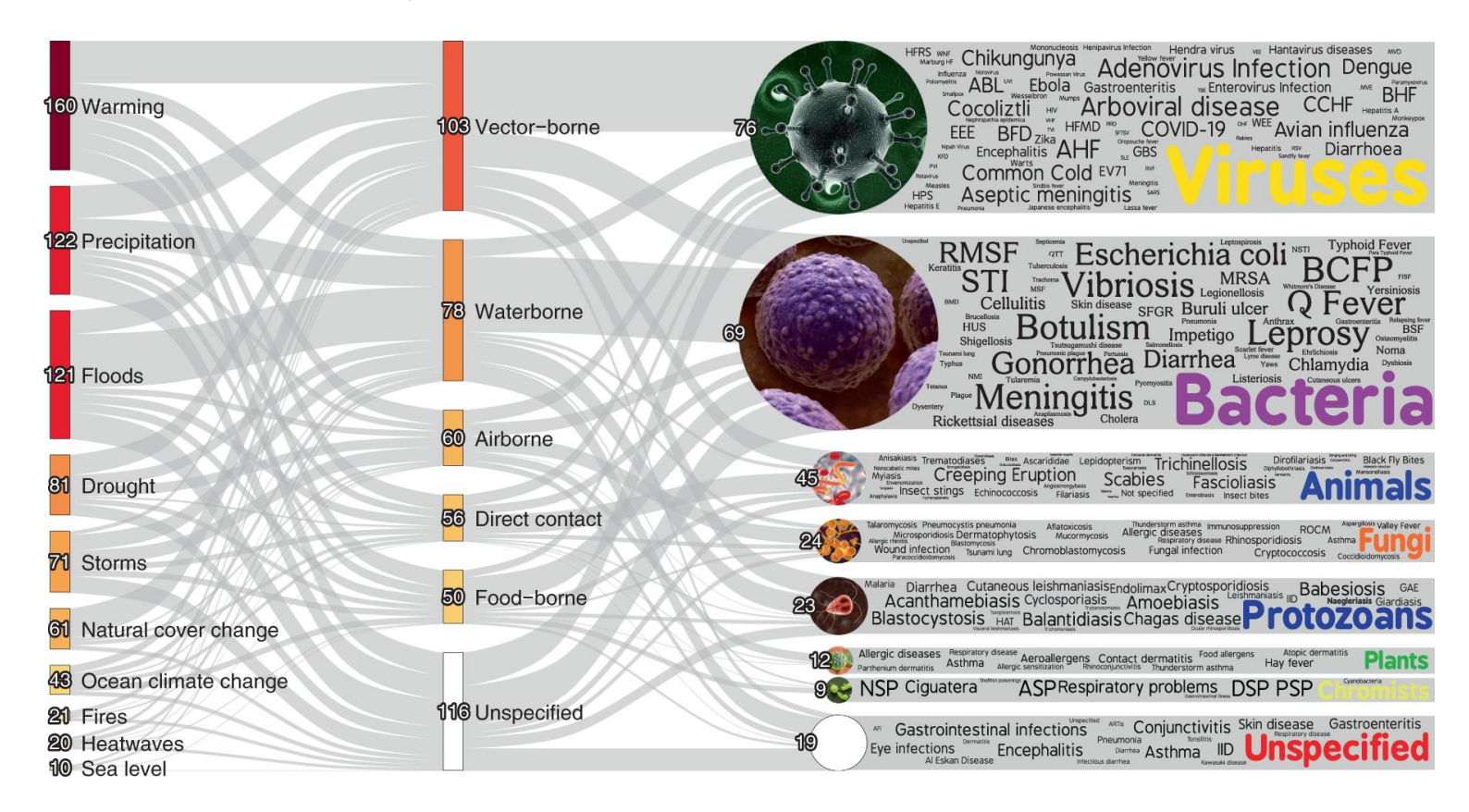
Over half of known human pathogenic diseases can be aggravated by climate change

Camilo Mora ☑, Tristan McKenzie, Isabella M. Gaw, Jacqueline M. Dean, Hannah von Hammerstein,

Tabatha A. Knudson, Renee O. Setter, Charlotte Z. Smith, Kira M. Webster, Jonathan A. Patz & Erik C.

Franklin

Nature Climate Change 12, 869–875 (2022) | Cite this article



Traditional methods for bacterial detection



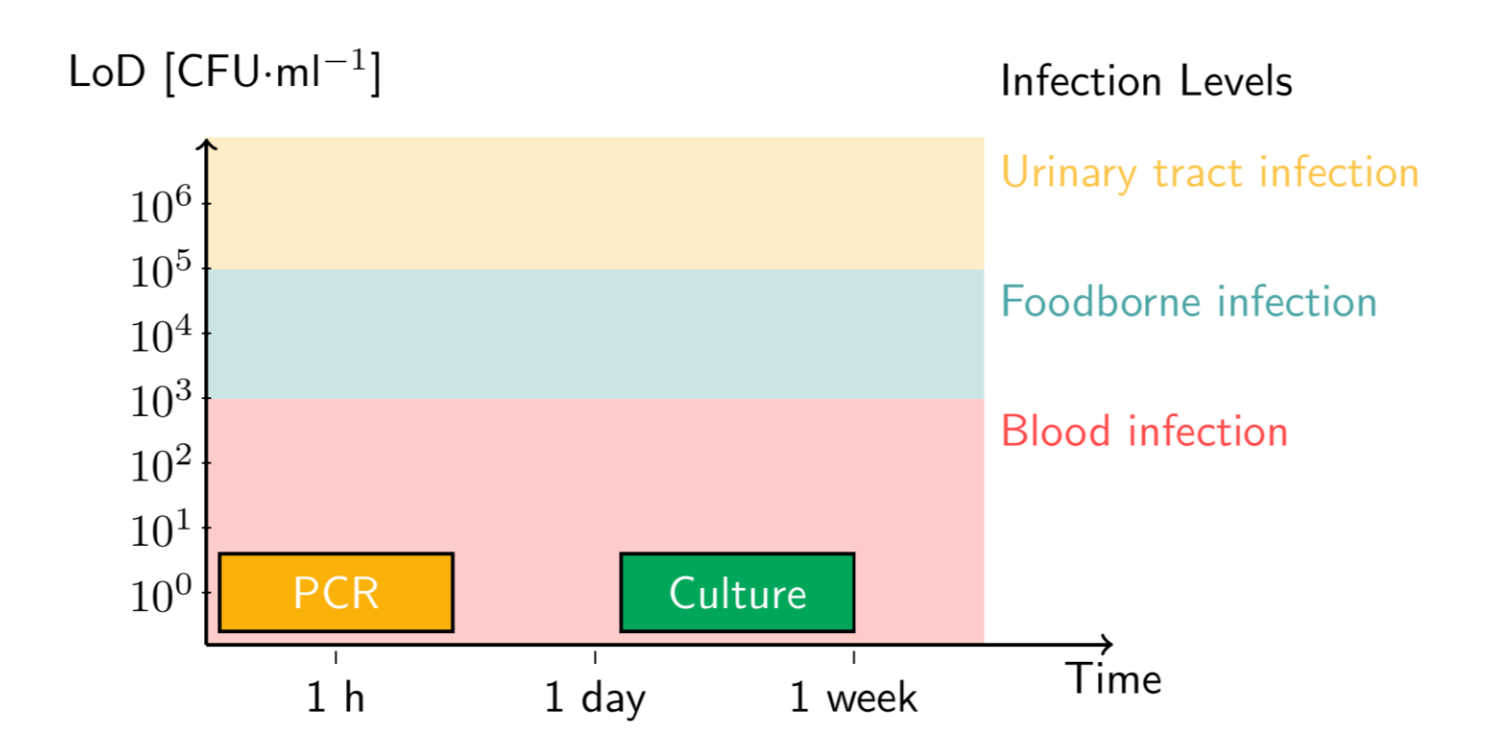
- ✓ Cost-effective
- ✓ Specific
- ✓ Sensitive (1 CFU*/mL)
- Time-consuming (>12h)
- × Prone to errors



- ✓ Fast (>2h)
- ✓ Specific
- ✓ Sensitive (1-10 CFU*/mL)
- Expensive



- ✓ Fast (>1h)
- ✓ Specific
- ✓ Sensitive (1 CFU*/mL)
- Expensive
- High-end instrumentation
- Prior knowledge of suspected pathogen



Assay time
Sensitivity
Selectivity
Reliability/Robustness
Complex sample
Versatility
Cost
Portability

PSI MEMBRANES

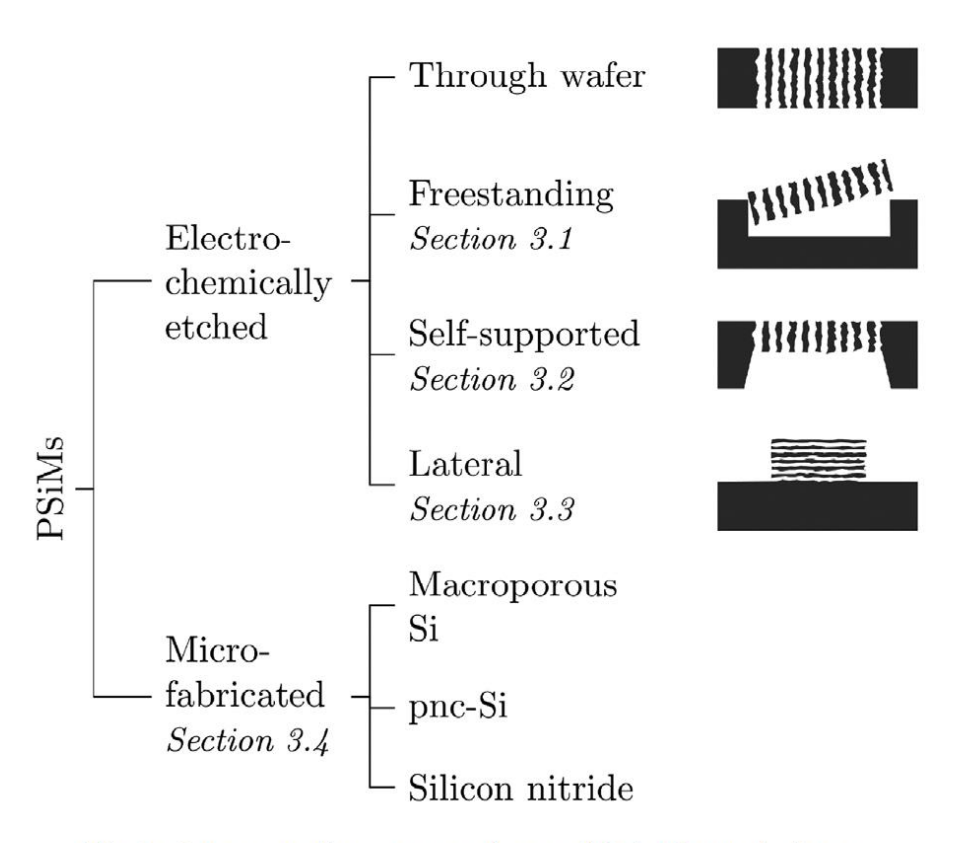


Fig. 2. Summary of porous membranes fabrication techniques.

R. Vercauteren; G. Scheen; J.-P. Raskin; L. A. Francis; Porous silicon membranes and their applications: Recent advances, *Sens. Actuator A-Phys.* **2021**, 318, 112486,

 Table 1

 Recent advances in the applications fields of porous silicon membranes (Note: C, F, FT, L, M, S stand for, respectively, Commercial, Freestanding, Full Thickness, Lateral, Microfabricated and Self-supported.)

Application field	Membrane characteristics	Membrane thickness	Detailed application	Ref.
Microfluidics	M, mesoporous	15 nm	Size and charge selective filtration	[150]
Medical	S, mesoporous	5 μm	Filtration of small biological molecules from mixtures	[81]
	L, mesoporous	$10-20\mu m$	Size and charge selective filtration	[99,151,152,100,153
	S, macroporous	215 μm	Electro-osmotic pump	[90]
	F, macroporous	4.29 μm	Drug delivery patch and optical monitoring of drug release	[7]
	M, macroporous	50-60 nm	Culture of human umbilical vein vascular endothelial cells	[8]
	M, macroporous	500 nm 75 nm	Reconstruction of the intestinal barrier of a trout via cell culture	[9]
	M, mesoporous	75 nm 30 μm	Small-format hemodialysis with high toxin elimination capabilities	[10]
	M, macroporous F, mesoporous	30 μm 276 μm	Transmigration assay for cancer cells Scaffold for the culture of oral mucosal epithelial cells	[11] [12]
	C, macroporous	276 μm 1 – 10 μm	Support for the investigation of pore-spanning lipid membranes	[154–160]
	M, mesoporous	30 nm	Cell culture of endothelial cells	[13]
	F, macroporous	12 – 15 μm	Tissue scaffold integrated with cell-laden hydrogel biomaterials	[14]
	M, macroporous	5 μm	Lung-on-chip microfluidic device	[15,161]
	M, macroporous	10 μm	Culture of intestinal epithelial cells	[16]
	S, macroporous	130 – 150 μm	Mechanical cell lysis and DNA isolation	[17,88]
	F, mesoporous	$4-5 \mu m$	Implantable scaffold for cell culture	[18]
Energy conversion	S, macroporous	~50 µm	Electrophysical NO2-gas detector	[85]
	F, mesoporous	1.7 μm	Silver-modified sensor for SERS-based detection of miRNA	[59]
	L, mesoporous	10 μm	Interferometric transducer for solvent detection	[153]
	F, mesoporous	1.6 μm	Optical detection of ethanol vapour	[138]
	S, mesoporous	2.5 μm	Impedance spectroscopy of the formation of a lipid membrane	[94,95]
	F, mesoporous	29 μm	Electrostatic isopropanol vapour sensor	[20]
	F, mesomacroporous	5.5 μm	Optical detection of Bovine Serum Albumin	[21]
	F, mesoporous	$17 - 21 \mu m$	Optical detection of dissolved gas concentrations in liquids	[137]
	M, mesoporous	50 nm	Nanopore-based sensing of DNA translocation	[110]
	S, mesoporous	20 μm	Multi-assay solvent vapour optical detection	[162]
	F, mesoporous	870 nm	Multianalyte detection using silver-decorated sensors	[67,68]
	M, mesoporous	15 nm	Optical detection of Bovine Serum Albumin permeation	[22]
	F, mesomacroporous	4.5 μm	Electrochemical detection of MS2 bacteriophage	[71]
	F, mesomacroporous	4.5 μm	Label-free electrochemical detection of bacterial toxin	[163]
	M, mesomacroporous	50 nm	Electrochemical detection of ion-transfer across the PSiM	[113] [164]
	C, macroporous S, mesoporous	475 μm 340 nm	3D liquid core sensor array DNA translocation detection	[96,97]
	M, macroporous	50 μm	Immunoassay for specific leukocyte subsets	[103]
	S, macroporous	1 – 3 μm	Transmembranes proteins sensing	[87]
	C, mesomacroporous	10-15 nm	DNA translocation detection	[165–167]
	F, mesoporous	19.9 μm	Optical aptasensors with multiple target-binding sites	[23]
	S, mesoporous	4 – 15 μm	Optical detection of enzyme adsorption and streptadivin binding	[19,79,168]
	F, micro/macroporous	10 – 30 μm	Wide-gap absorber for solar cells	[66,64]
	S, mesoporous	~70 µm	Implantable glucose biofuel cell	[89]
	S, mesoporous	5 – 20 μm	Ion-exchange membrane for micro fuel cells	[27]
	S, mesoporous	50 μm	Anion exchange membrane for Glucose/O2 micro fuel cell	[28]
	S, macroporous	125 μm	Membrane-electrode assembly for H ₂ /air-fed micro fuel cells	[29]
	S, macroporous	230 μm	Microfluidic electric generator	[91]
	S, mesoporous	13 μm	Monolithic Si electrode for micro fuel cells	[30,98]
	F, macroporous	50 μm	Anode for lithium-ion batteries	[63,60,65]
	F, mesoporous	200 μm	Anode for lithium-ion batteries	[31]
	M, macroporous	5 μm	Electrode grids for micro fuel cells	[32]
	S, micro/macroporous	210 μm	High-conductivity electrodes for micro fuel cells	[33]
	M, macroporous	280 μm	Ion-exchange membrane for photoelectrochemical cell	[34]
	S, macroporous	50 μm	Electrode for methanol micro fuel cell	[35]
	S, macroporous	60 μm 500 μm	Cathode for self-breathing microfuel cells Mambrane electrode assembly for hydrogen/oxygen micro fuel cells	[36]
	FT, meso/macroporous S, mesoporous	500 μm 100 μm	Membrane-electrode assembly for hydrogen/oxygen micro fuel cells Proton exchange membrane for methanol micro fuel cells	[57,37] [83,84]
Electronics	S, mesoporous S, meso/macroporous	100 μm 80 – 100 μm	Pervaporation membrane for methanol vapour-fed micro fuel cells	[83,84] [80]
	F, mesoporous	80 – 100 μπ 46 μm	RF insulating and supporting substrate for microfabricated inductors	[61]
	S, mesoporous	46 μm 10 μm	MEMS-based superheated loop heat pipes	[24]
	M, macroporous	600 nm	Thermal management device	[25]
	S, mesoporous	300 μm	Thermal isolation layer for high temperature micro-hotplates	[26]
	F, macroporous	2.46 μm	Flexible optoelectronics device	[72]
	F, mesoporous	1.92 μm	Modulator for photodetector	[74,75]
	FT, mesoporous	380 μm	CMOS compatible RF insulating substrate	[58]

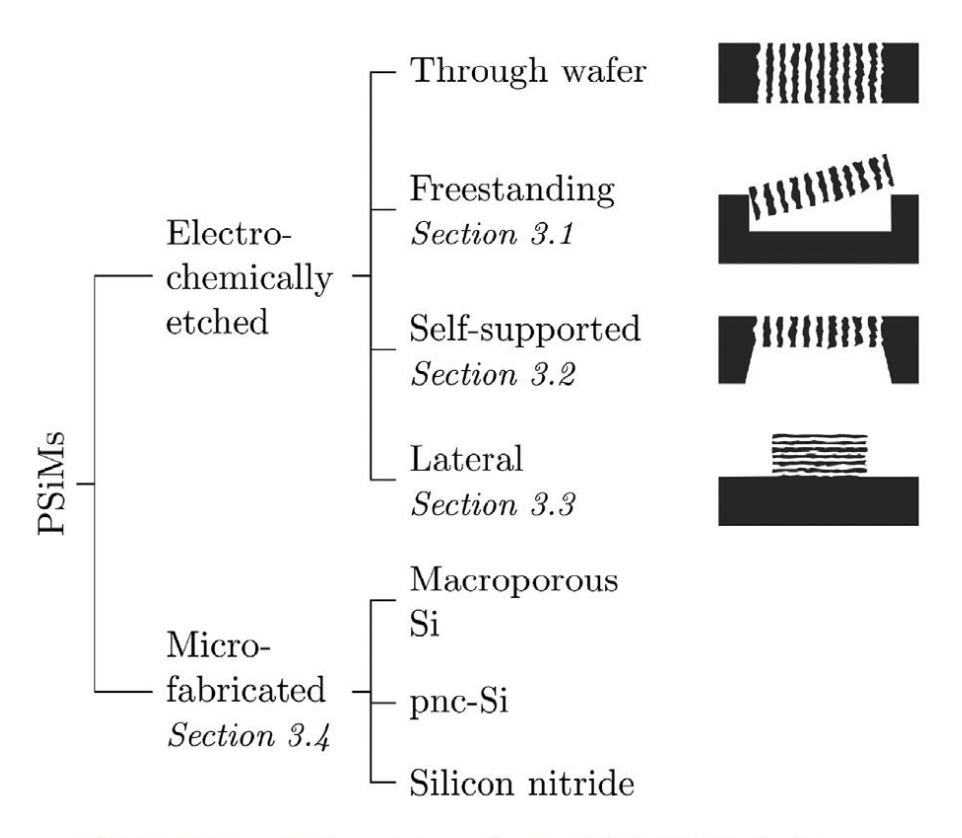


Fig. 2. Summary of porous membranes fabrication techniques.

R. Vercauteren; G. Scheen; J.-P. Raskin; L. A. Francis; Porous silicon membranes and their applications: Recent advances, *Sens. Actuator A-Phys.* **2021**, 318, 112486,

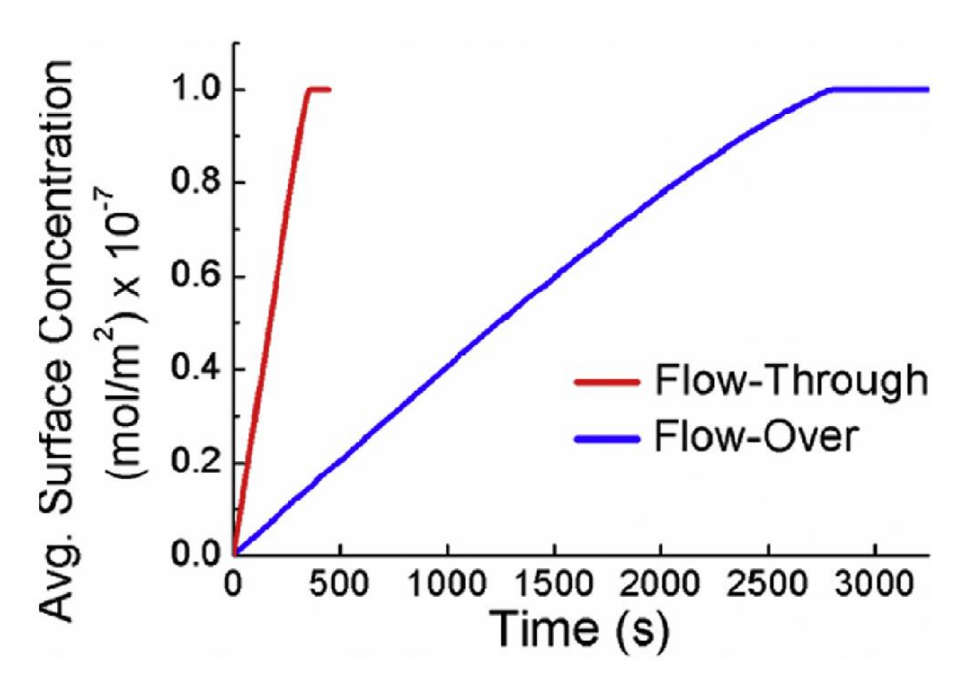


Fig. 11. Simulated average surface concentration of analyte with the same diffusivity, captured by close- and open-ended PSi sensors as a function of time; reprinted from [19], Copyright (2016), with permission from American Chemical Society.

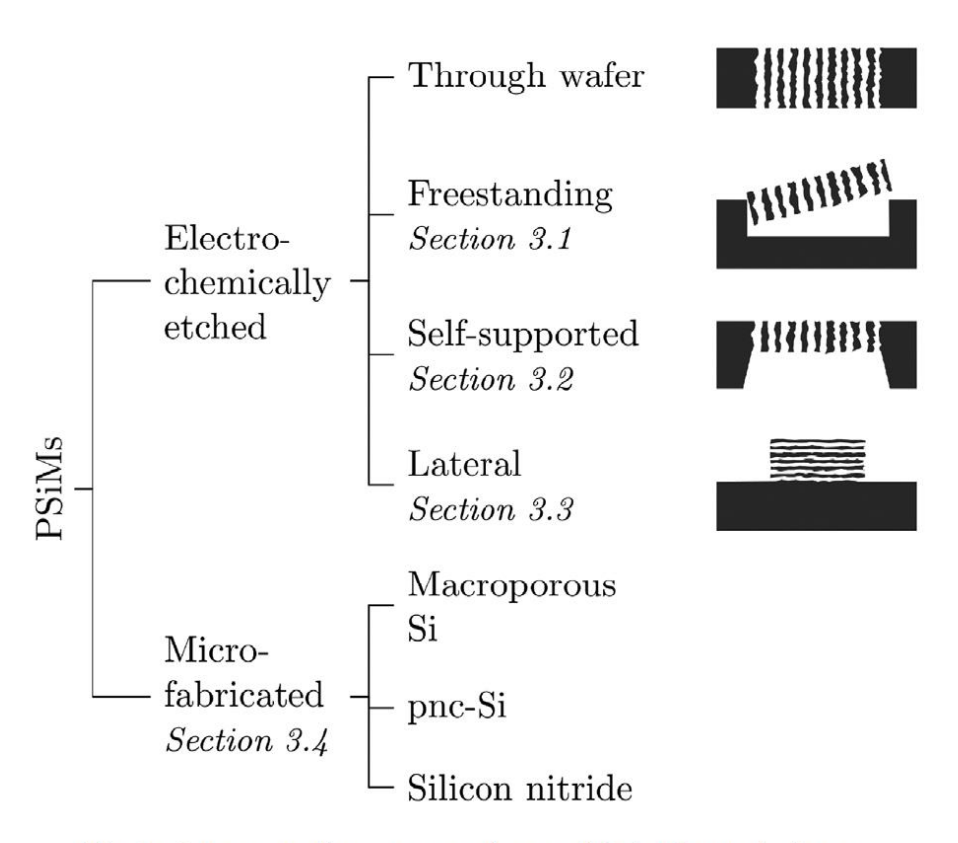
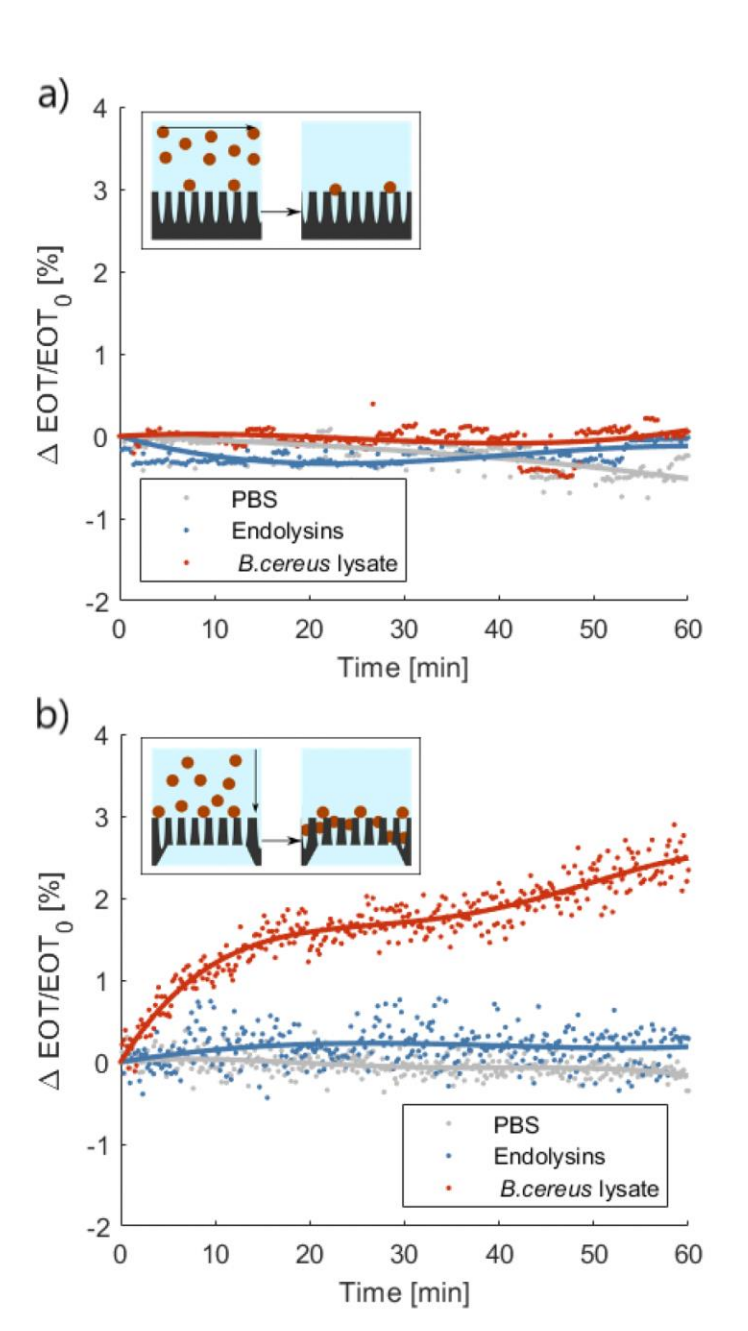
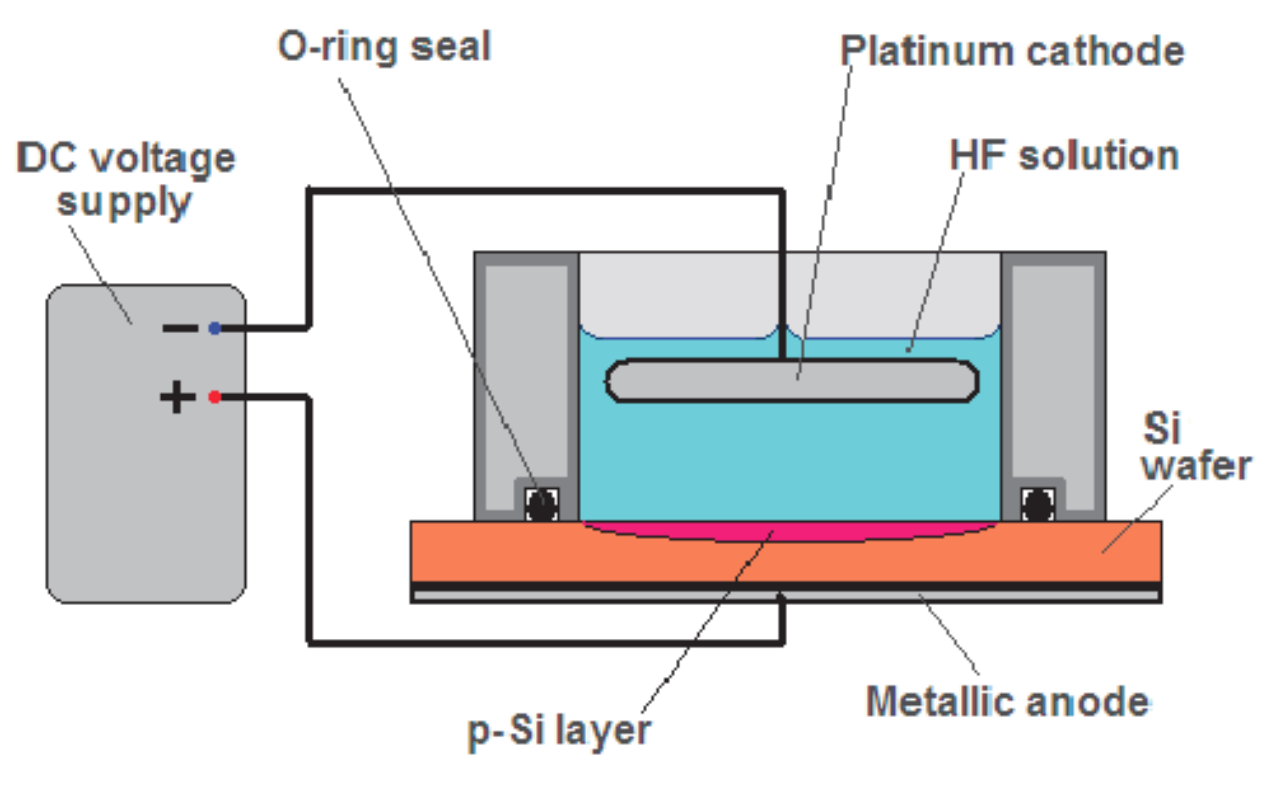


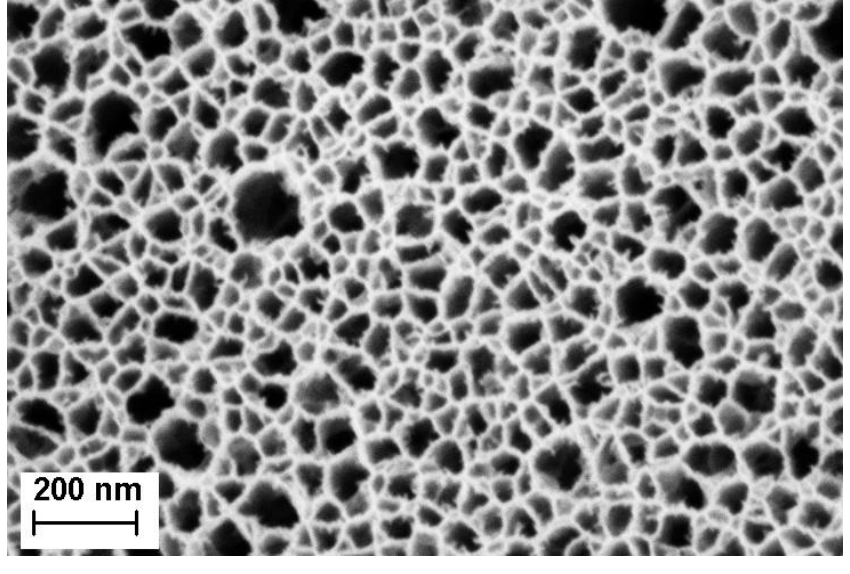
Fig. 2. Summary of porous membranes fabrication techniques.

R. Vercauteren; G. Scheen; J.-P. Raskin; L. A. Francis; Porous silicon membranes and their applications: Recent advances, *Sens. Actuator A-Phys.* **2021**, 318, 112486,



Electrochemical etching





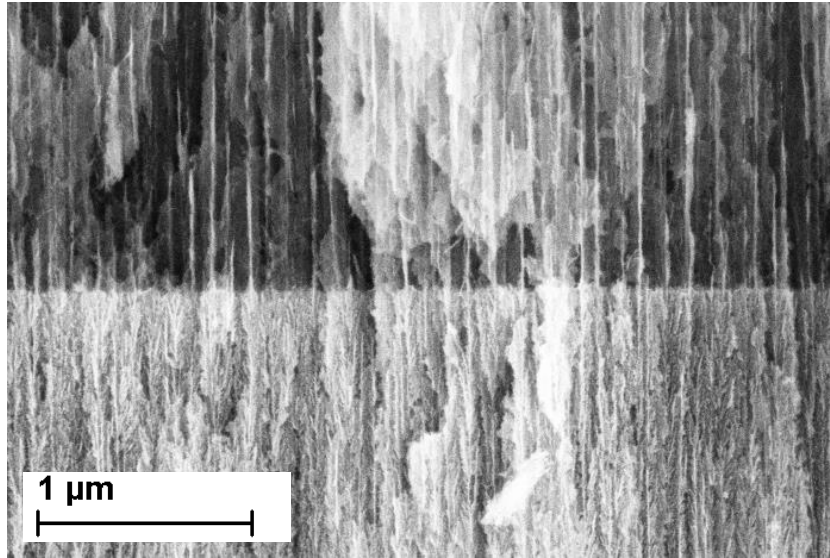
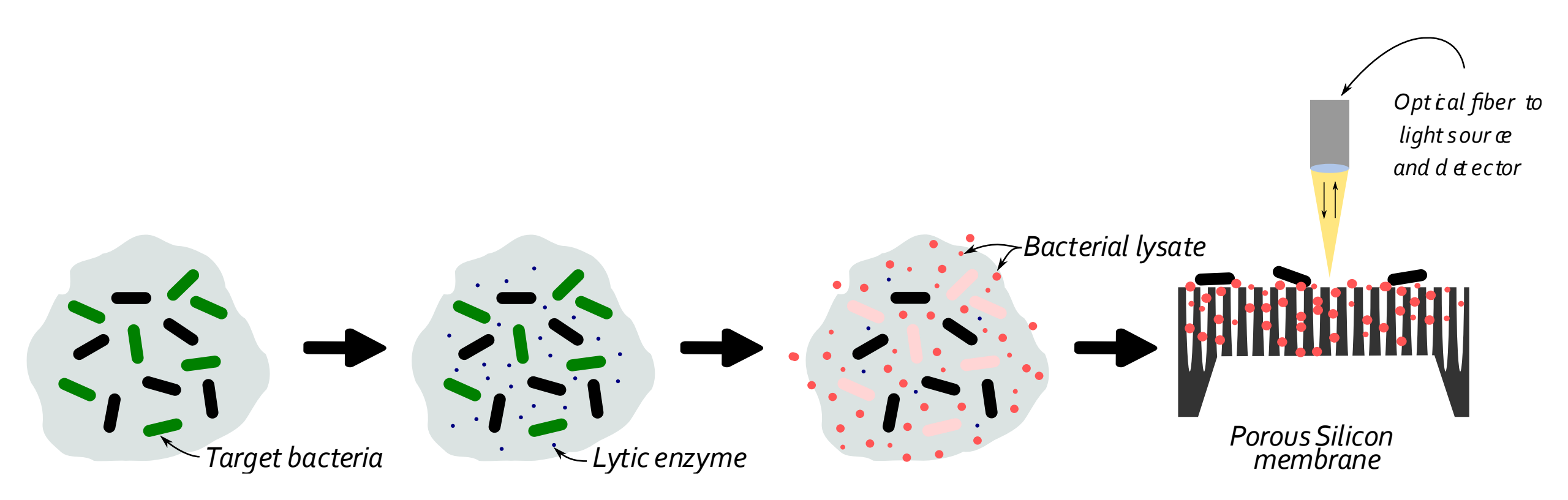
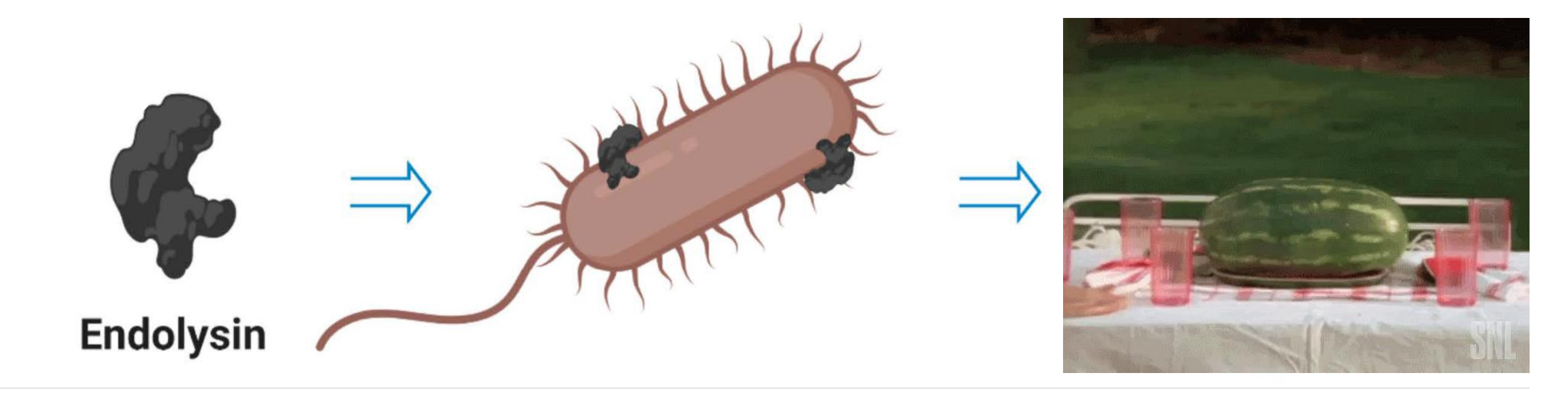
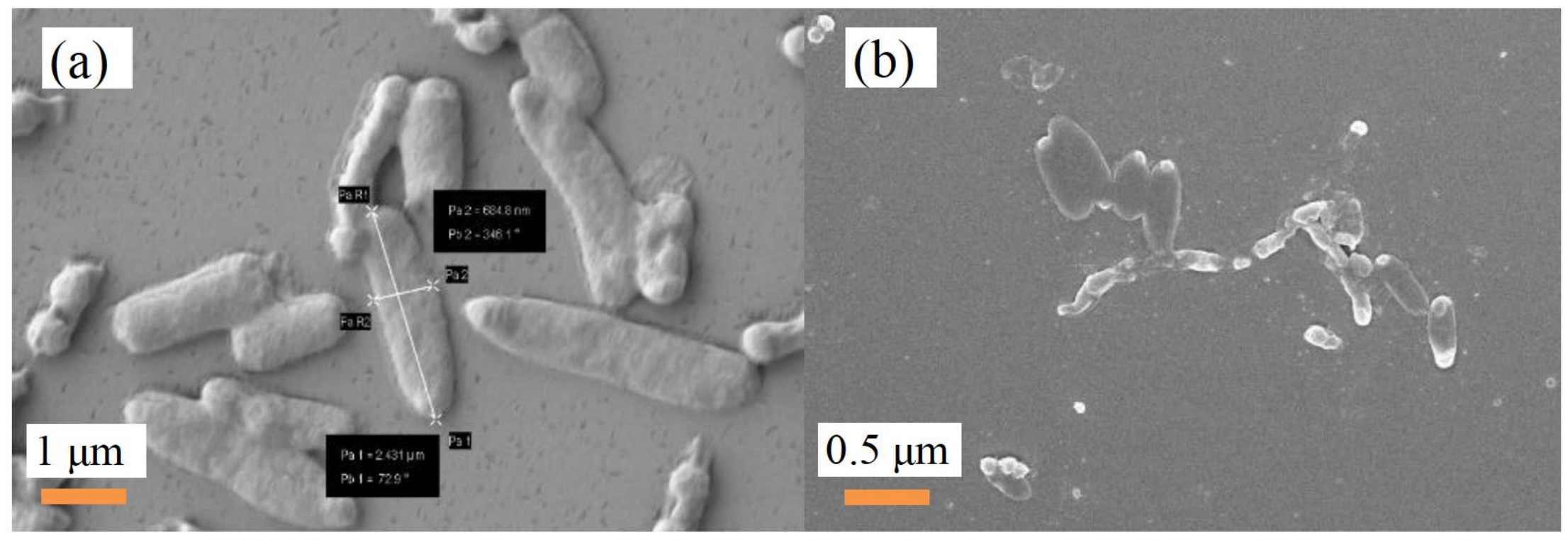


Image from de la Mora, Bety & Lugo, Eduardo. (2013). Porous Silicon Biosensors. 10.5772/52975.



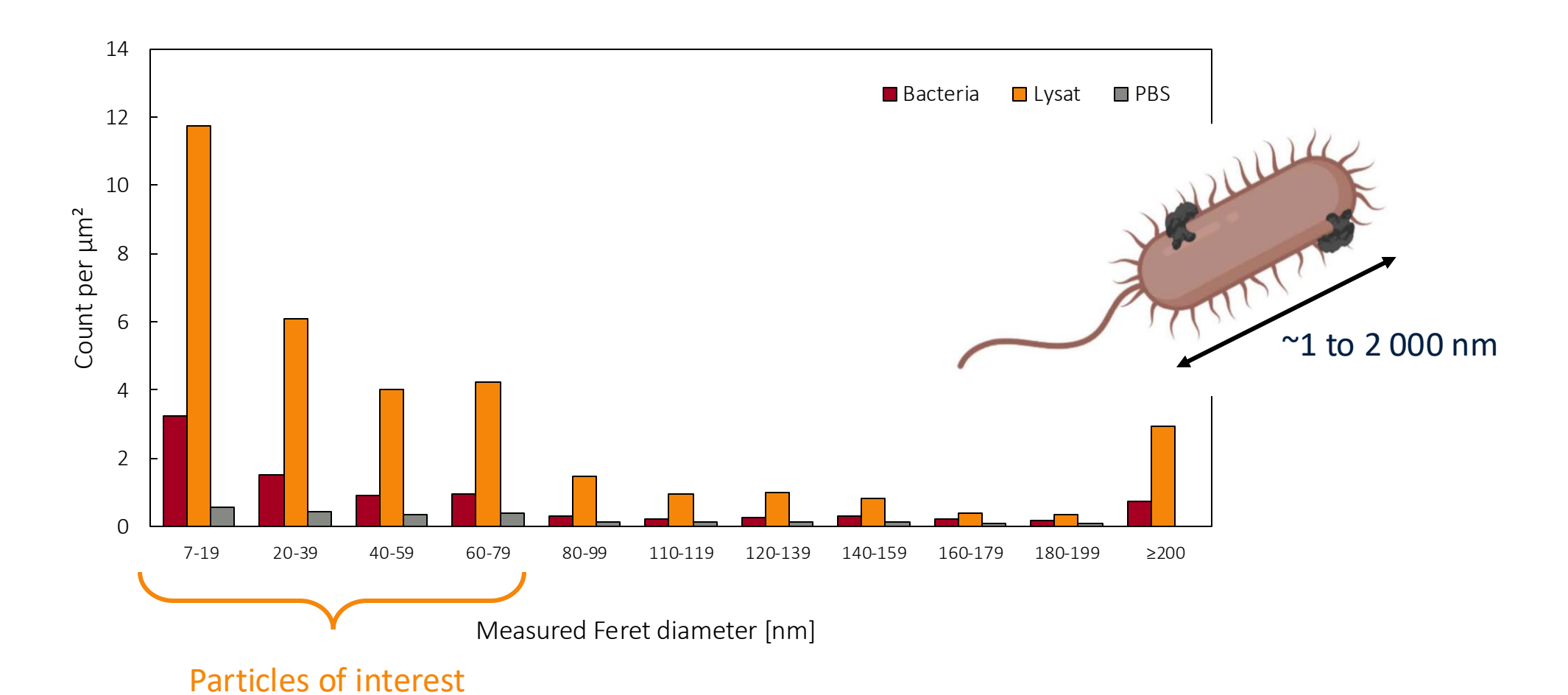


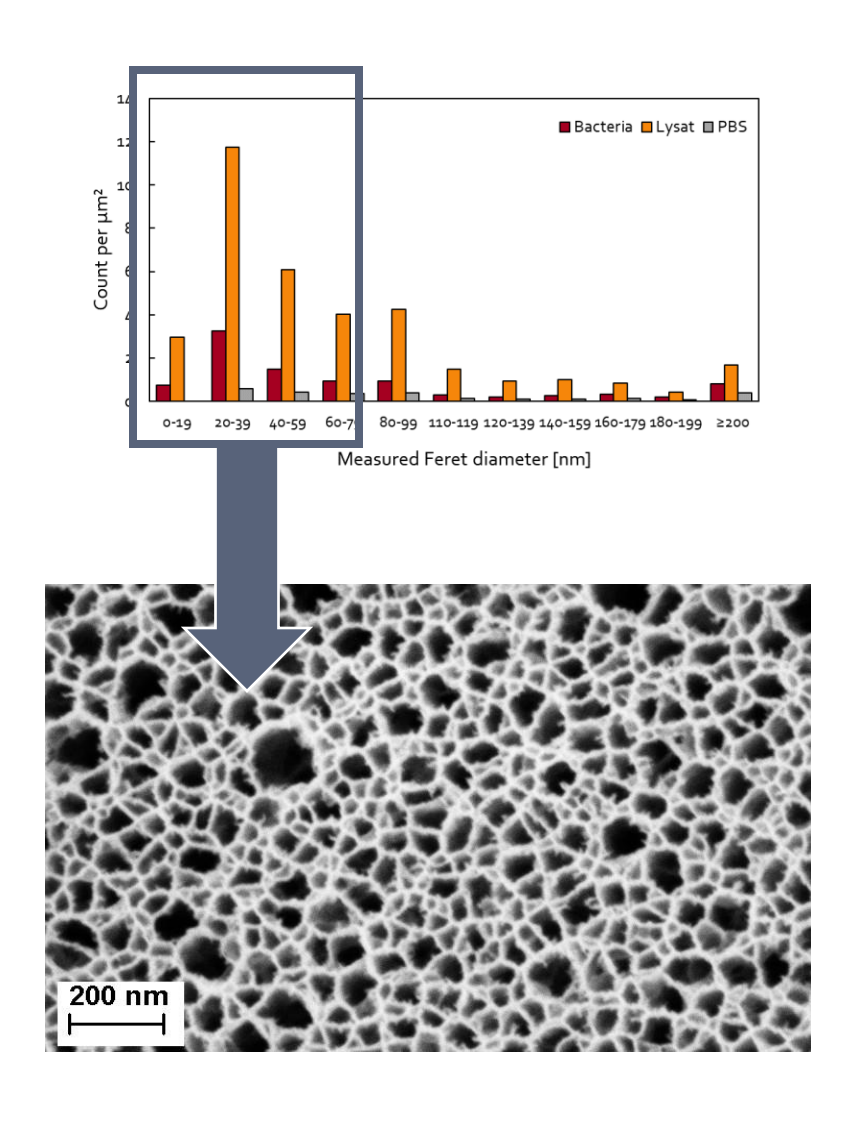
Lytic enzymes can be produced by bacteria or bacteriophage



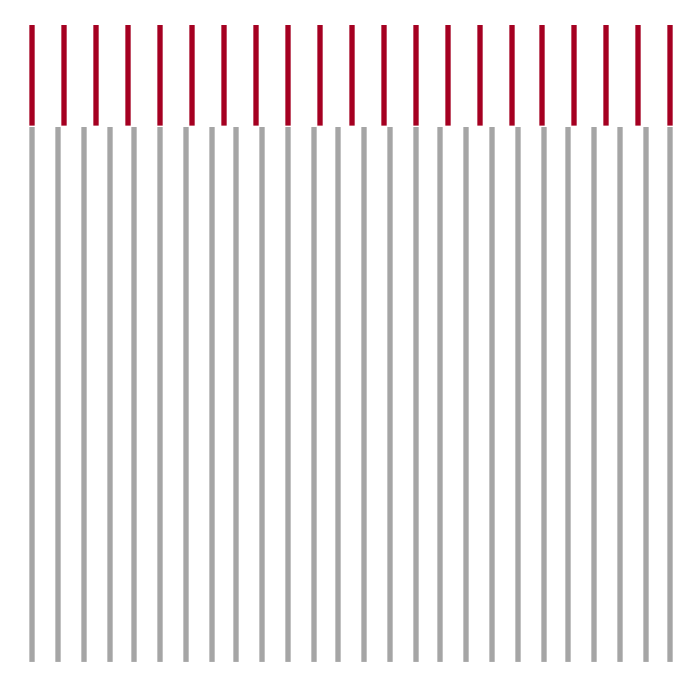
SEM observations of (a) *E. coli* bacteria and (b) *E. coli* lysate (through phage lysis).

Model: *Bacillus cereus* (ATCC10987)



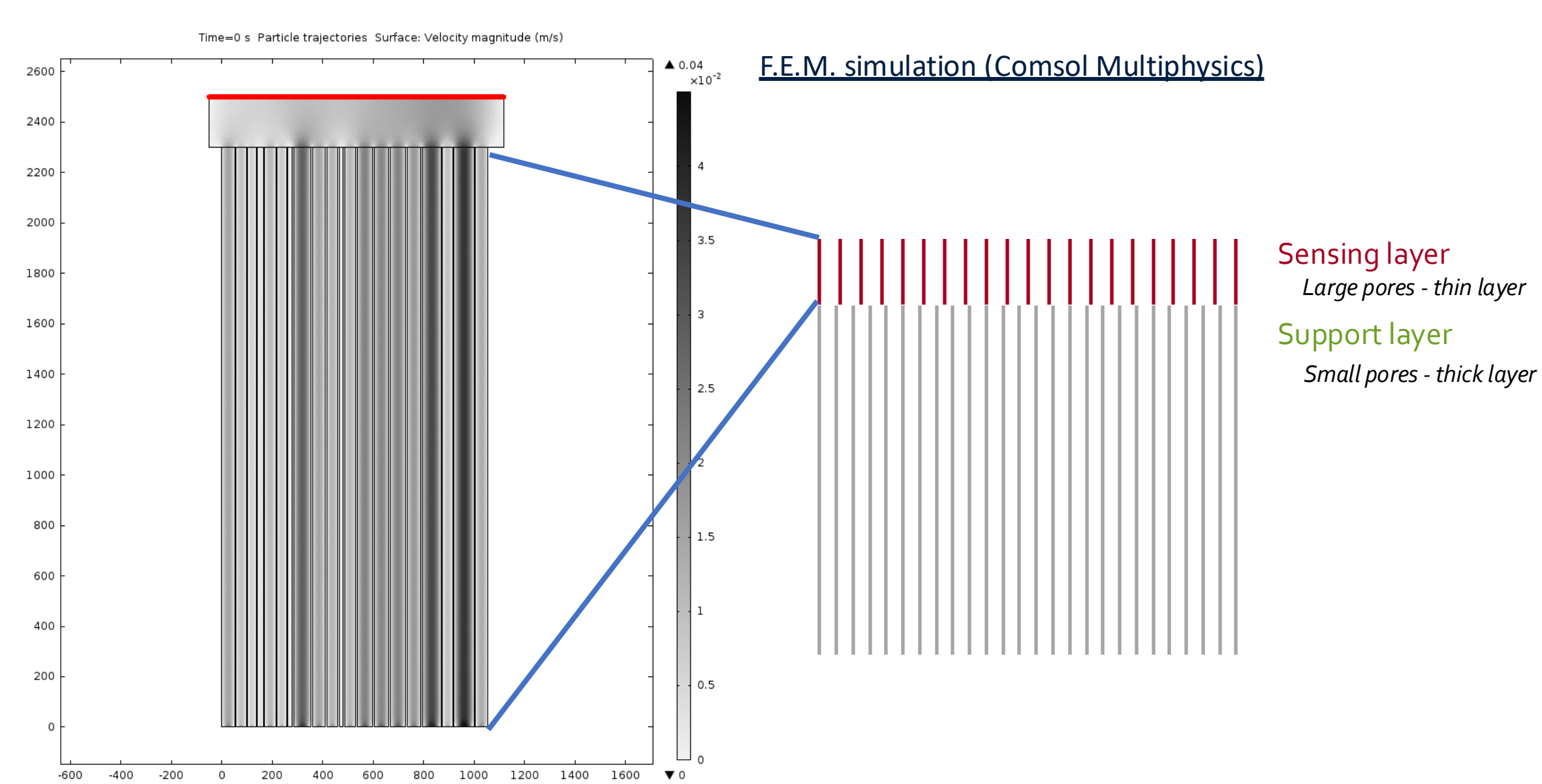


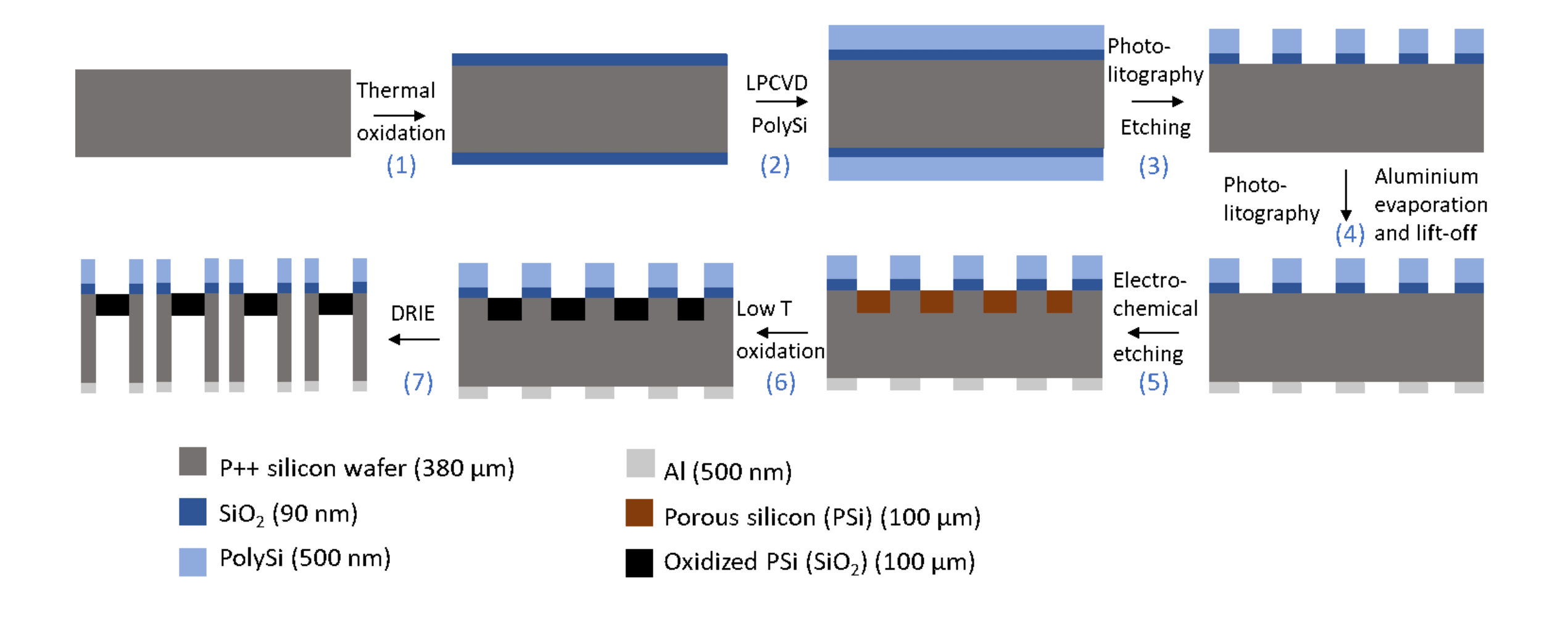
Porous silicon **interferometer**



Sensing layer Large pores - thin layer

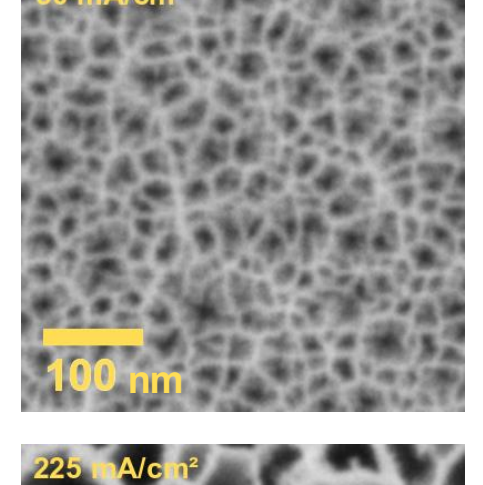
Support layer
Small pores - thick layer

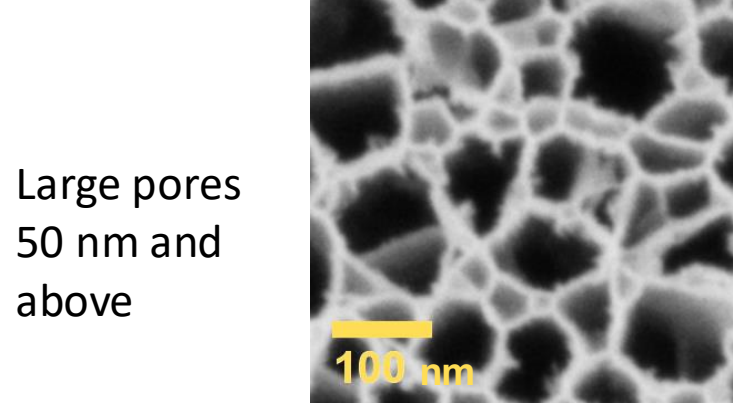


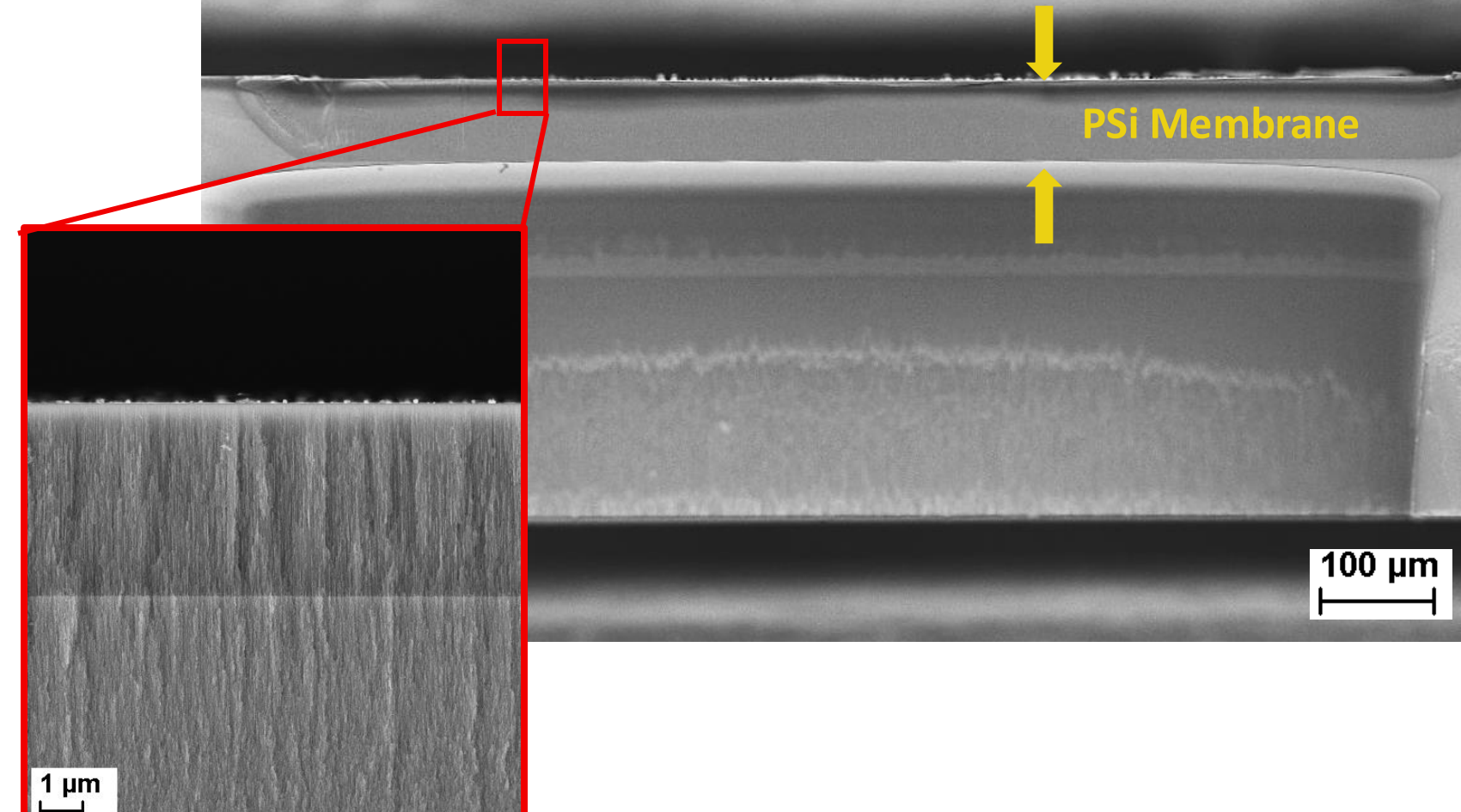


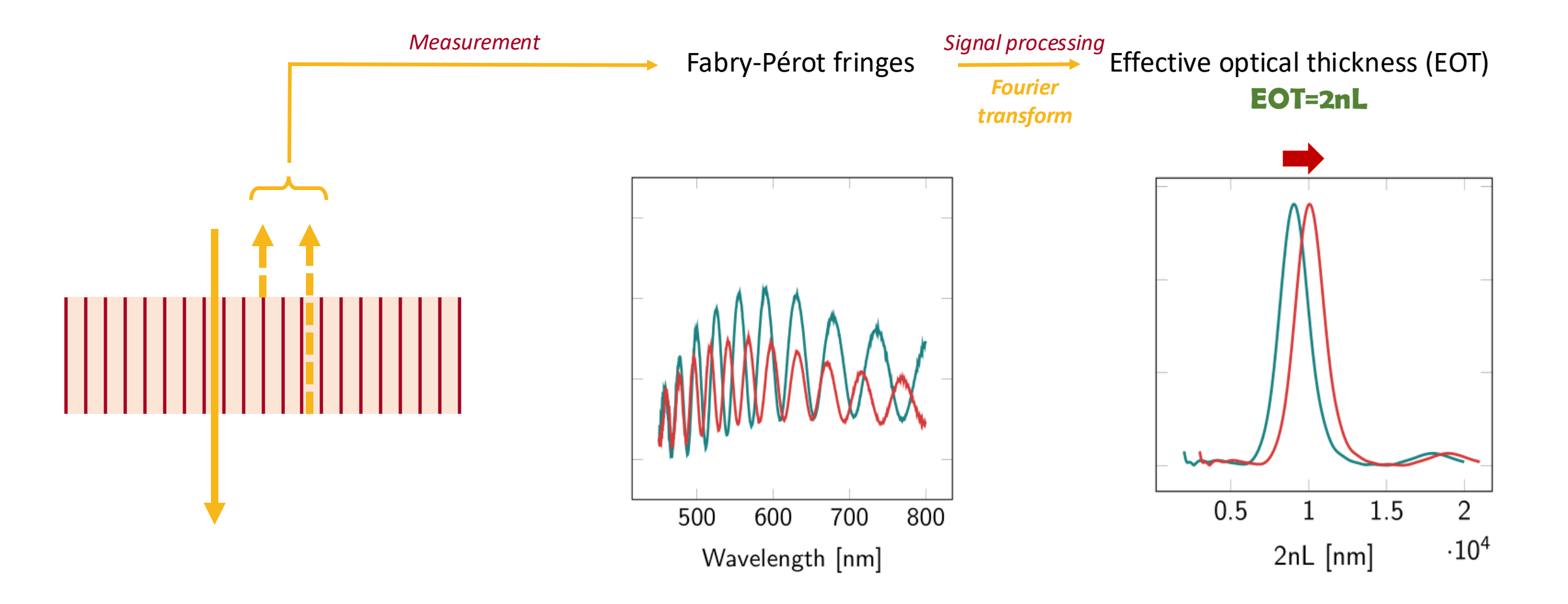
Filtration membrane/sieve

Small pores ~15 nm

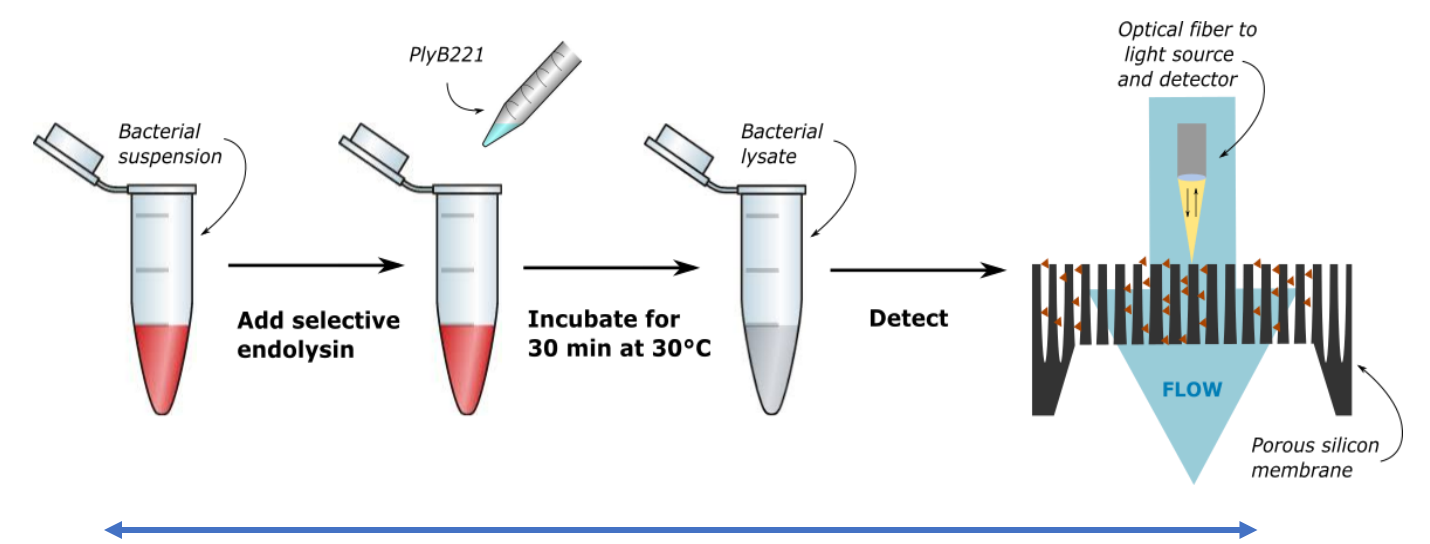




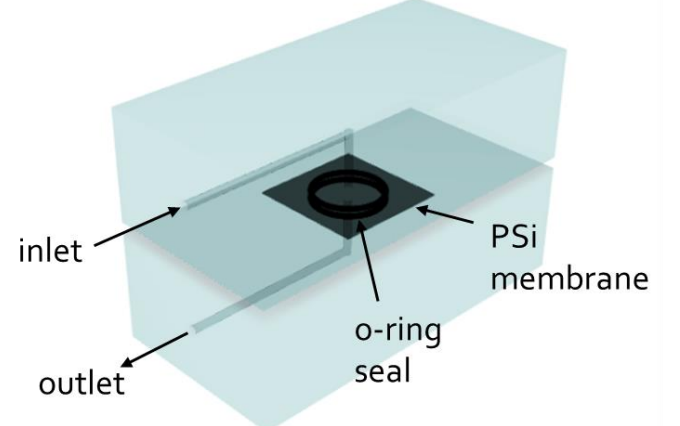


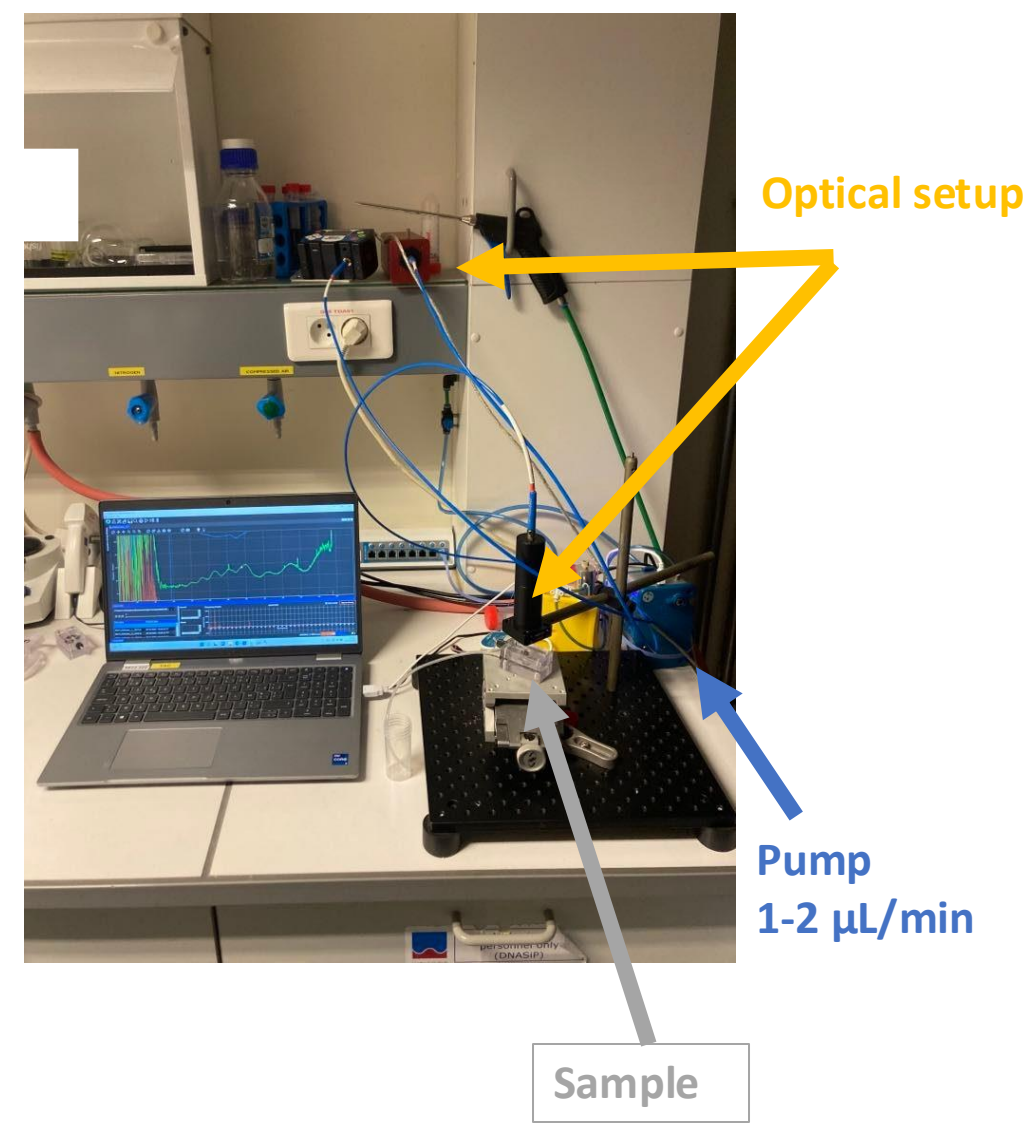


The detection of *Bacillus cereus* lysed by PlyB221 endolysins



1h30 max

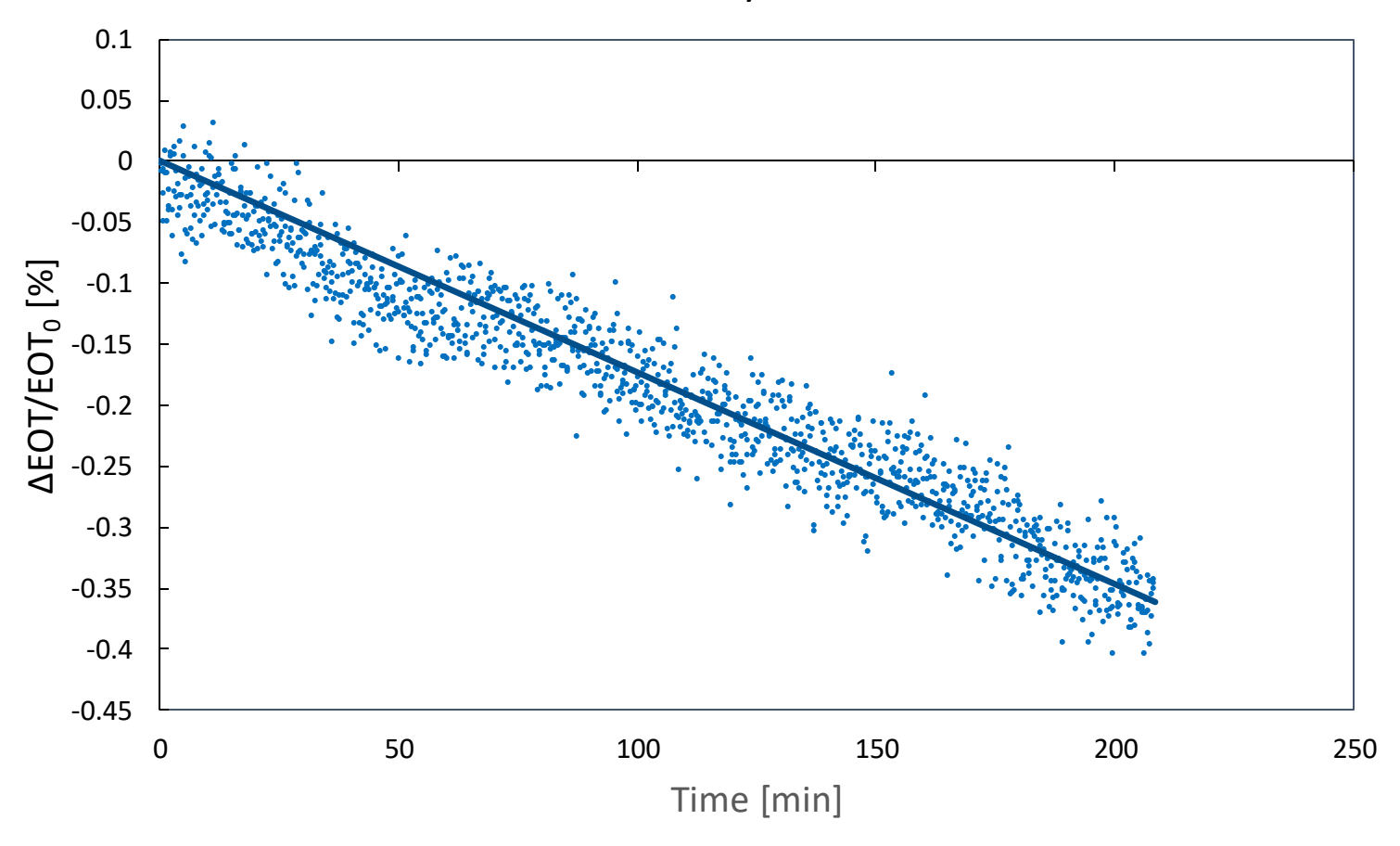


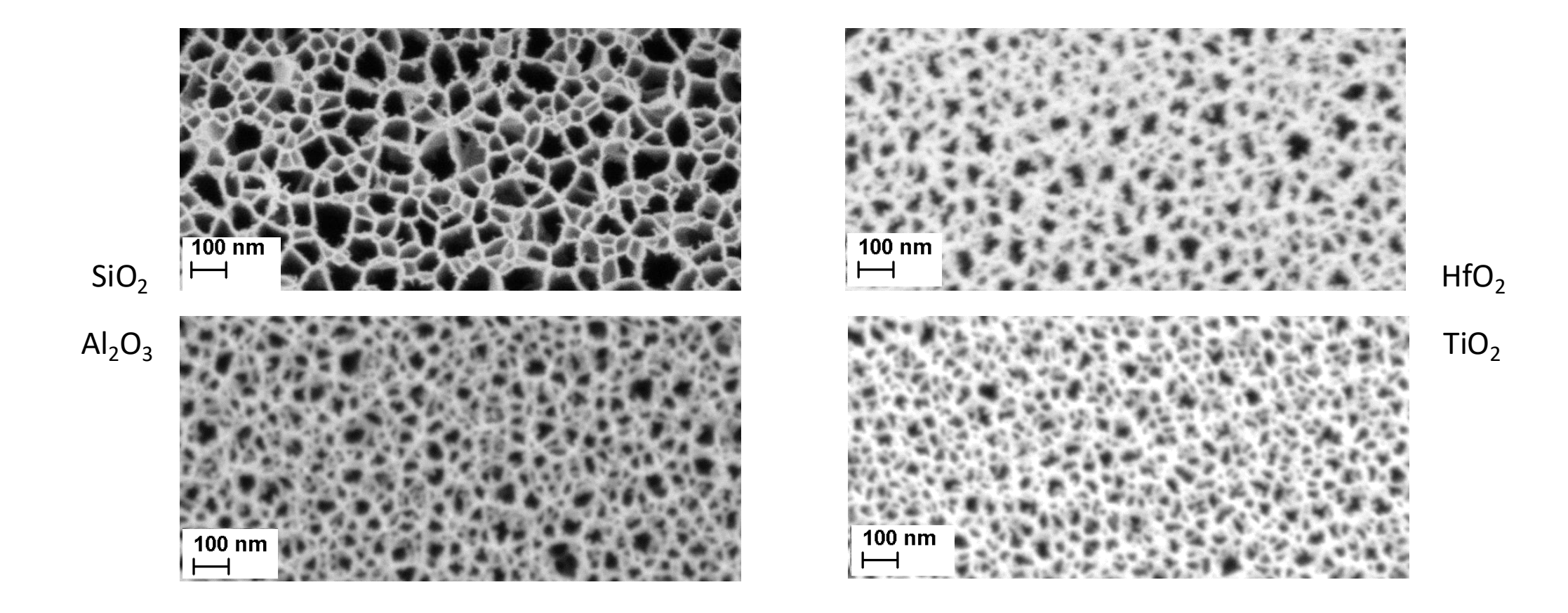


inlet PSi membrane o-ring seal

C. Whyte Ferreira, UCLouvain, 2021

RIFTS Stability in PBS

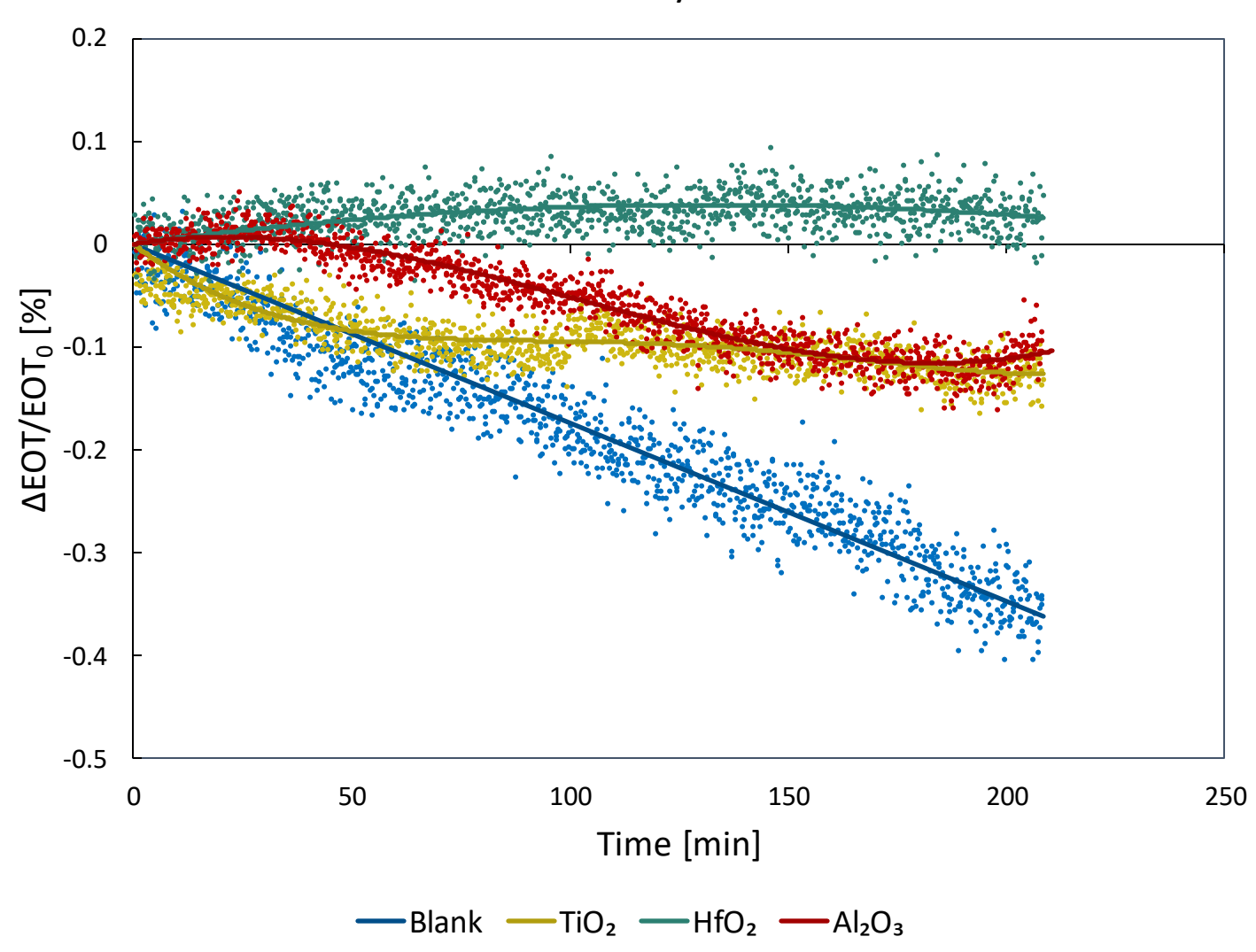




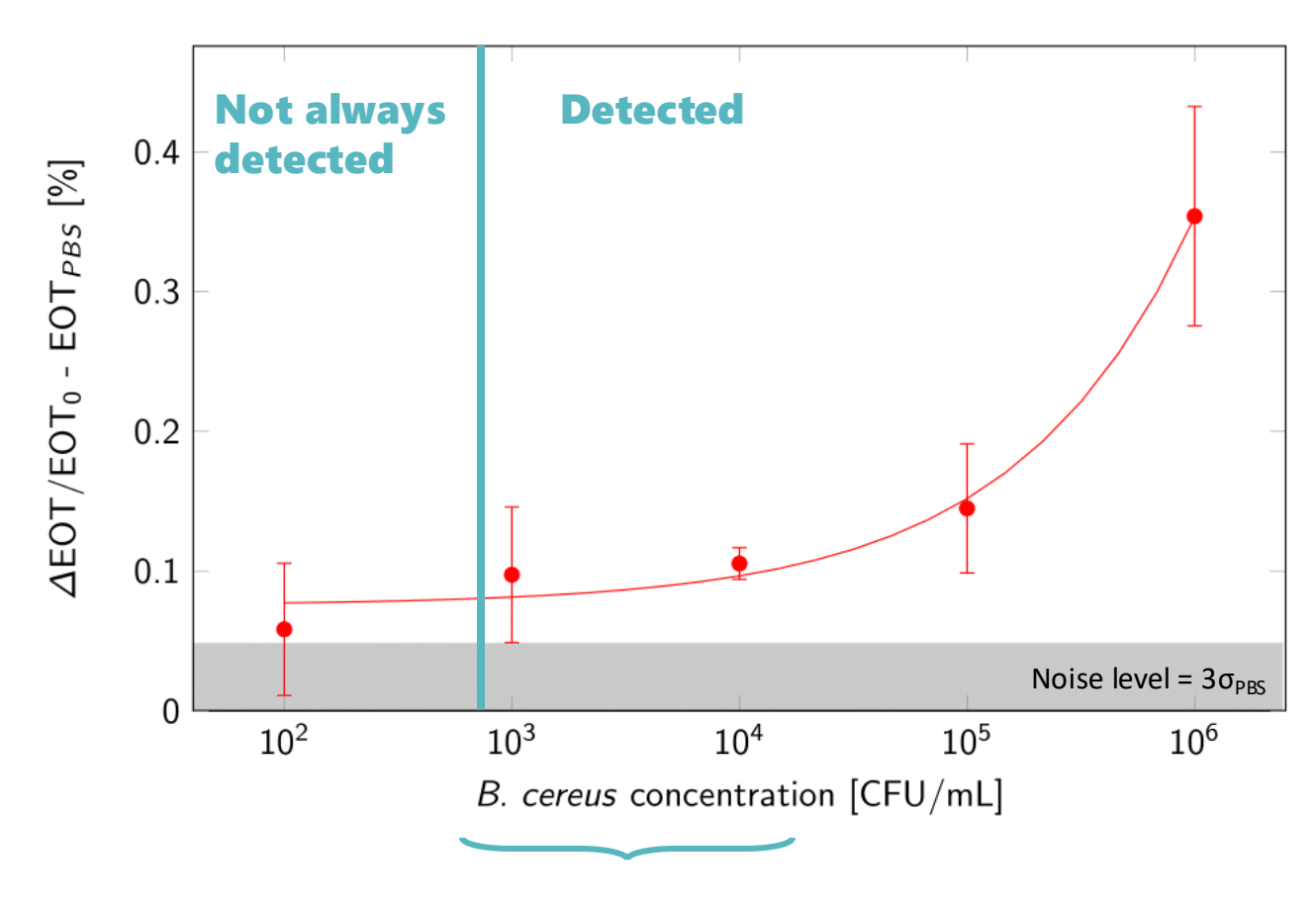
inlet PSi membrane o-ring seal

C. Whyte Ferreira, UCLouvain, 2021

RIFTS Stability in PBS



Sensitivity

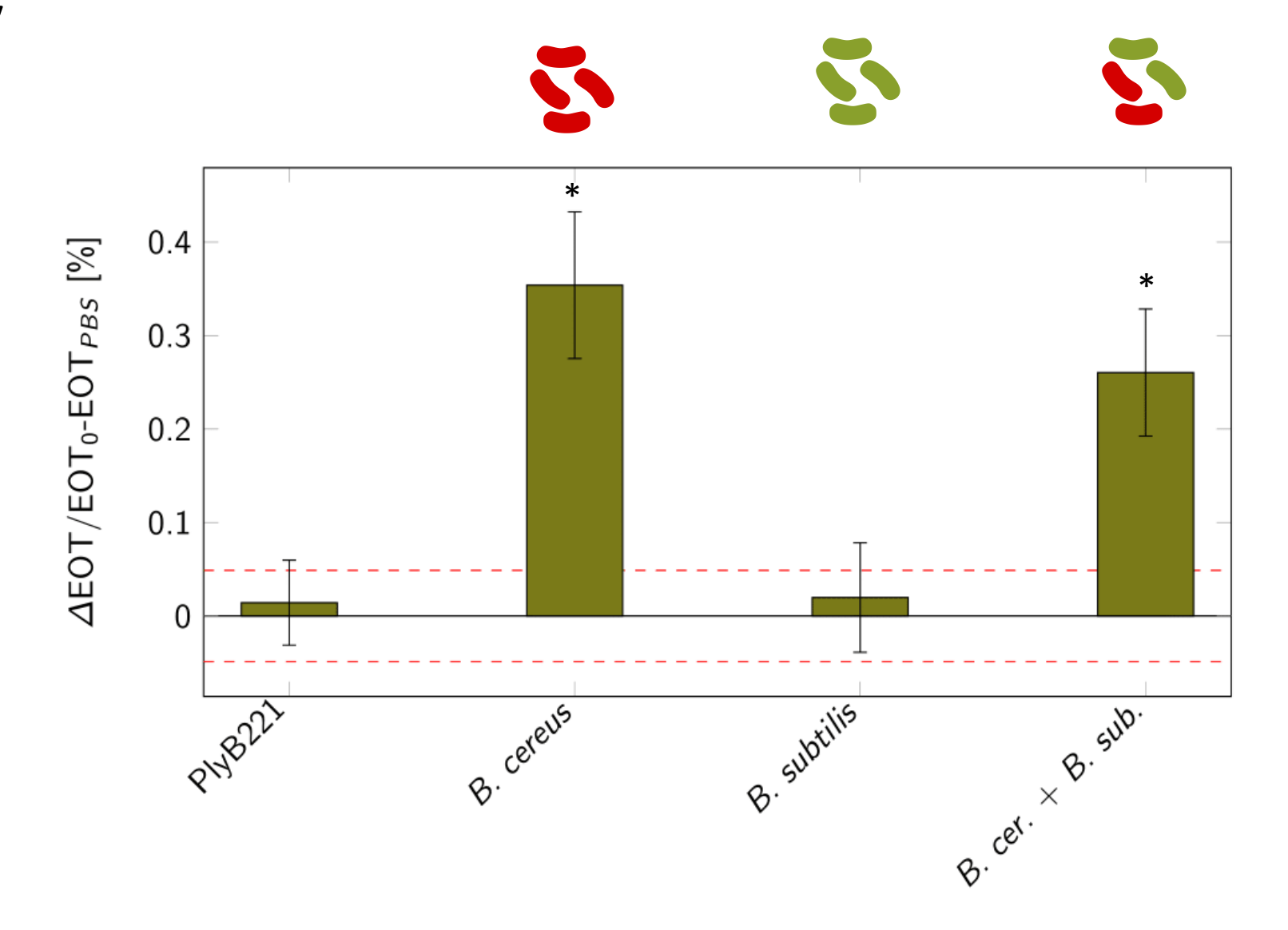


Infection levels for foodborne infection

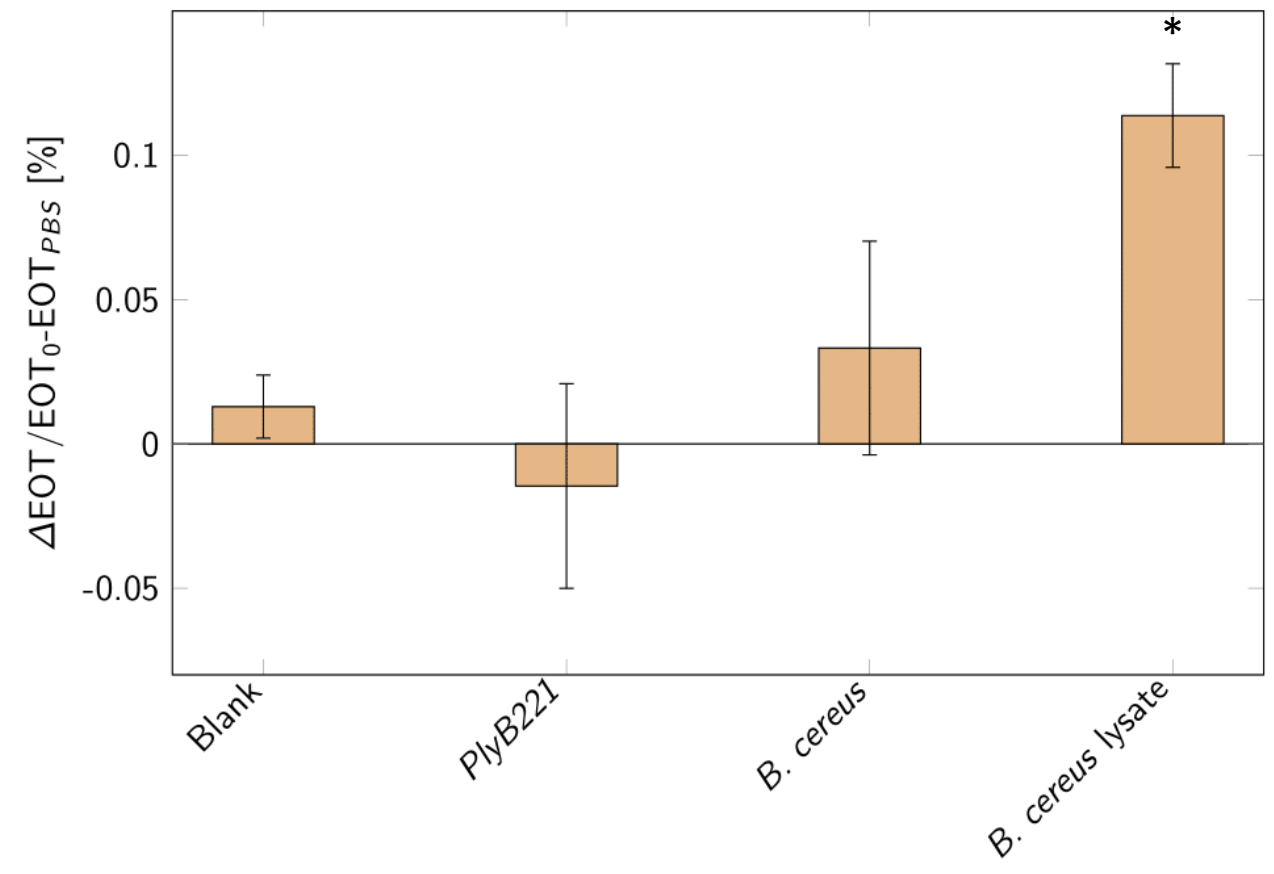
10² CFU/mL ⇒ Detected but not *reliably* (p-value>0.05)

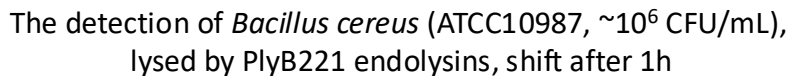
10³ CFU/mL ⇒ <u>Limit of Detection (LoD)</u> (p-value<0.05)!

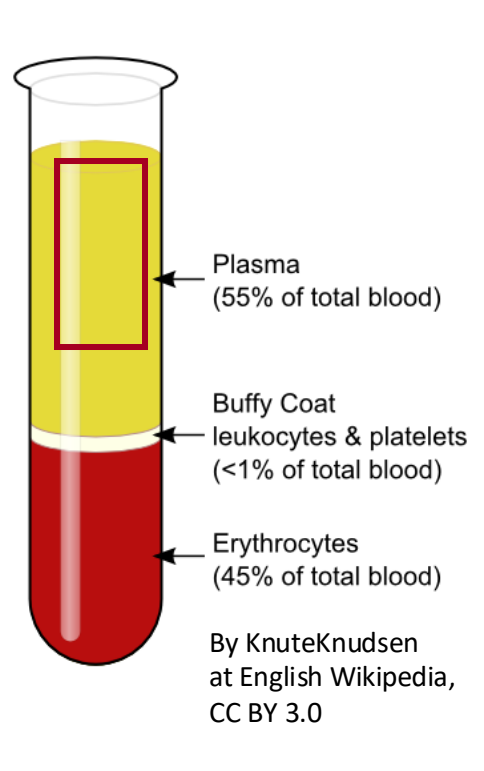
Selectivity



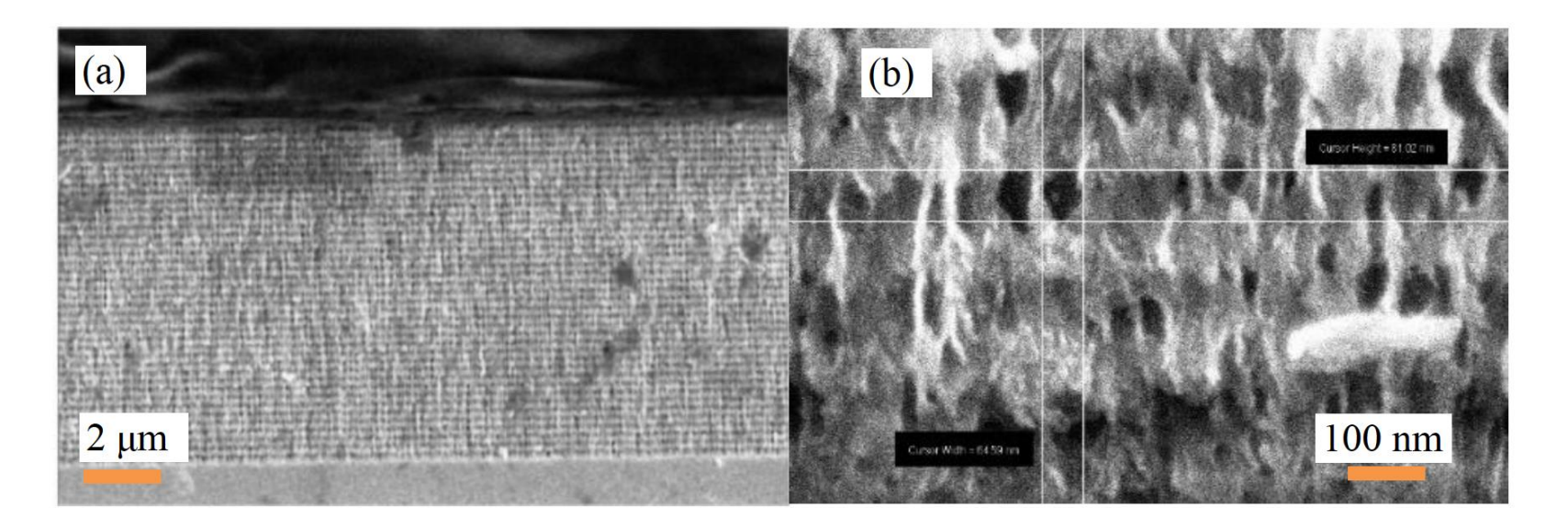
Complex sample: human plasma Blood without white blood cells, red blood cells and platelets

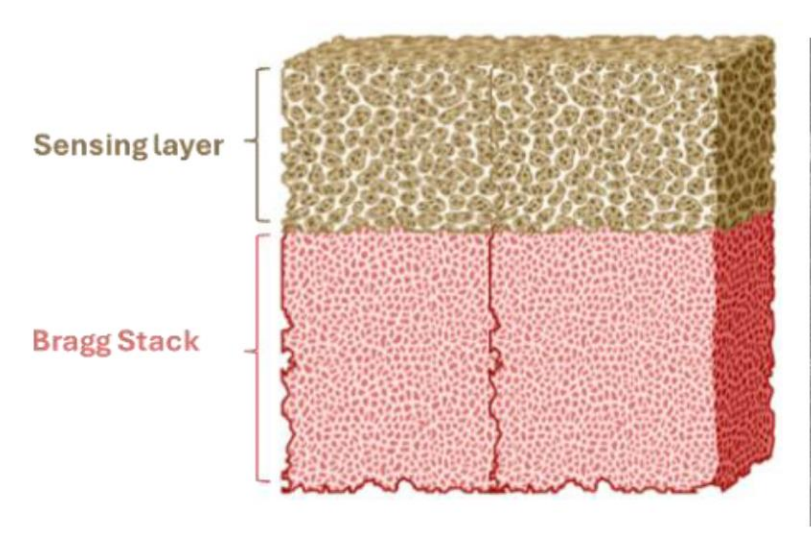


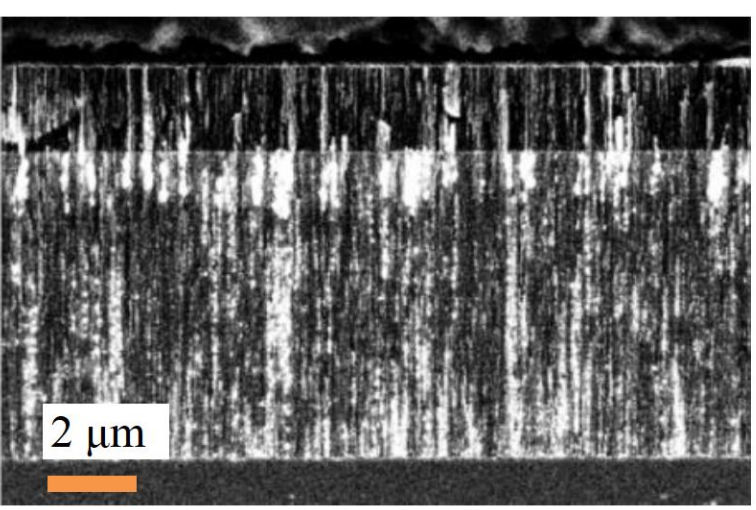


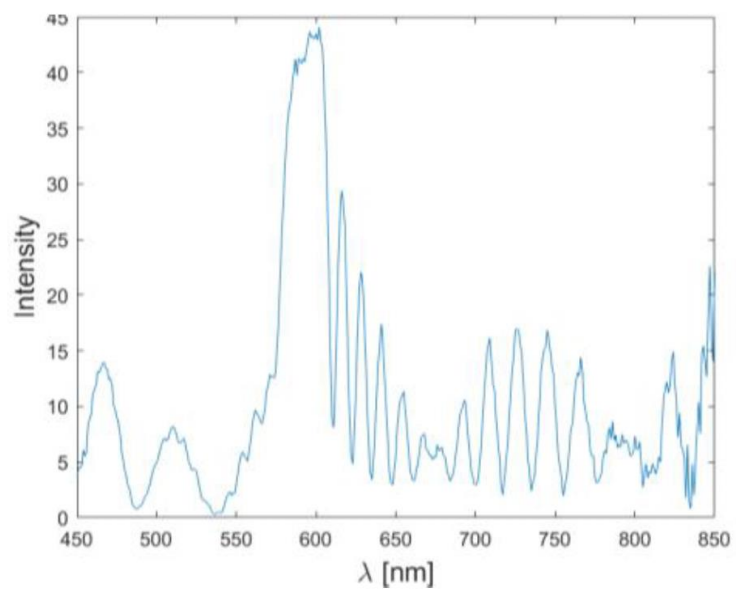


BRAGG MIRROR



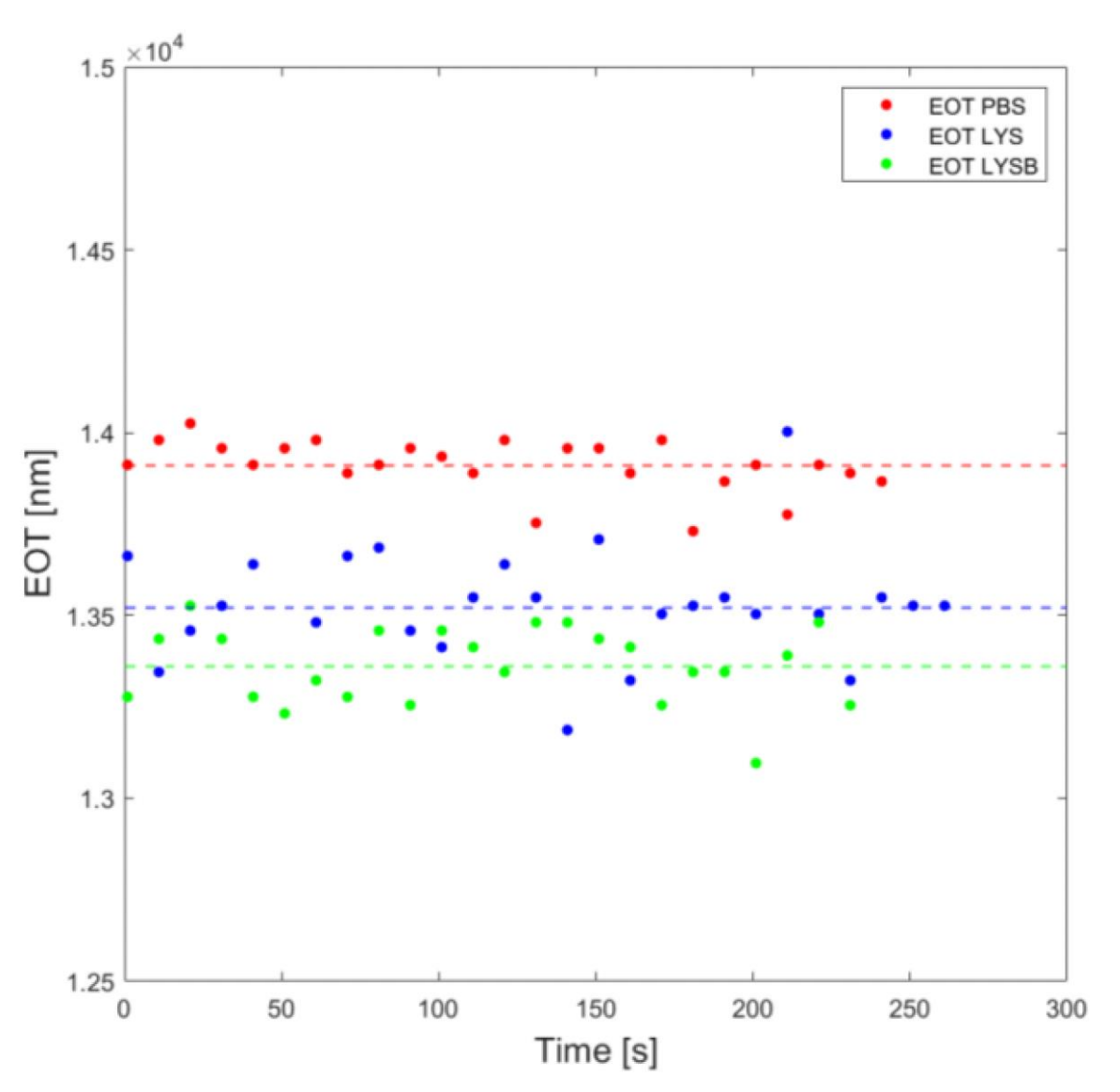






Work of E. Colomer Clavel and C. Gevers

BRAGG MIRROR



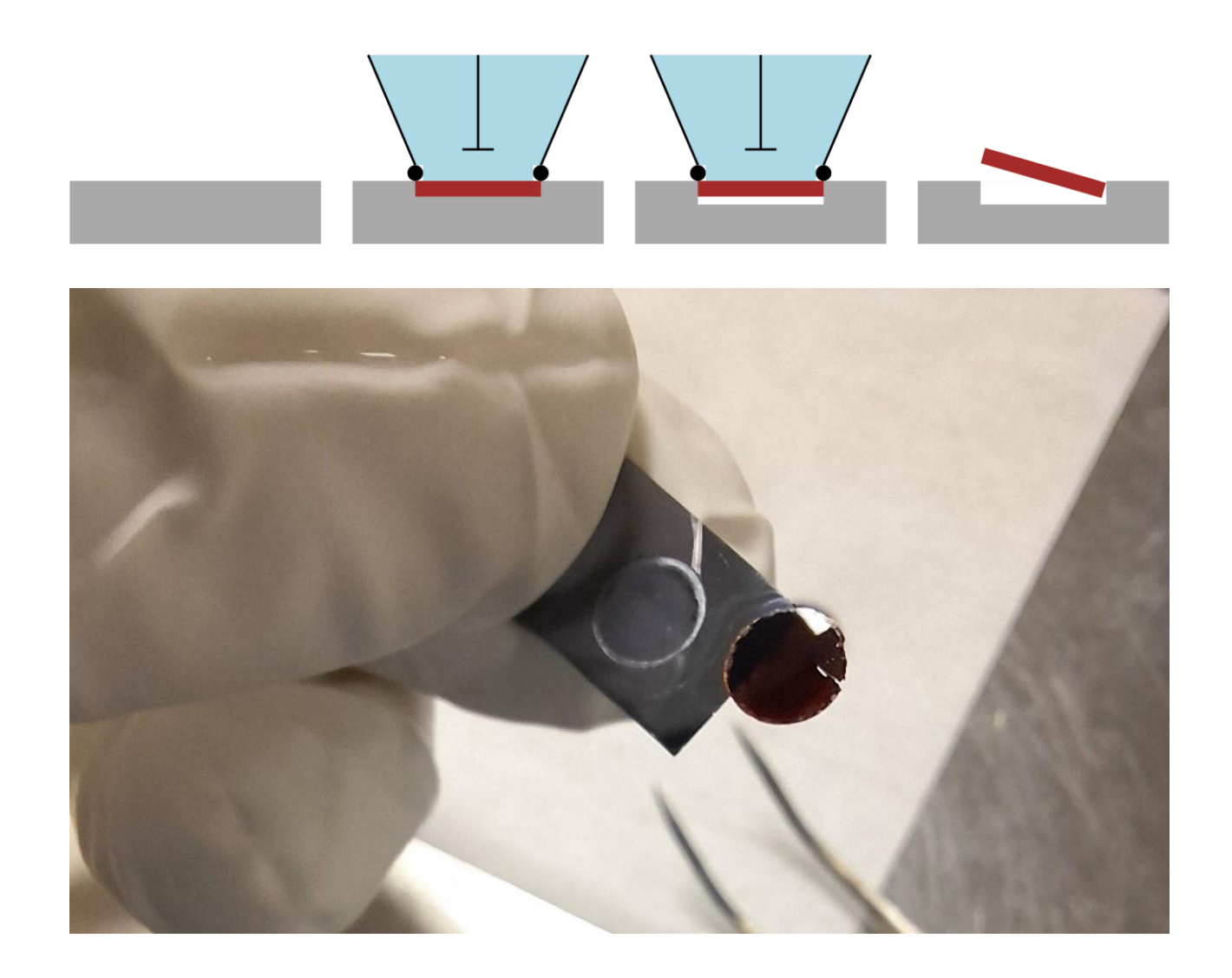
4% EOT shift

Theoretical LoD

PSi 2.15·10⁻¹ RIU

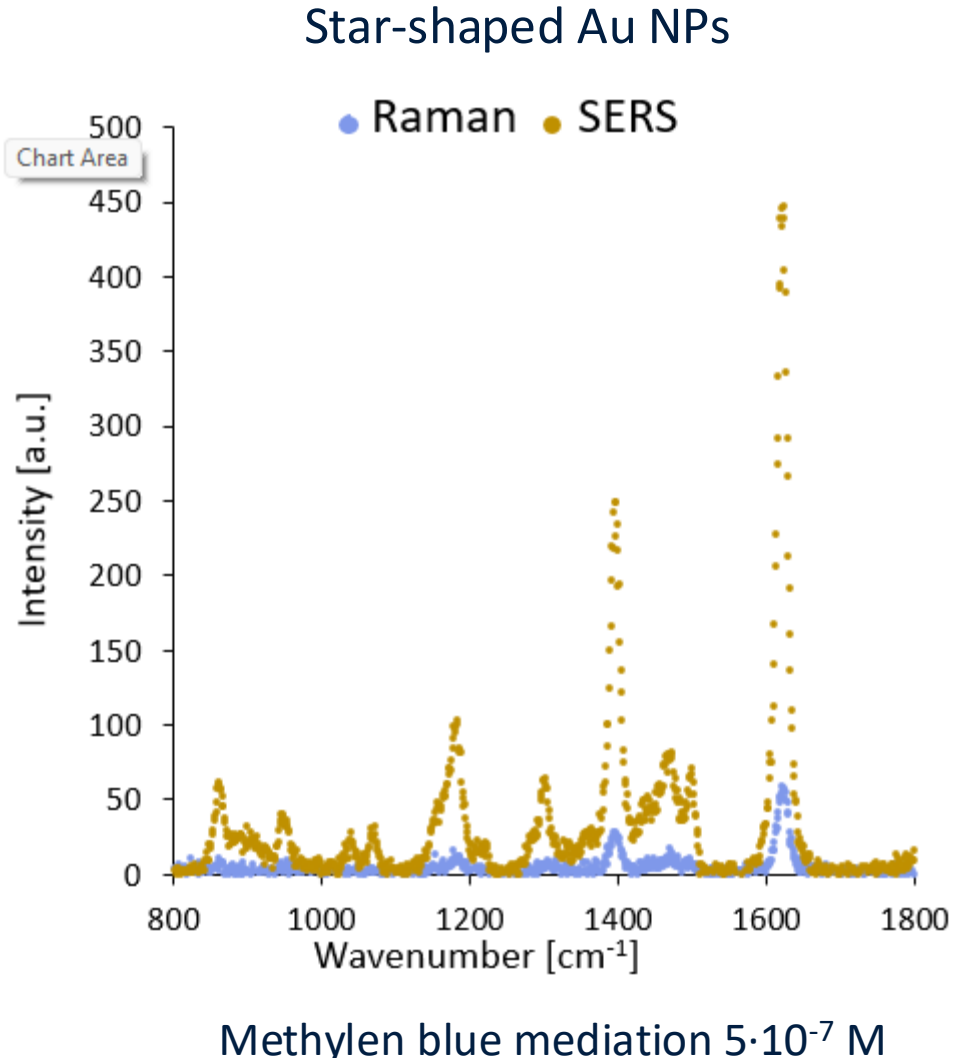
PSi+Bragg mirror 1.35·10⁻³ RIU

Much simpler method to achieve the fabrication of membranes, if we cope with the mechanical fragility ...

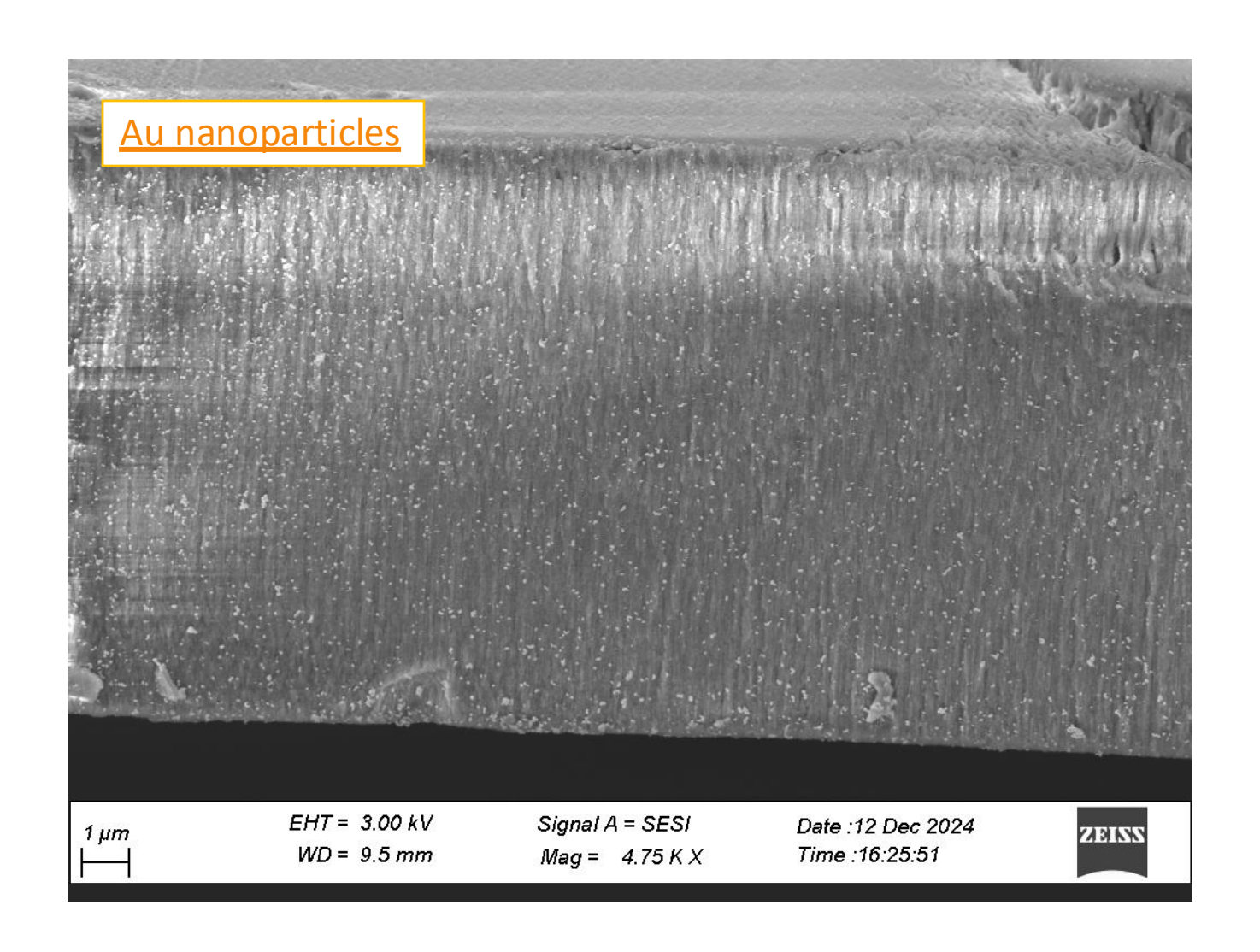


Work of R. Hanus & C. Gevers

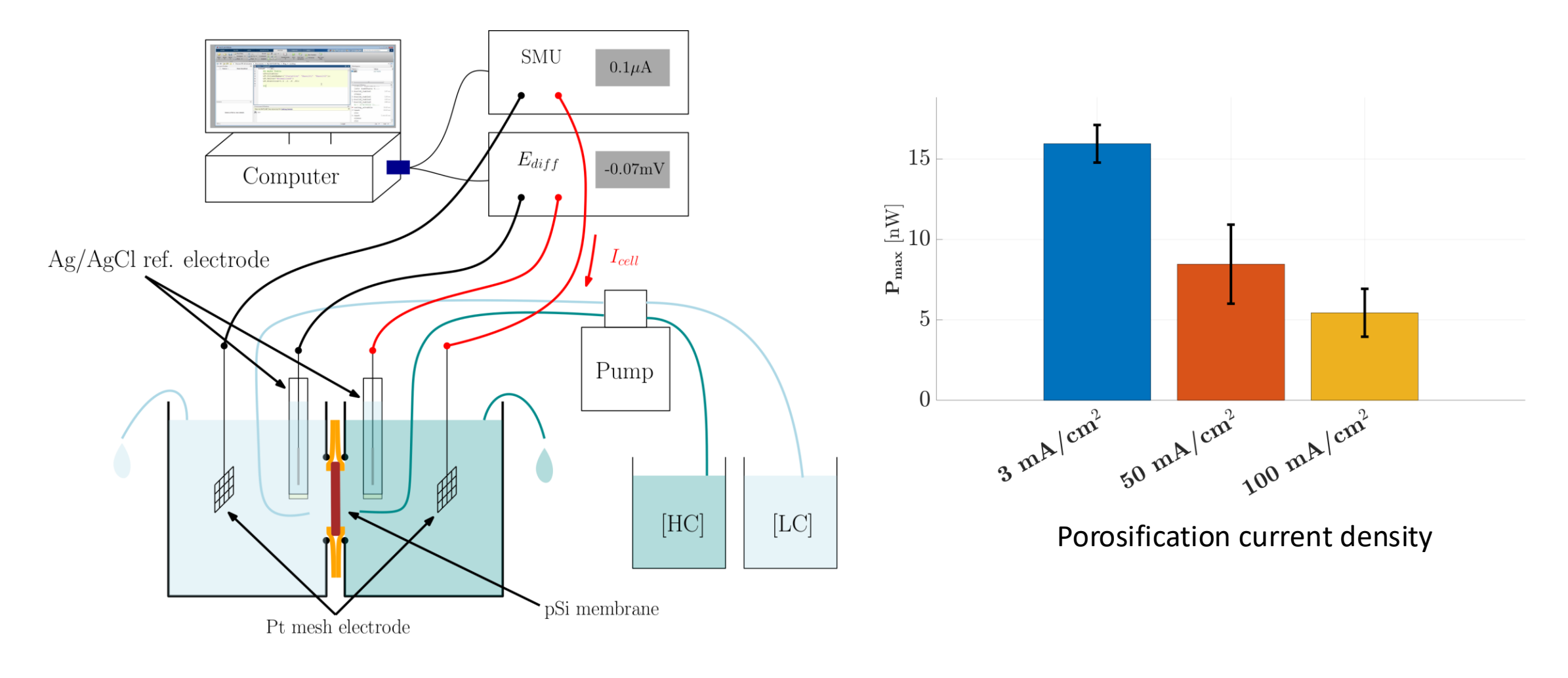
AU NP FOR SERS



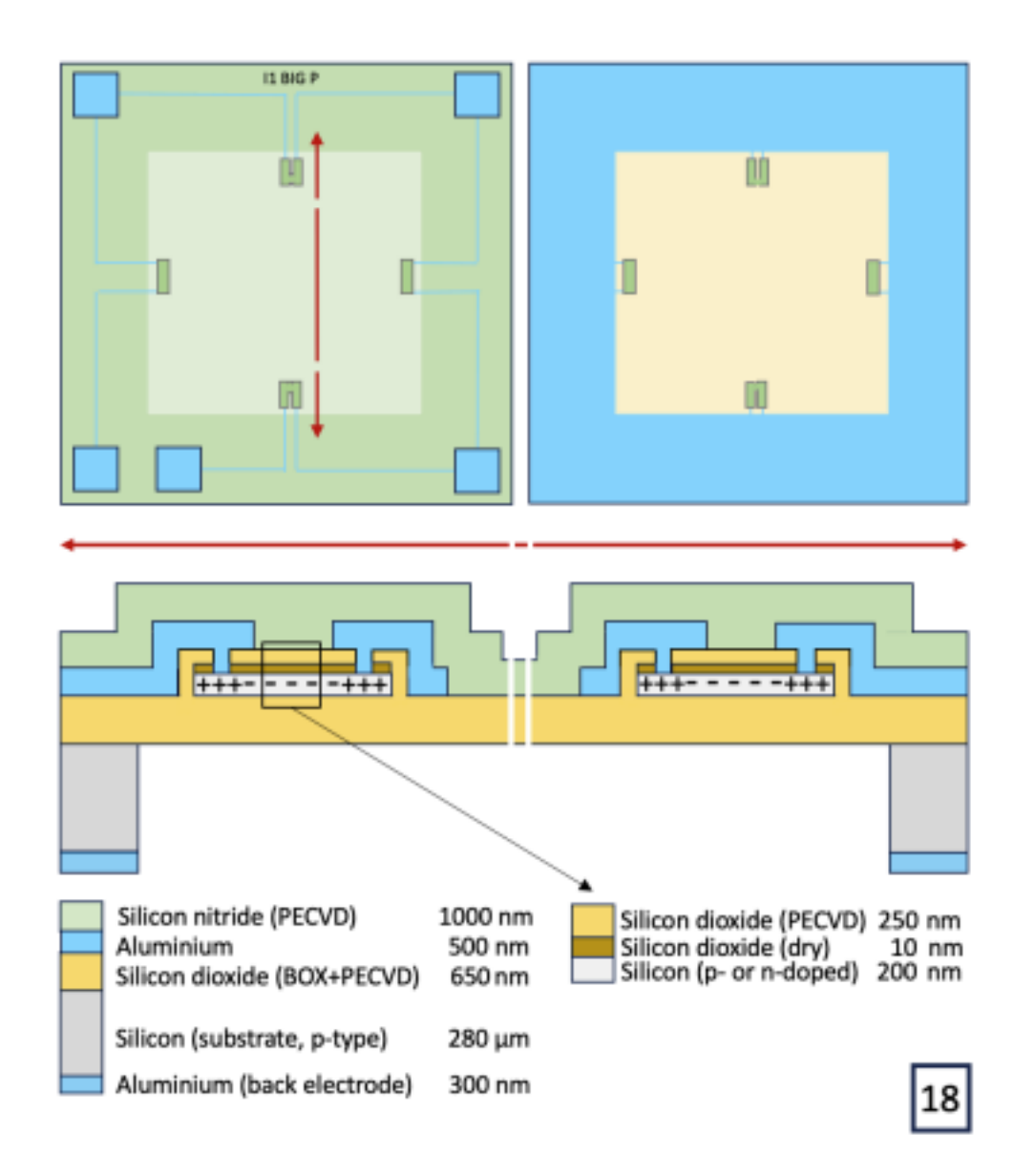
Methylen blue mediation 5·10⁻⁷ M



Blue Energy harvesting



SOI irradiated membranes



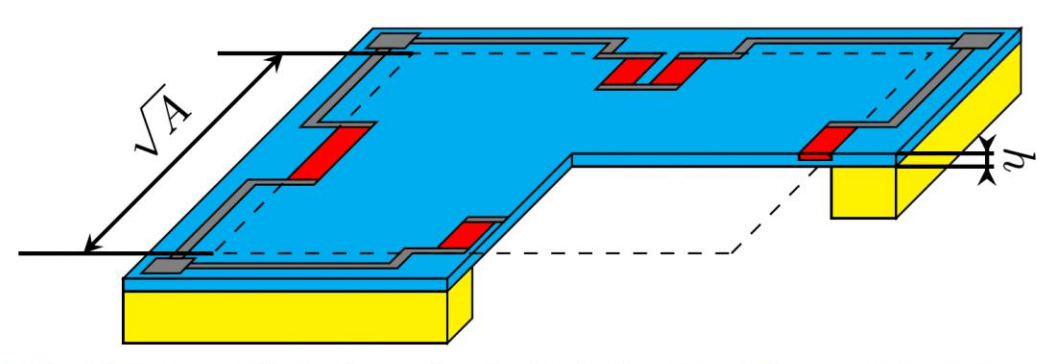


Fig. 1. Cross-section view of a typical piezoresistive pressure sensor: silicon handle wafer is in yellow, silicon or silicon dioxide membrane of thickness *h* and area *A* is in blue, piezoresistors are in red and aluminum conductive lines are in gray, dashed lines delimit the membrane.

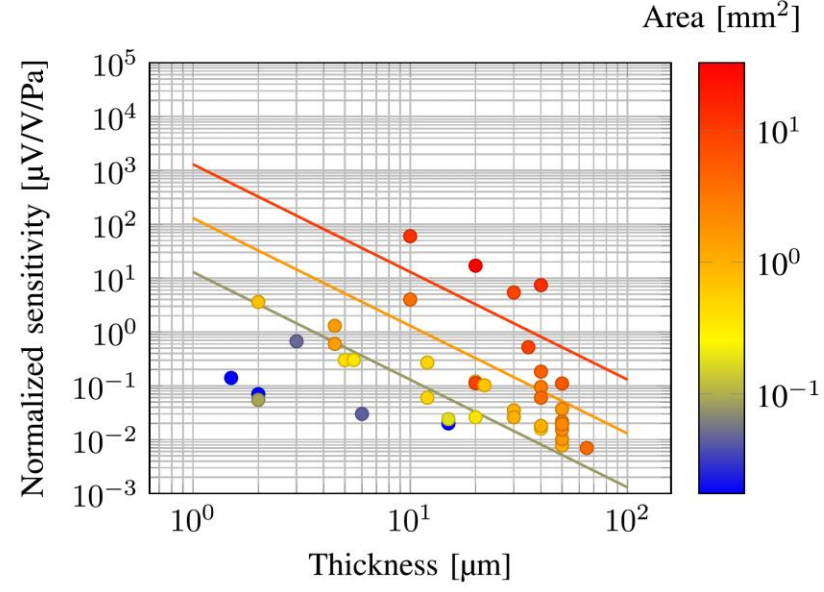
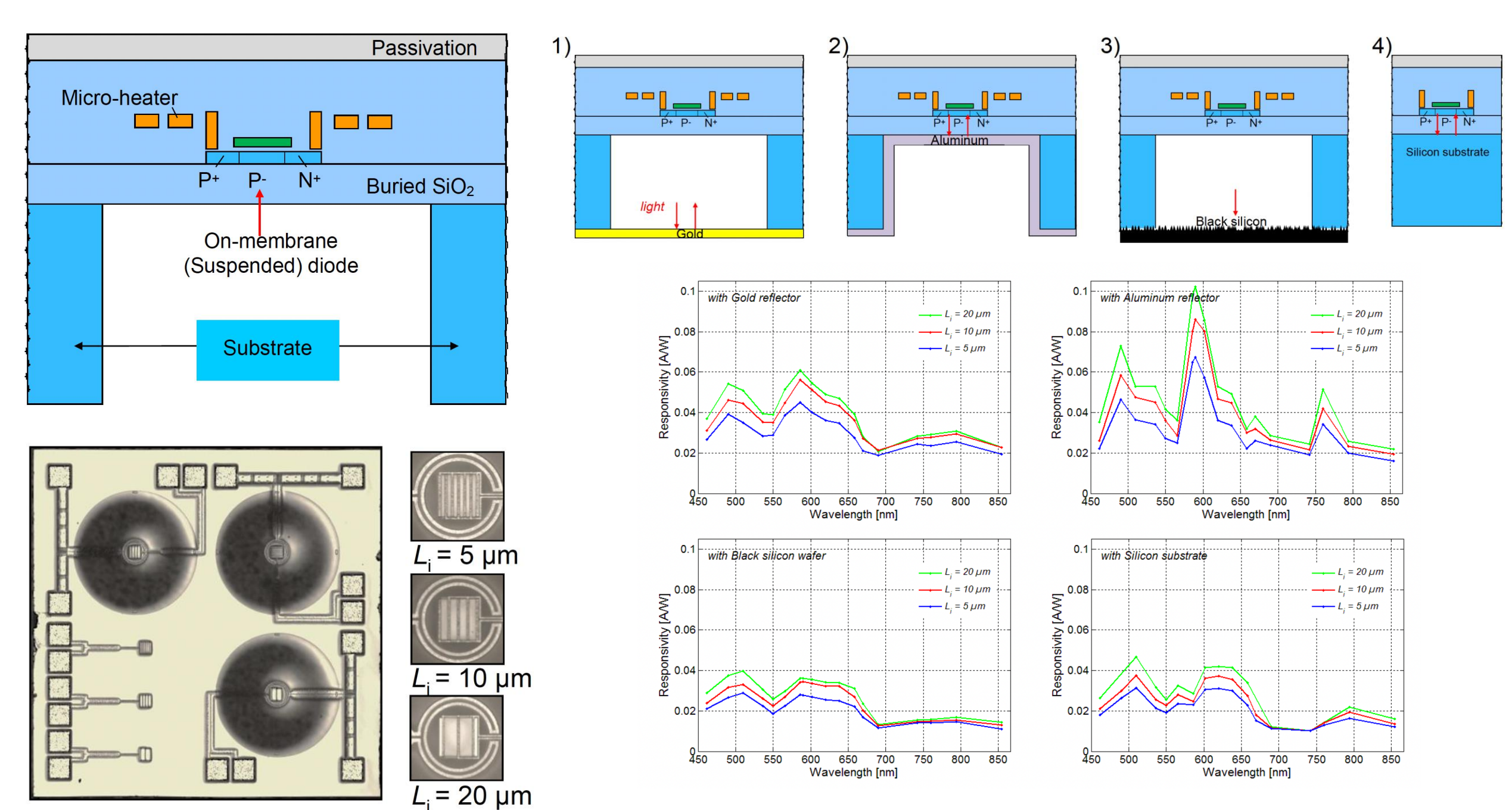
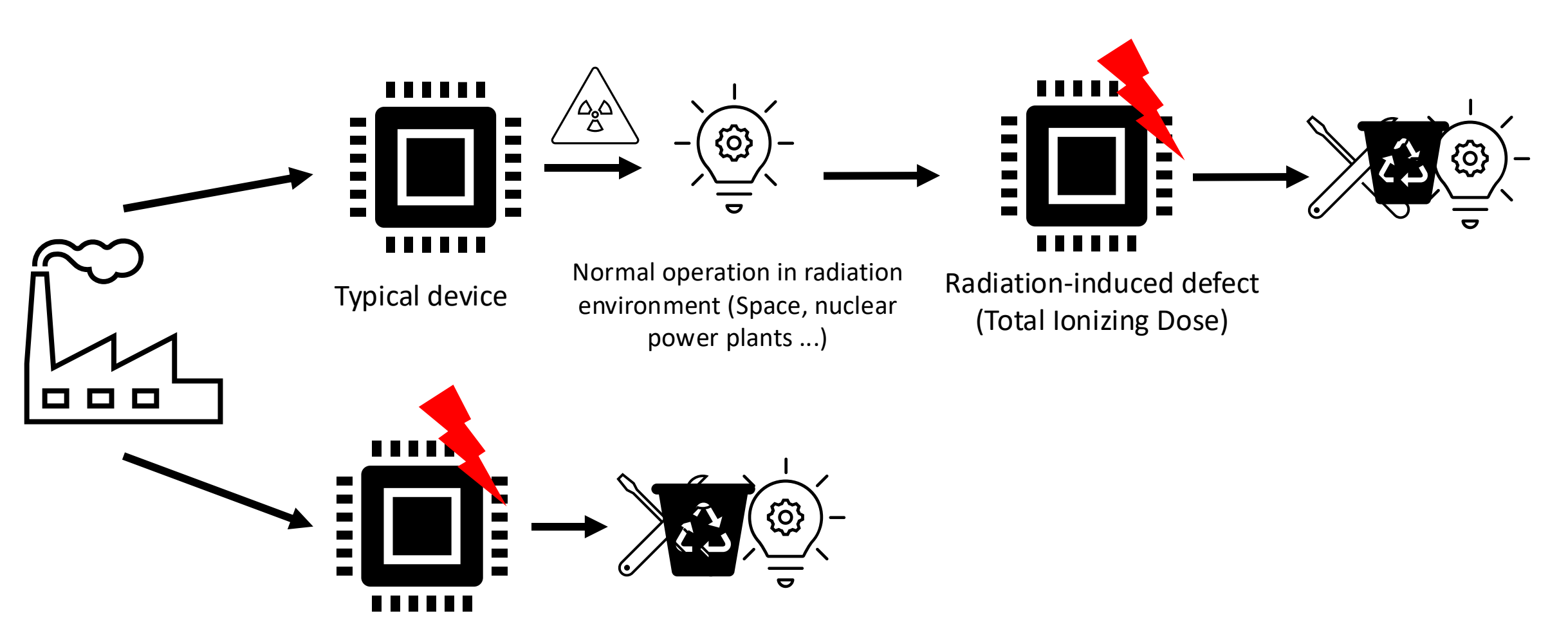


Fig. 4. Normalized sensitivity versus membrane thickness (x-axis) and membrane area (color circles). Lines are theoretical trends obtained with the simple model, eq. (9), for areas of 0.1, 1 and 10 mm², from bottom to top.

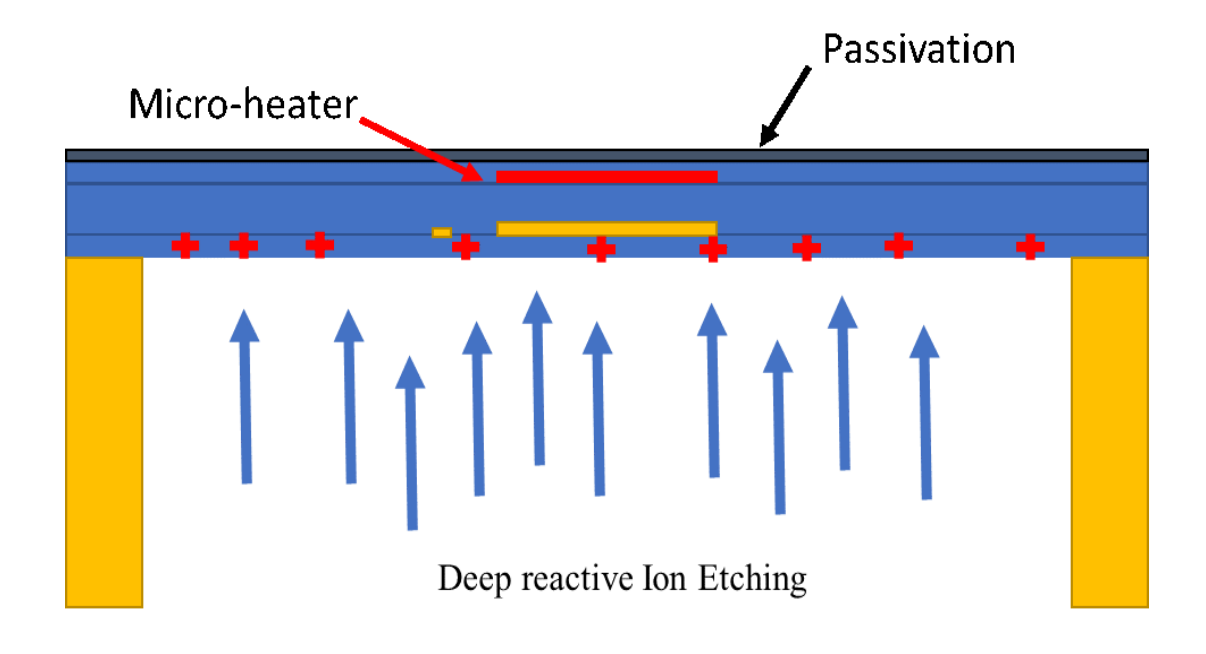


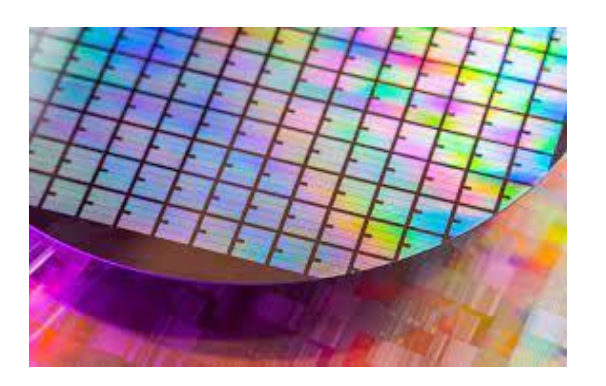
Courtesy of Guoli Li et al., in collaboration with Cambridge U. 45



Process-induced defect

Process-induced defects





- Hot Carrier Injection
- Deep reactive Ion Etching
- Doping variations
- > Positive oxide trapped charges.
- **➤** SiO2-Si Interface states.
- > Stress-induced defects
- Shift of parameters (V_{th}, gm, SS)
- Leakage current.
- Reduce lifetime.

Radiation-induced defects

Total Ionizing Dose (TID)

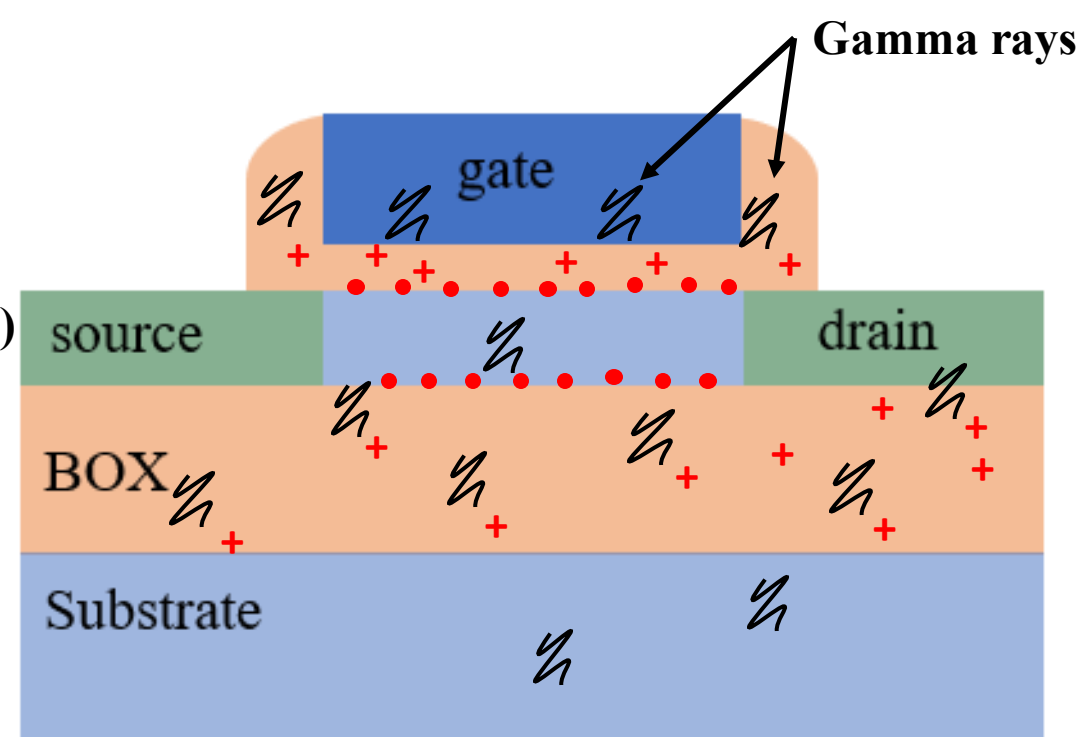
Positive oxide trapped charges. Interface states.

- Shift of parameters (V_{th}, gm, SS)
- Cumulative degradation
- **Reduce lifetime**

Permanent failure!!

- Shielding
- Radiation hardening by design

In-situ thermal annealing !!!?

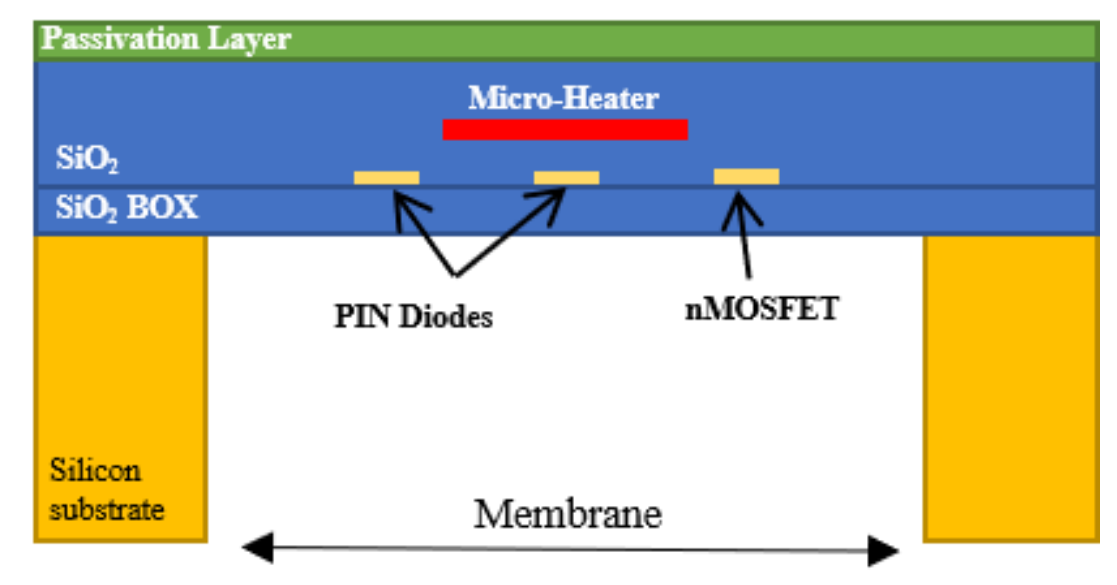




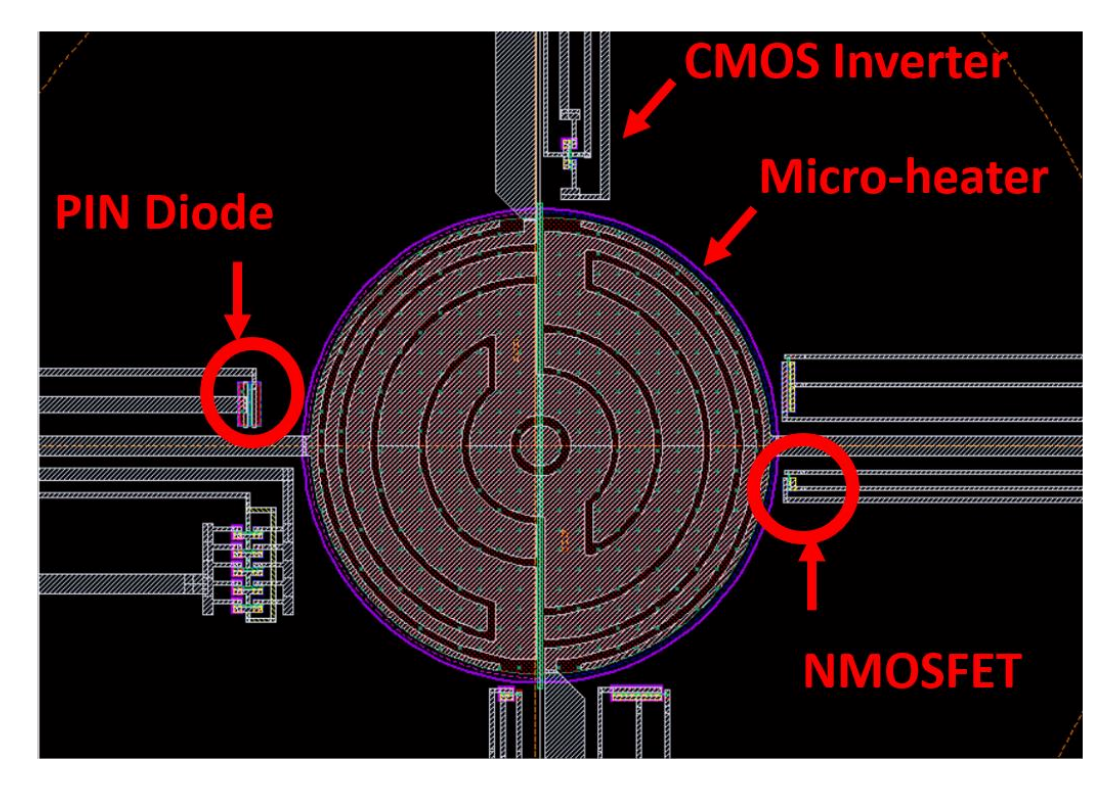




1.0 μm Partially-Depleted SOI technology (XI.10 from XFAB, Germany).

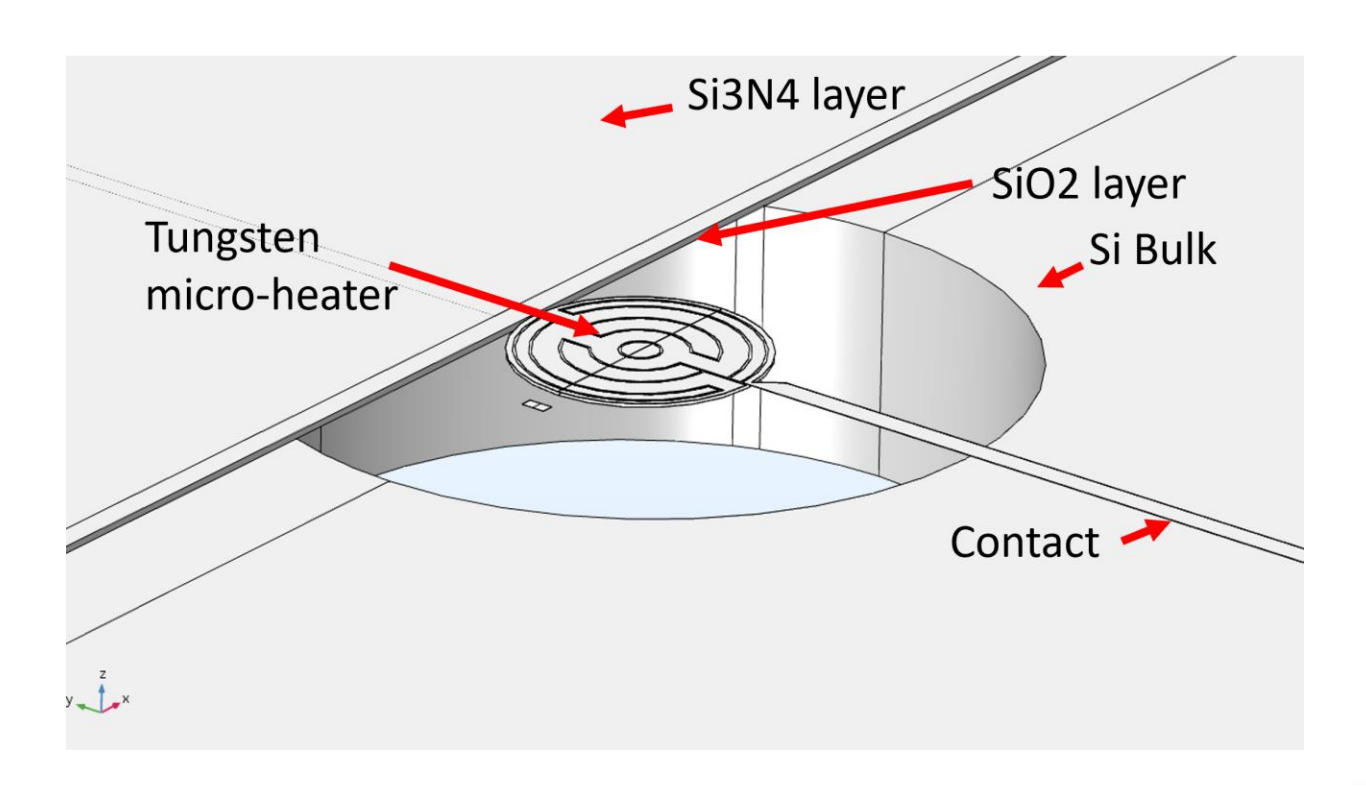


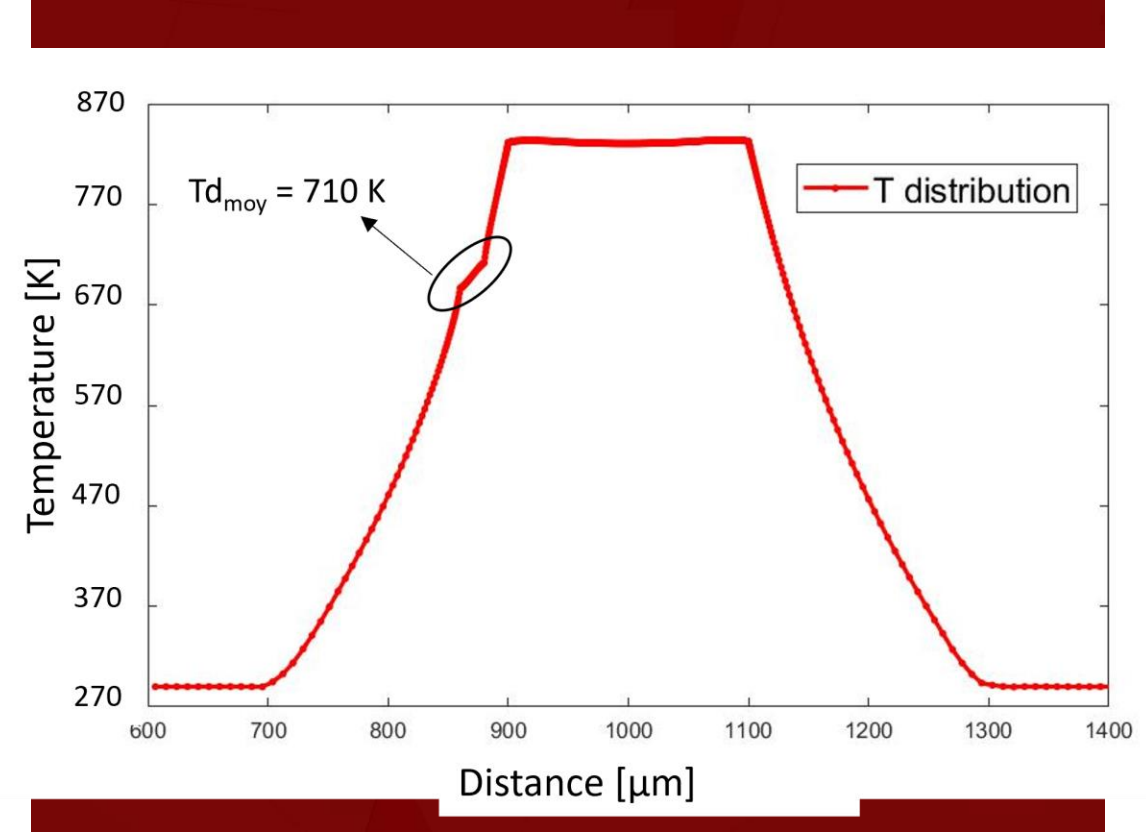
Schematic cross section of the device under test. (S Amor, et al, Semicond.Sci. and Techn., vol. 32, 2016.)



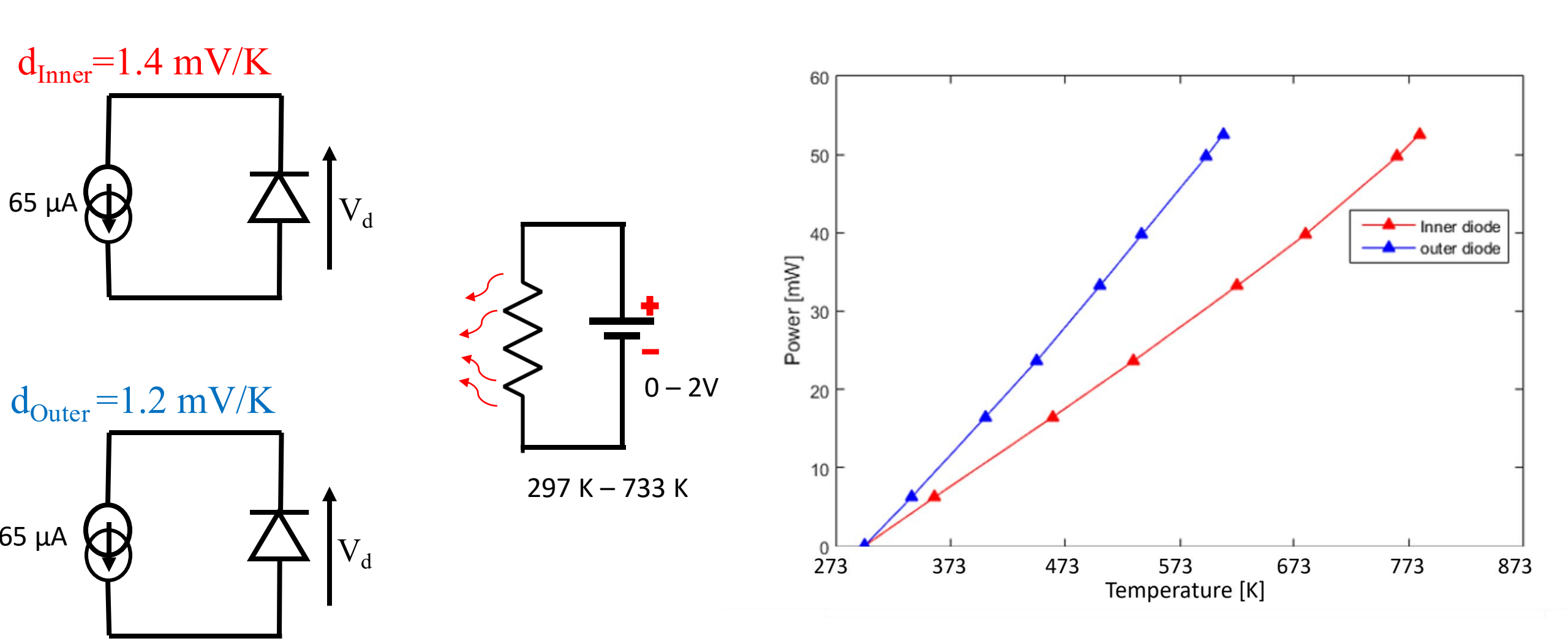
Layout image showing the location of the components around the micro-heater.

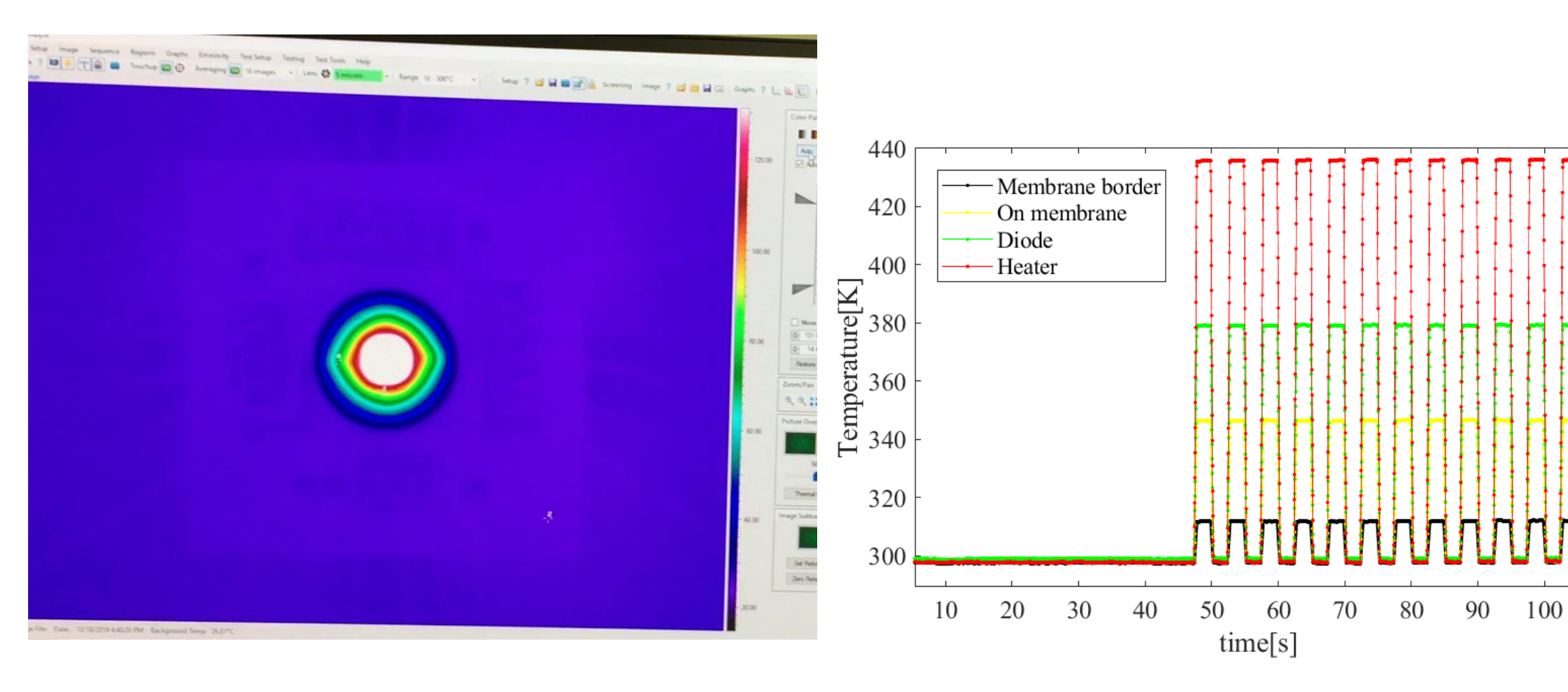
Comsol simulation of the on-membrane micro-heater.

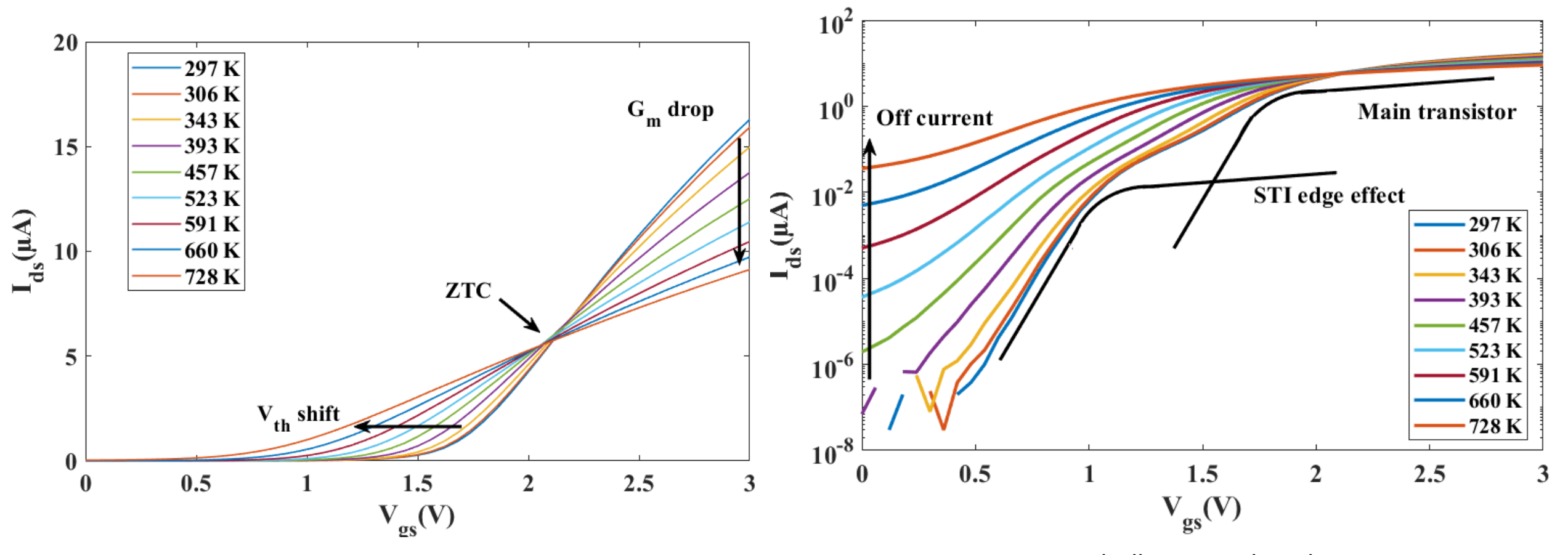




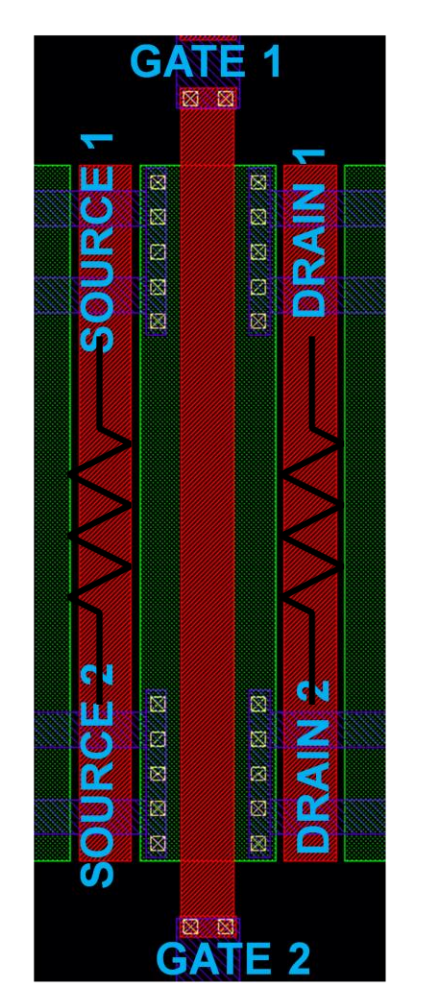
$$V_d = V_0 - d (T - T_0)$$

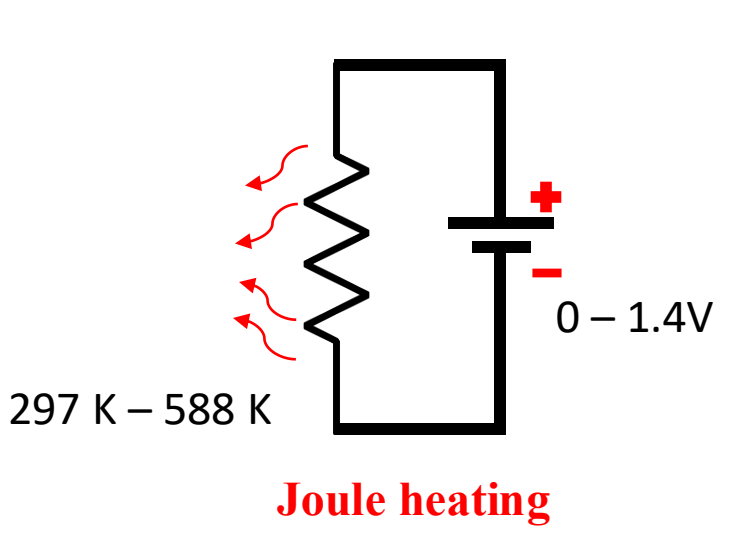


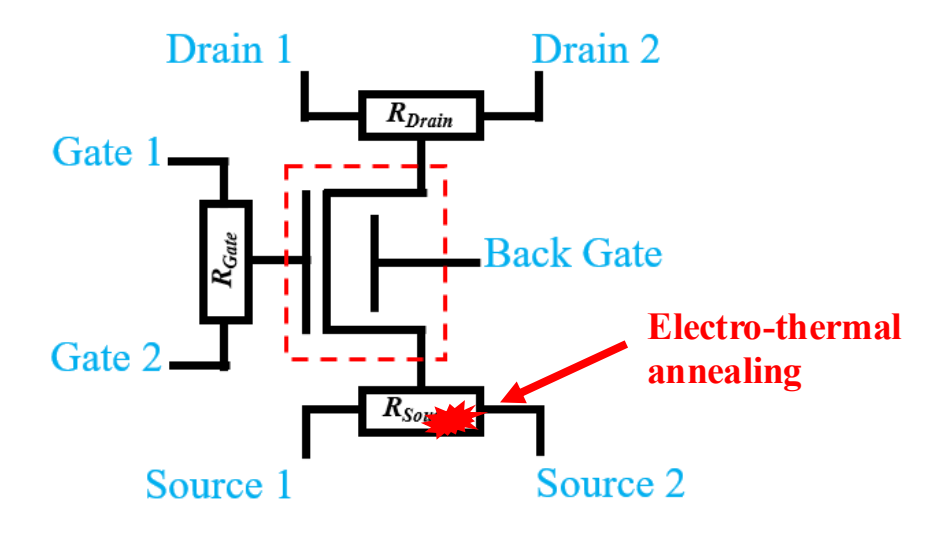




STI = shallow trench isolation

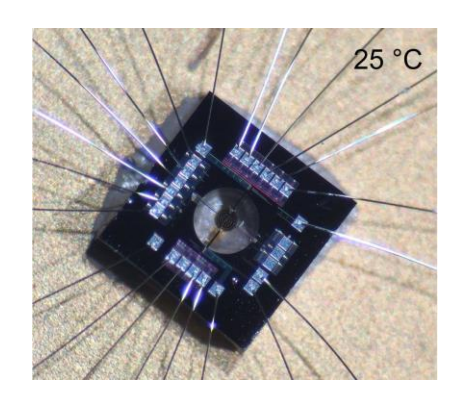






Schematic representation of N-type MOS with 3 embedded micro-heaters based on 28 nm FDSOI technology.

Layout of N-type MOS transistor with thick high-k metal gate oxide, from 28 nm Fully Depleted Silicon-On-Insulator (FDSOI) process.

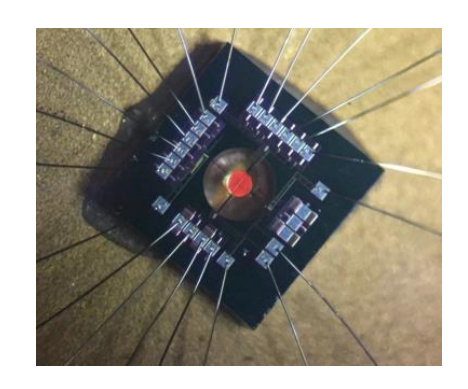




• Cadence simulation based on the pdk of the technology.

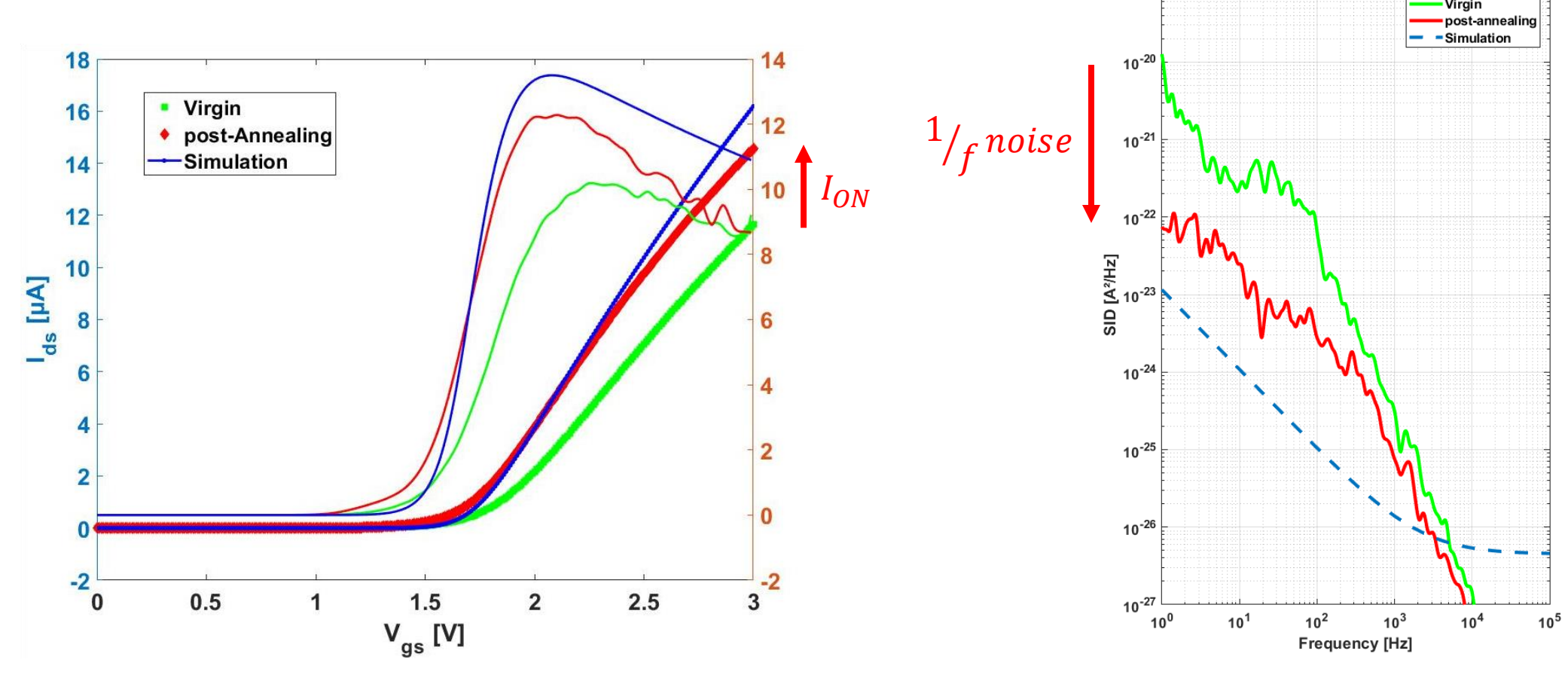
DRIE etching

- I-V measurements.
- LFN measurements.



Thermal annealing at 538 K

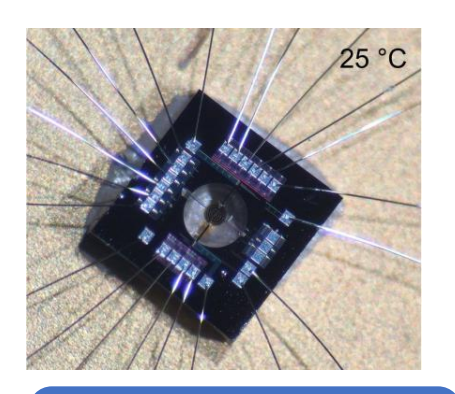
- In-situ thermal annealing for 2 minutes .
- IV and LFN measurements after annealing.



I-V (thick lines) and transconductance g_m (thin lines) measurements of onmembrane n-MOSFET, before and after thermal annealing, compared to Cadence simulation of the ideal MOSFET model in linear regime with V_{ds} =50 mV.

Measured noise power spectral density of the on-membrane n-MOSFET in weak inversion regime, before and after thermal annealing, and compared to 1/f noise Cadence simulation.

10⁻¹⁹



Fresh measurements

• I-V and Low Frequency Noise (LFN) measurements in normal conditions.

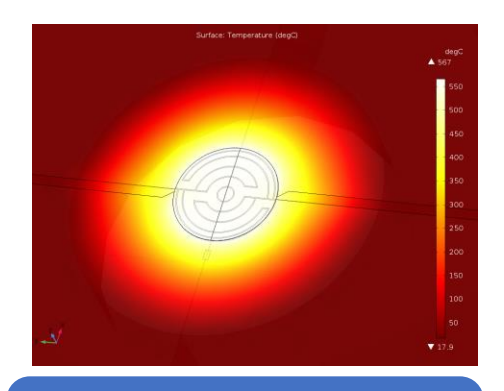


348 krad (Si)



Gamma irradiation

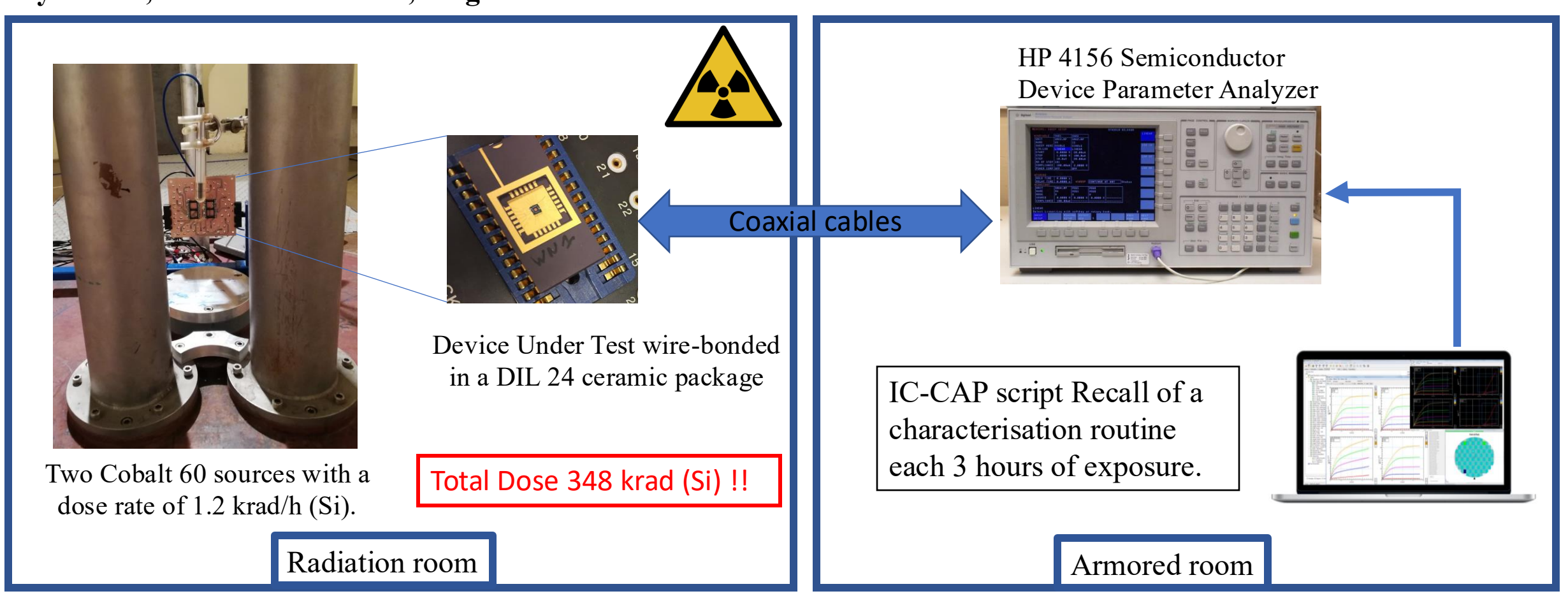
- I-V measurements after each irradiation dose of 1.2 krad (Si).
- I-V and LFN measurements after irradiation.

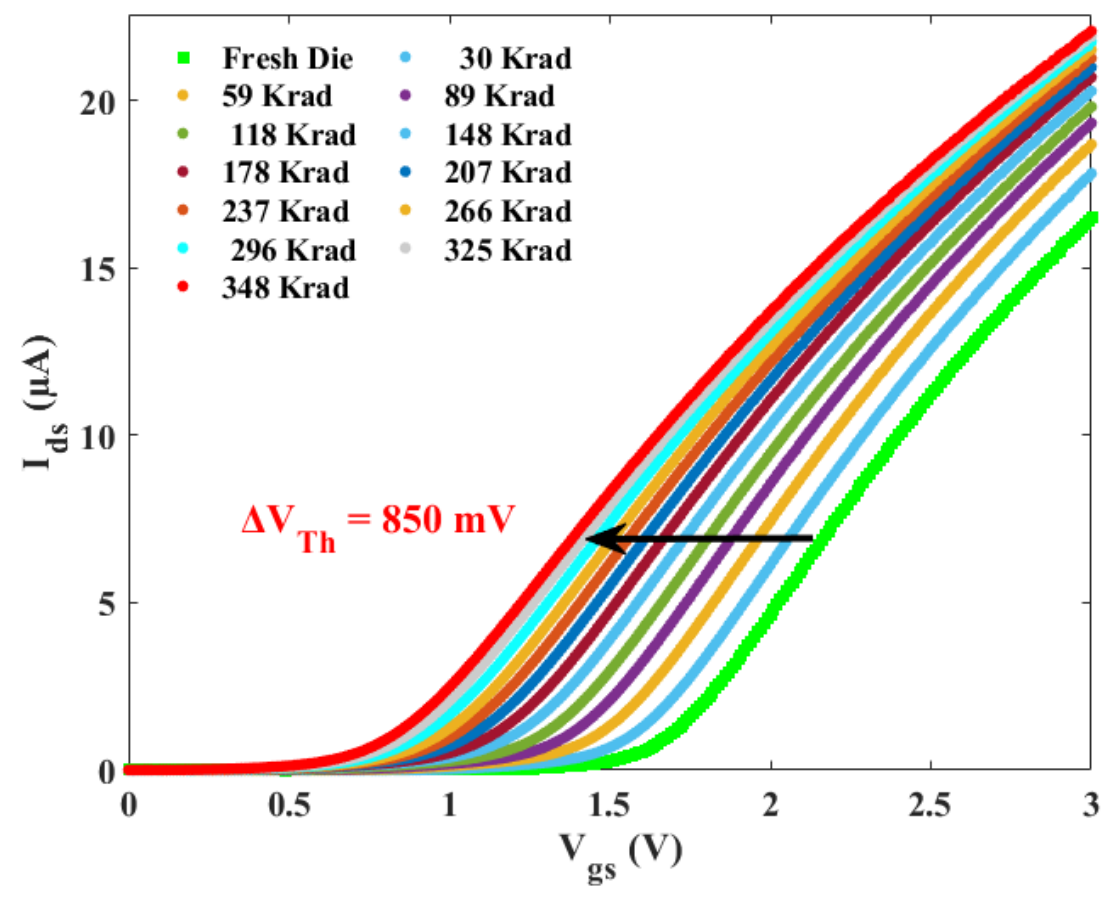


Thermal annealing up to 638 K

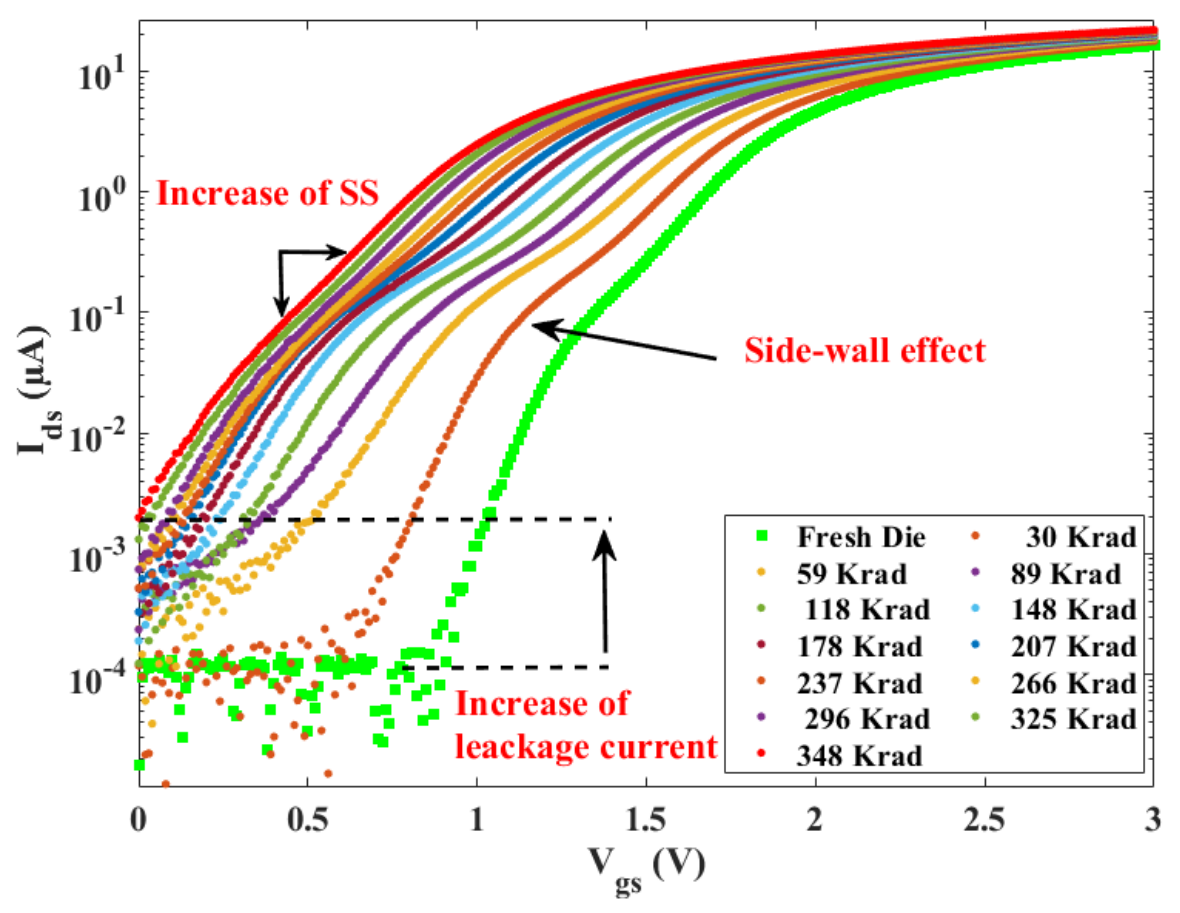
- I-V measurements after each step of 30s thermal annealing.
- LFN measurements after annealing.

Cyclotron, Louvain-La-Neuve, Belgium.

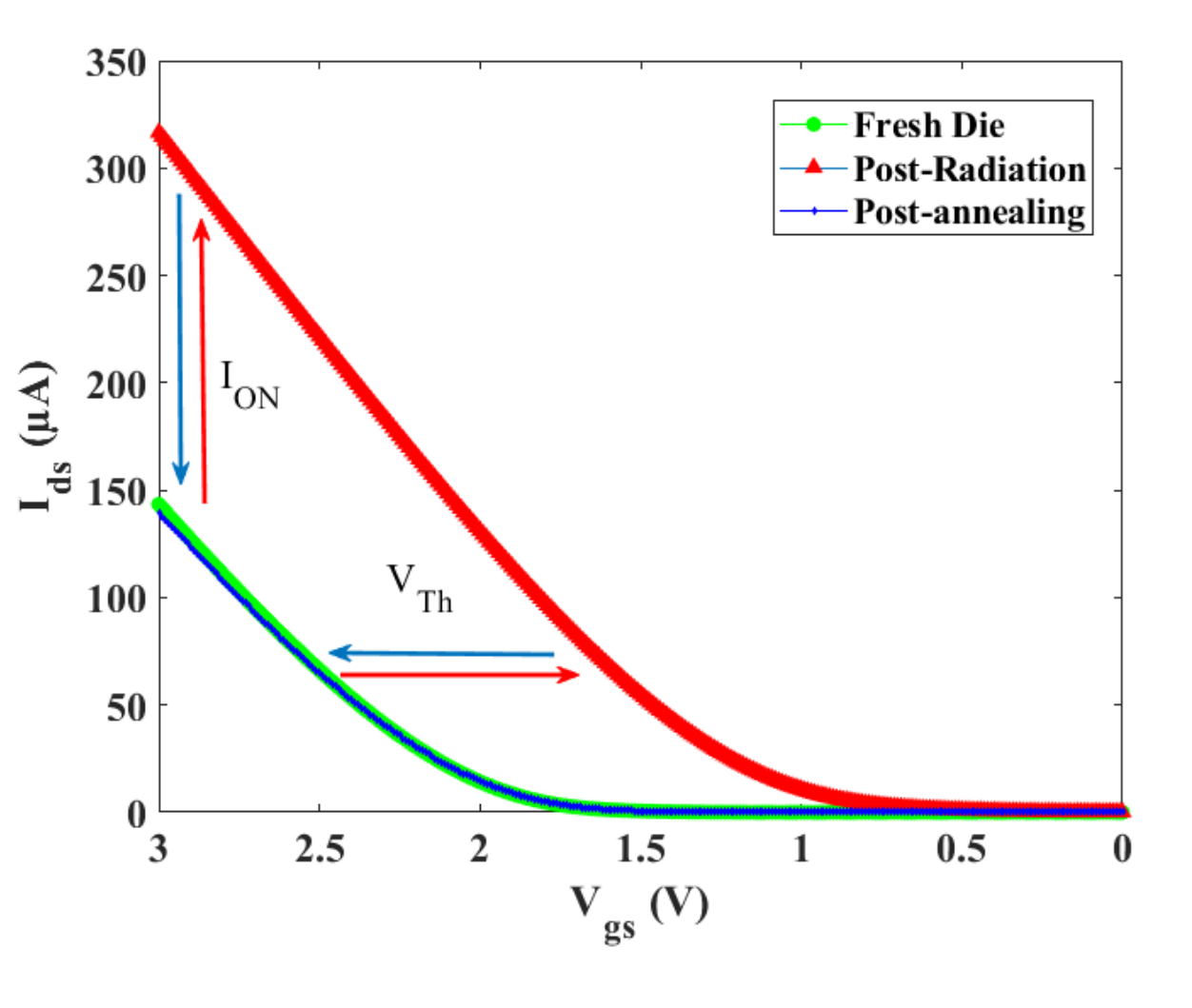


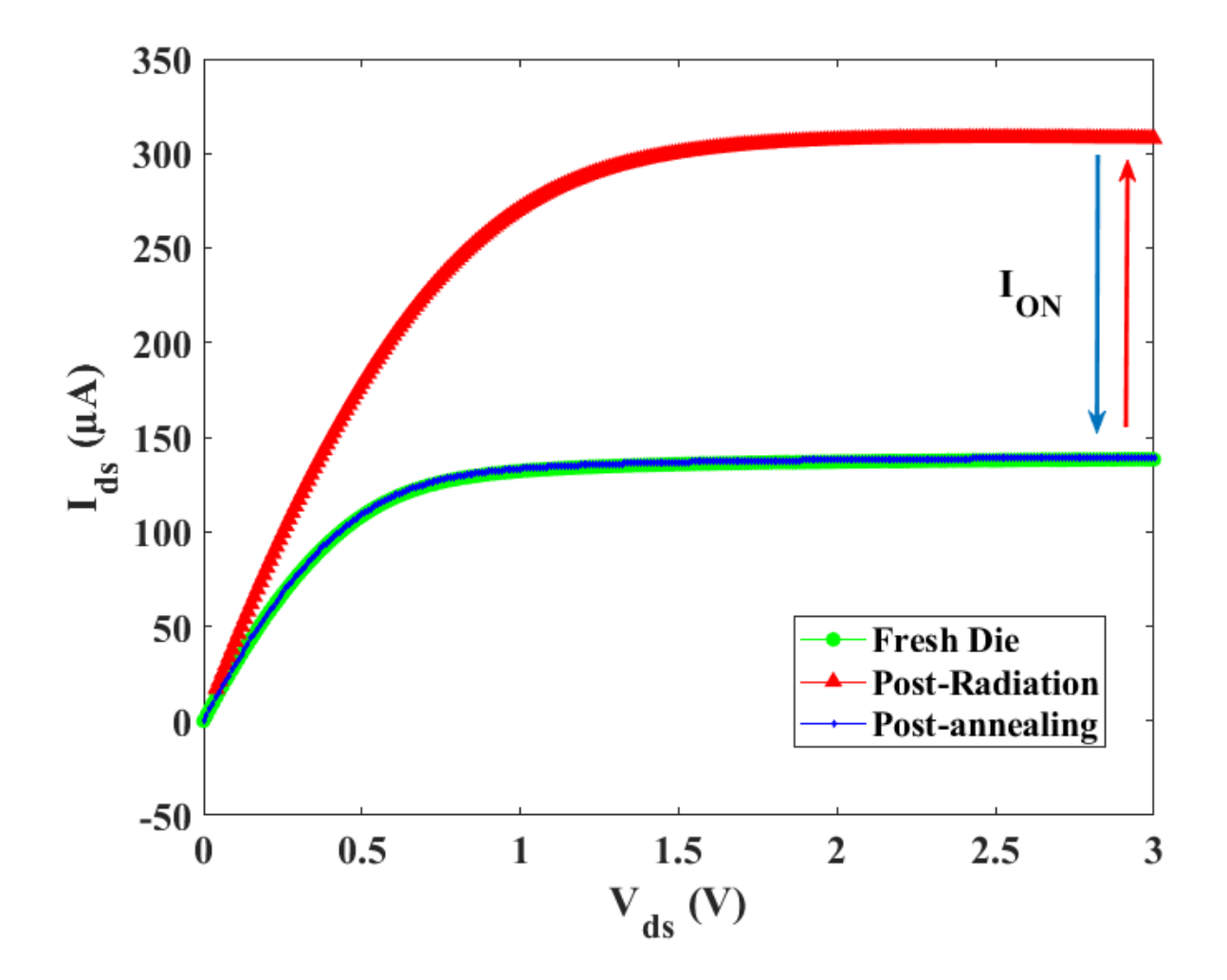


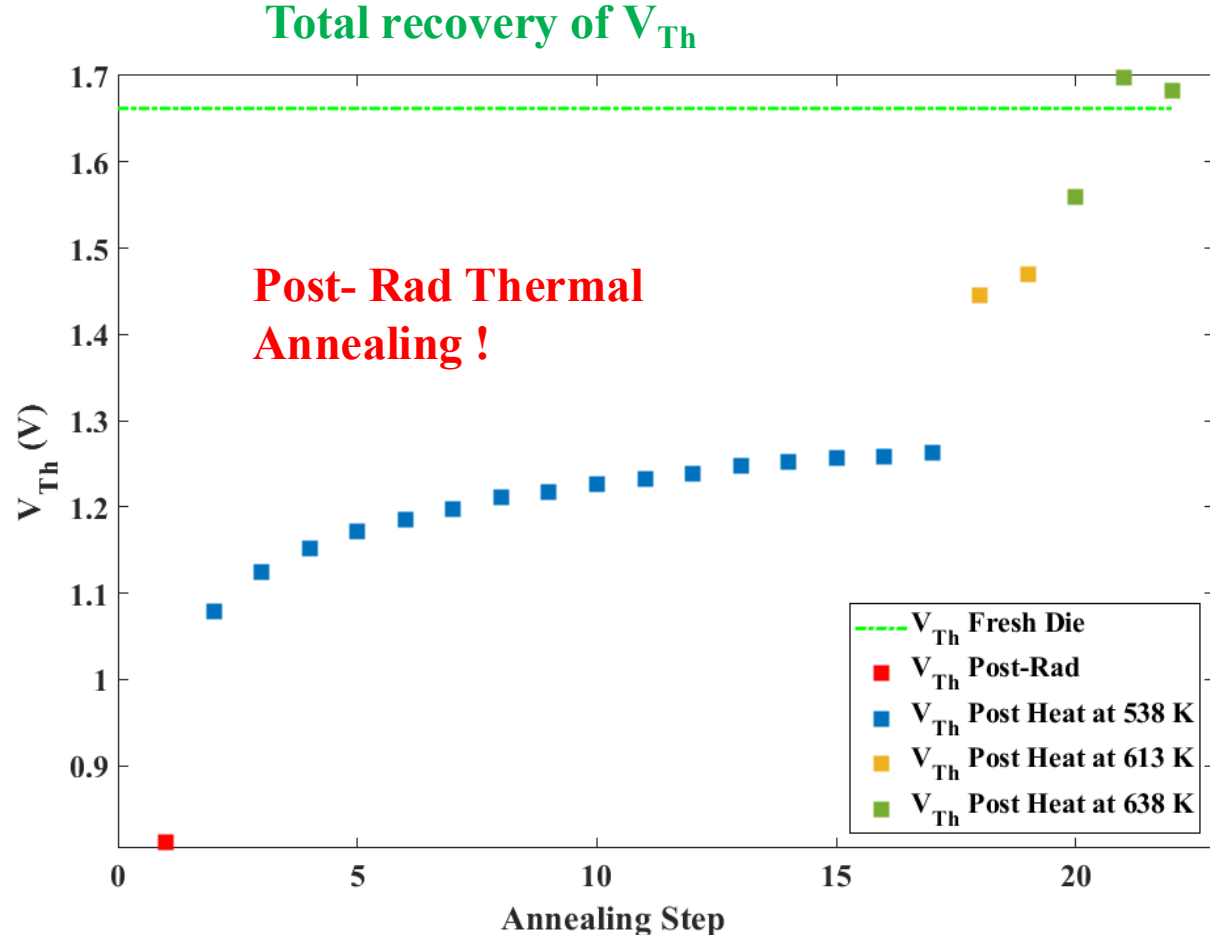
 $I_{ds}\ vs\ V_{gs}$ characteristics of the 6µm wide transistor. Measured in linear regime under after each 60 krad (Si) of gamma radiation .



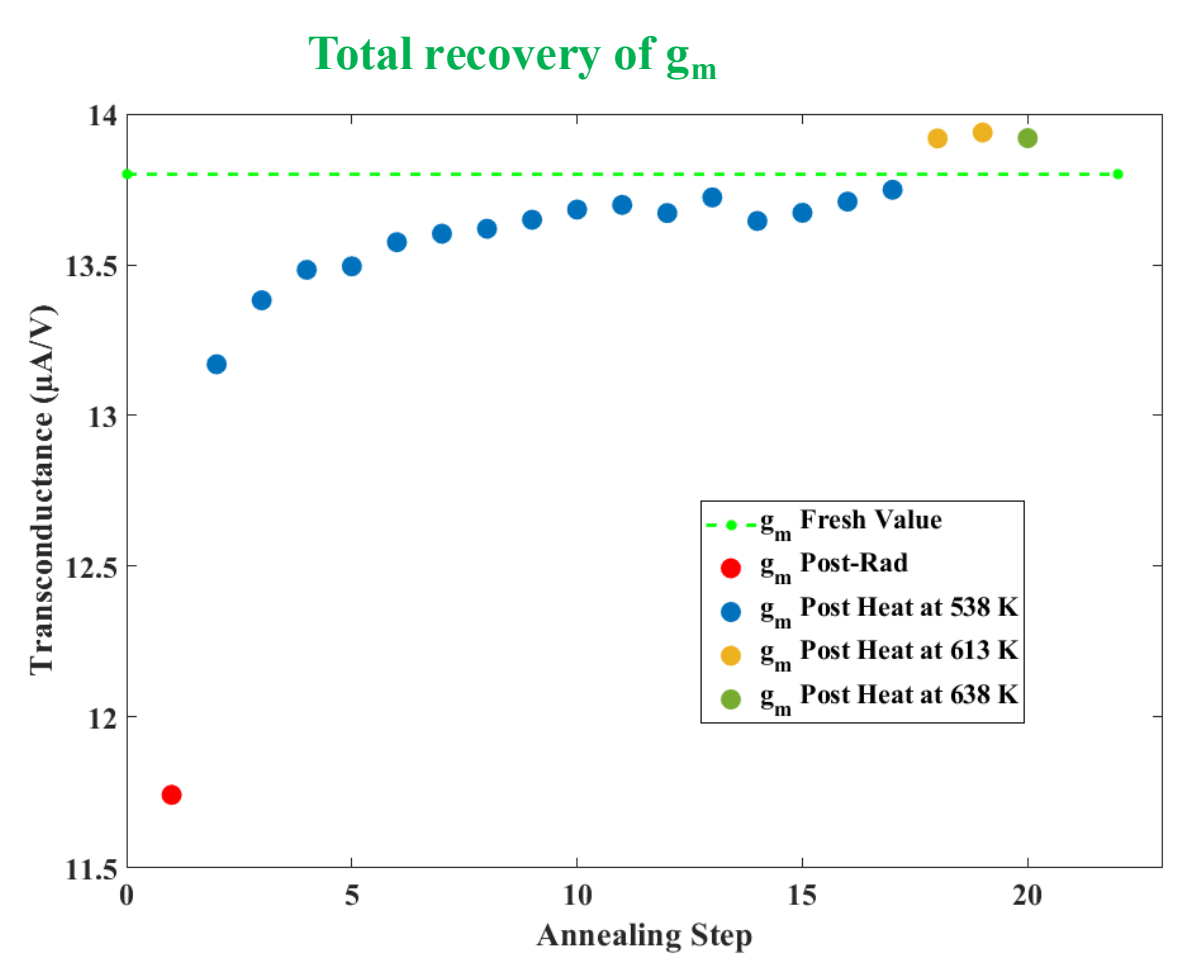
Logscale representation of the transistor's I-V characteristics. Measured under gamma radiation after each 60 krad (Si).



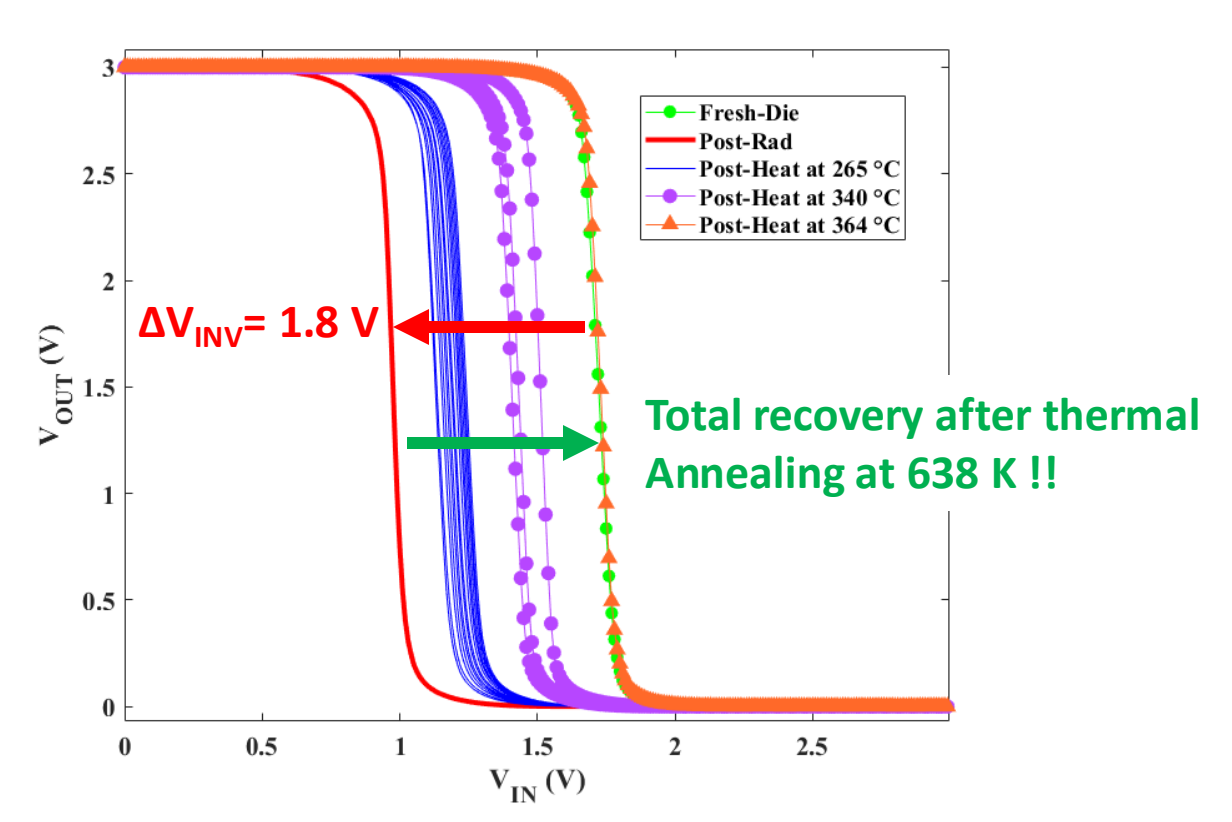




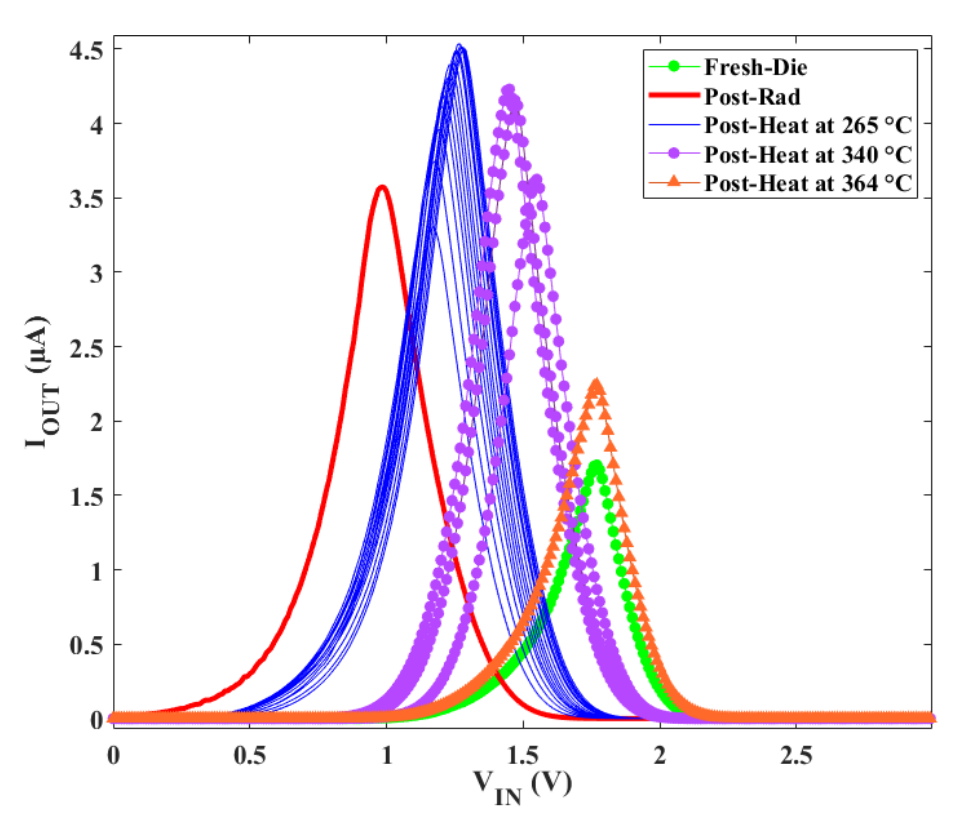
Threshold voltage of the transistor in fresh condition, after irradiation and after each annealing step.



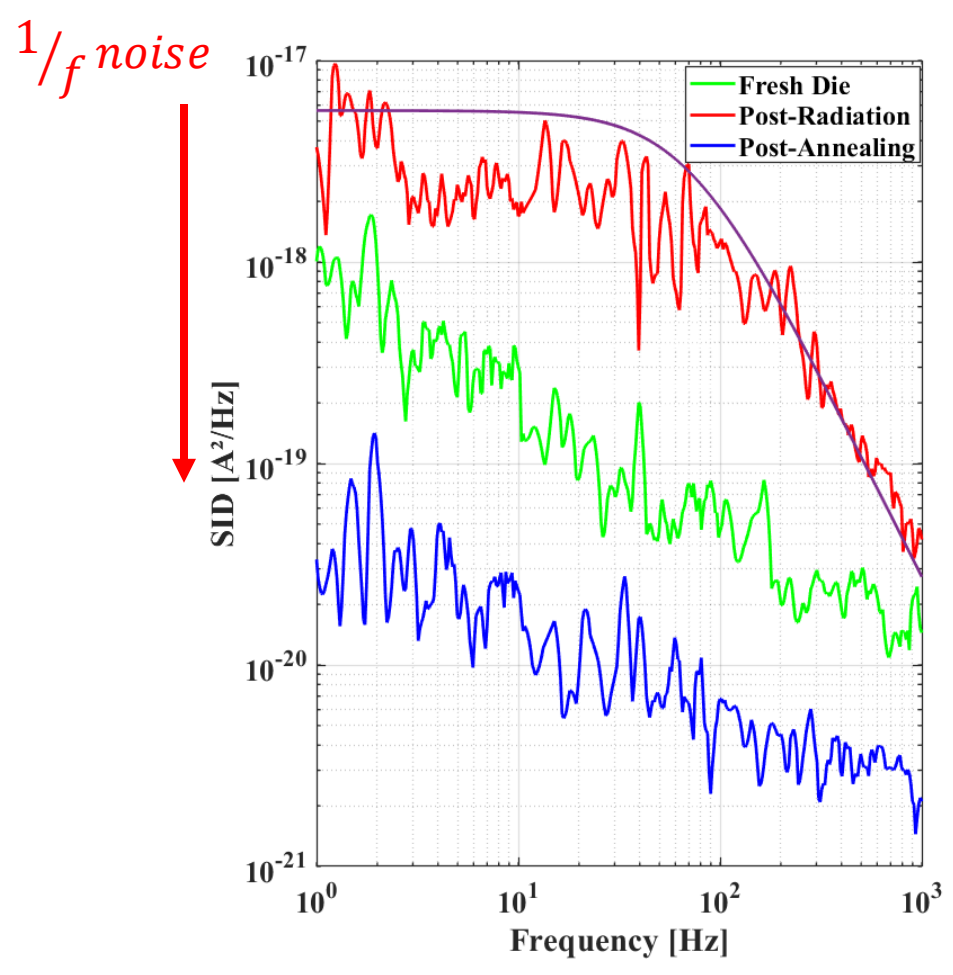
Maximum transconductance in linear regime, extracted in fresh condition, after irradiation and after each annealing step.



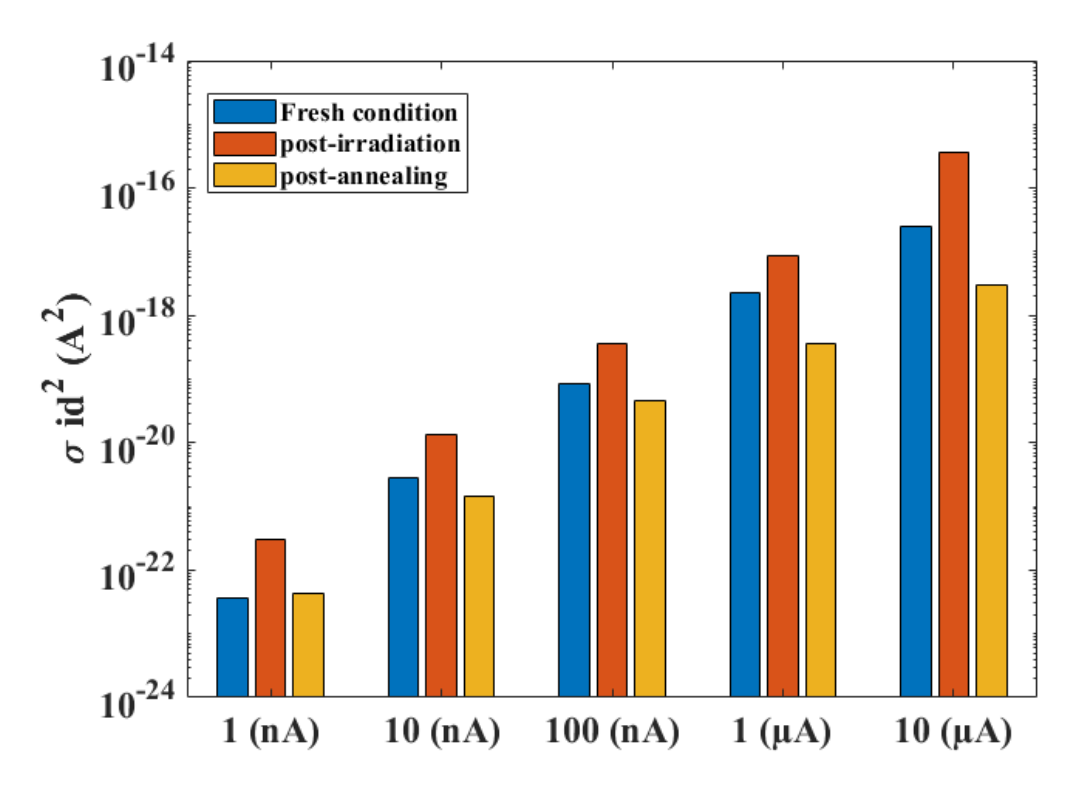
Voltage transfer characteristics of the CMOS inverter after each annealing step



Output current of the CMOS Inverter measured after each annealing step



Noise power spectral density of the MOSFETs. Measured Pre-Post radiation and after annealing at $V_{ds} = 3 \text{ V}$.



Total power noise at different drain currents (from weak to strong inversion integrated from 1 Hz to 606 Hz).

Summary

- > Supported membranes in MEMS applications
 - ➤ Porous silicon acts as particles sieve for lysed bacteria
 - Silicon-on-Insulator (SOI) with embedded electronics can be heated up to high temperatures, providing *in situ* low-power annealing of various types of defects

Conferences announcement



scope2025 : Journées SCOPe 2025

23-24 Oct 2025 Louvain-la-Neuve (Belgium)



ACKNOWLEDGEMENTS

- Prof. Denis Flandre and Prof. Jean-Pierre Raskin for their continuous presence and precious help on so many topics
- The past and current porous team @UCL members: Dr. Gilles Scheen, Dr. Jonathan Rasson, Dr. Roselien Vercauteren, Ir. Clara White Fereira, Ir. Romain Hanus, Ir. Clémentine Gevers, Dr. Romain Tuyaerts and Elia Colomer Clavel
- Dr. Sedki Amor for the bulk of the work on the recovery of irradiated SOI membranes
- Pr. em. Jacques Mahillon and his team, in particular to Audrey Leprince and Manon Nuytten for endolysin synthesis
- Prof. Florin Udrea and Dr. Zeeshan Ali from the University of Cambridge/CCMOS Sensors Ltd. (now with AMS)
- Pr. Sophie Hermans and Louise Lejeune for Au NPs
- UCLouvain's cleanroom WINFAB and electronic measurement platform WELCOME's technical teams for assistance

- Funding:
 - EU F.P. Horizon 2020
 - Fonds de la Recherche Scientifique FRS-FNRS, through FRIA fellowships
 - UCLouvain







Thank you for your attention!

Laurent.Francis@uclouvain.be